TR 82-2

Nonrandom Behavior in Field Wave Spectra and Its Effect on Grouping of High Waves

by

Edward F. Thompson

TECHNICAL REPORT NO· 82-2

AUGUST 1982

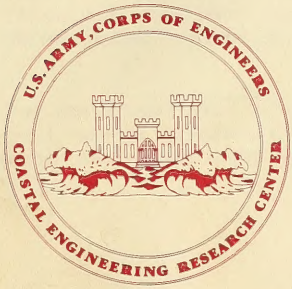

Approved for public release;
distribution unlimited.

U.S. ARMY, CORPS OF ENGINEERS
COASTAL ENGINEERING
RESEARCH CENTER
Kingman Building
Fort Belvoir, Va. 22060

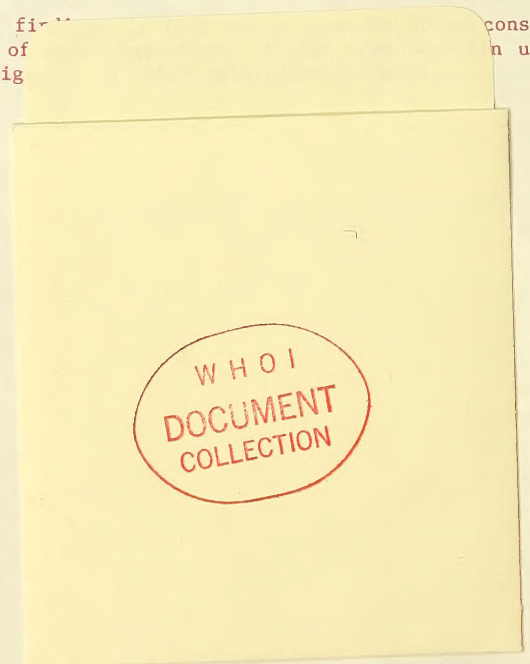

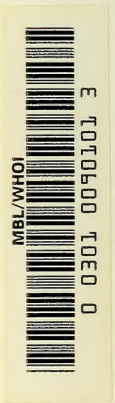

REPORT DOCUMENTATION PAGE

READ INSTRUCTIONS BEFORE COMPLETING FORM

1. REPORT NUMBER: TR 82-2	2. GOVT ACCESSION NO.
3. RECIPIENT'S CATALOG NUMBER	
4. TITLE *(and Subtitle)*: NONRANDOM BEHAVIOR IN FIELD WAVE SPECTRA AND ITS EFFECT ON GROUPING OF HIGH WAVES	5. TYPE OF REPORT & PERIOD COVERED: Technical Report
	6. PERFORMING ORG. REPORT NUMBER
7. AUTHOR(s): Edward F. Thompson	8. CONTRACT OR GRANT NUMBER(s)
9. PERFORMING ORGANIZATION NAME AND ADDRESS: Department of the Army, Coastal Engineering Research Center (CERRE-CO), Kingman Building, Fort Belvoir, Virginia 22060	10. PROGRAM ELEMENT, PROJECT, TASK AREA & WORK UNIT NUMBERS: A31592
11. CONTROLLING OFFICE NAME AND ADDRESS: Department of the Army, Coastal Engineering Research Center, Kingman Building, Fort Belvoir, Virginia 22060	12. REPORT DATE: August 1982
	13. NUMBER OF PAGES: 110
14. MONITORING AGENCY NAME & ADDRESS*(if different from Controlling Office)*	15. SECURITY CLASS. *(of this report)*: UNCLASSIFIED
	15a. DECLASSIFICATION/DOWNGRADING SCHEDULE

16. DISTRIBUTION STATEMENT *(of this Report)*

Approved for public release; distribution unlimited.

17. DISTRIBUTION STATEMENT *(of the abstract entered in Block 20, if different from Report)*

18. SUPPLEMENTARY NOTES

19. KEY WORDS *(Continue on reverse side if necessary and identify by block number)*

Fast Fourier transform
Multiple regression screening
Spectral analysis
Wave height
Wave spectra

20. ABSTRACT *(Continue on reverse side if necessary and identify by block number)*

Wave measurements are examined from three relatively deepwater field sites in Lake Michigan, the Pacific Ocean, and the Gulf of Mexico. Approximately 1 hour of data representing high waves, single-peaked spectra, and nearly constant significant heights and peak spectral periods was selected for analysis. The data represent actively growing waves at two sites and swell at the third site.

(continued)

Analysis is done in both the frequency and the time domain. The fast Fourier transform (FFT) spectral analysis procedure is shown to possess limitations in resolution of frequency and phase. Phases are shown to be subject to erratic variations. Shortcomings of the FFT procedure are circumvented by using a multiple regression screening (MRS) technique to identify frequency, amplitude, and phase for major constituents in the frequency domain.

The time domain analysis is designed to extract wave grouping information directly from the time series. A wave group is conceptualized as a small area of sea surface containing relatively high energy. Groups are identified as sections of the time series in which the local variance is high relative to the variance of the complete record. Local variance is computed over a time approximately equal to twice the peak spectral period. Fluctuations in local variance provide information on both the intensity and time scale of wave grouping. A new dimensionless parameter indicative of wave grouping is defined as the ratio of standard deviation of local variance fluctuations to variance of the time series. The autocorrelation between individual wave heights, between periods, and between amplitudes is also considered. The autocorrelation between successive heights ranged from about 0.2 to 0.5.

Analyses of the data are used to test the following six hypotheses about the nature of ocean waves:

(a) Spectral components are sometimes discrete and are not smeared over a broad continuous spectrum.

(b) Spectral components are sometimes related in a deterministic, nonrandom way.

(c) The detailed spectral shape may be partially explained by the theory of Benjamin and Feir (1967).

(d) Waves in deep water tend to be organized so that high waves occur in groups.

(e) The modulation period of wave groups is sometimes related to the period and steepness of the waves.

(f) The extent of grouping in each time series and the modulation period are related to certain features of the spectrum.

Evidence supporting the hypotheses leads to the conclusion that some commonly held conceptions of ocean waves, including the notion of a random wave field represented by a continuous random-phase spectrum, are open to serious question.

PREFACE

The tendency for high waves to group is a phenomenon of considerable interest in the coastal and ocean engineering community. This grouping has special importance in the Corps of Engineers because several high waves in succession can represent a more severe design condition for coastal structures than ungrouped waves. In particular, recent evidence indicates that grouped waves can be more damaging to a rubble-mound structure than ungrouped waves with the same heights. This report deals primarily with relatively simple cases of waves in deep water. However, it is hoped (and expected) that the analysis techniques and results developed in this study will lead to a better understanding of wave grouping characteristics in shallow water. The work was carried out under the U.S. Army Coastal Engineering Research Center's (CERC) Wave Estimation for Design work unit, Coastal Flooding and Storm Protection Program, Coastal Engineering Area of Civil Works Research and Development.

The report was prepared by Dr. Edward F. Thompson, Hydraulic Engineer, under the supervision of Dr. C.L. Vincent, Chief, Coastal Oceanography Branch, and Mr. R.P. Savage, Chief, Research Division.

The author acknowledges the guidance and encouragement throughout this study provided by Dr. J.E. Feir, Associate Dean of the School of Engineering and Applied Science, George Washington University; Dr. D.L. Harris, formerly with CERC and currently Research Scientist, College of Engineering, University of Florida; Dr. R.M. Sorensen, Chief, Coastal Processes and Structures Branch, CERC; and Dr. B.E. Herchenroder, Mathematician-Oceanographer, CERC. Dr. Harris also provided the computer program for multiple regression screening analysis. W. Buckley and M. Davis of the U.S. Navy David W. Taylor Naval Ship Research and Development Center made possible the inclusion of wave data from Hurricane Camille in this study.

The material included in this report provided the basis for a dissertation submitted to the George Washington University in partial satisfaction of the requirements for the Doctor of Science degree (Thompson, 1981).

Technical Director of CERC was Dr. Robert W. Whalin, P.E., upon publication of this report.

Comments on this publication are invited.

Approved for publication in accordance with Public Law 166, 79th Congress, Approved 31 July 1945, as supplemented by Public Law 172, 88th Congress, approved 7 November 1963.

TED E. BISHOP
Colonel, Corps of Engineers
Commander and Director

CONTENTS

TABLES

FIGURES

CONTENTS

FIGURES--Continued

CONTENTS

FIGURES--Continued

CONVERSION FACTORS, U.S. CUSTOMARY TO METRIC (SI) UNITS OF MEASUREMENT

U.S. customary units of measurement used in this report can be converted to metric (SI) units as follows:

Multiply	by	To obtain
inches	25.4	millimeters
	2.54	centimeters
square inches	6.452	square centimeters
cubic inches	16.39	cubic centimeters
feet	30.48	centimeters
	0.3048	meters
square feet	0.0929	square meters
cubic feet	0.0283	cubic meters
yards	0.9144	meters
square yards	0.836	square meters
cubic yards	0.7646	cubic meters
miles	1.6093	kilometers
square miles	259.0	hectares
knots	1.852	kilometers per hour
acres	0.4047	hectares
foot-pounds	1.3558	newton meters
millibars	1.0197×10^{-3}	kilograms per square centimeter
ounces	28.35	grams
pounds	453.6	grams
	0.4536	kilograms
ton, long	1.0160	metric tons
ton, short	0.9072	metric tons
degrees (angle)	0.01745	radians
Fahrenheit degrees	5/9	Celsius degrees or Kelvins[1]

[1]To obtain Celsius (C) temperature readings from Fahrenheit (F) readings, use formula: $C = (5/9)(F - 32)$.

To obtain Kelvin (K) readings, use formula: $K = (5/9)(F - 32) + 273.15$.

SYMBOLS AND DEFINITIONS

A_i amplitude for multiple regression screening (MRS) constituent

A(j) difference between j'th wave amplitude and mean amplitude for record

A_m amplitude of combined sine and cosine components of the Fourier transform of a time series

a wave amplitude

a_o constant equal to mean of time series

a_m amplitude of cosine component of the Fourier transform of time series

b_m amplitude of sine component of the Fourier transform of time series

c_i constant

d water depth

d_i constant

f_i arbitrary function

f_o carrier wave frequency

f_p frequency corresponding to highest spectral peak

G wave grouping parameter

g acceleration due to gravity

H amplitude of a sinusoidal wave

H(j) difference between height of j'th wave and mean wave height for record

H_s significant wave height

I integer constant; number of data points used in computing local variance

i,j summation index; arbitrary integer

J integer constant indicating number of nonoverlapped data points in partially overlapped time series; number of waves in record

K integer subscript

k wave number

k_o deepwater wave number

L constant

M	total number of points in zero-padded time series
m	summation index
$\hat{m}$	constant used to specify frequency of a sinusoidal wave
N	number of data points in time series
n	index to sequence of data points
p	number of functions used to estimate time series in MRS analysis
$R_A(\tau)$	autocorrelation between wave amplitudes
$R_H(\tau)$	autocorrelation between wave heights
$R_T(\tau)$	autocorrelation between wave periods
$R_{x_i y}$	correlation between the function x_i and the time series
$R_{x_{2i-1}x_{2i}y}$	multiple correlation between the functions x_{2i-1} and x_{2i} and the time series
$T(j)$	difference between j'th wave period and mean period for record
T_{LVTS}	time between high wave groups estimated from peaks in local variance time series (LVTS)
T_{mod}	time between high wave groups estimated from wave steepness
T_{MRS}	time between high wave groups estimated from MRS constituents
T_p	wave period corresponding to highest spectral peak
t_i	time associated with a data point in time series
$w(n\Delta t)$	cosine bell data window
X_i	selected function of time
x_i	selected function of time with mean removed
y, $y(n\Delta t)$	finite time series with zero mean
$\tilde{y}(n\Delta t)$	time series after application of cosine bell data window
$\overset{o}{y}(n\Delta t)$	squared time series
$\hat{y}(n\Delta t)$	time series padded symmetrically with zeros

$\hat{\hat{y}}(n\Delta t)$	time series containing periodic repetitions of short data record
$y_e(n\Delta t)$	estimate of finite time series
$y_1(n\Delta t)$	partially overlapped time series
$y_2(n\Delta t)$	partially overlapped time series
$y_i(n\Delta t)$	partially overlapped time series
$Z(n\Delta t)$	local variance time series (LVTS)
$Z(\Delta t)$	first point in LVTS
$z(n\Delta t)$	LVTS with mean removed
α_i	amplitude of sine component of MRS analysis of a time series
β_i	amplitude of cosine component of MRS analysis of a time series
Δf_{MRS}	frequency spacing between adjacent pair of prominent MRS constituents
Δt	time interval between data points
δ	a fraction
ε	wave steepness, ak
η_i	elevation represented by a data point in time series
π	constant equal to 3.14159
σ	frequency of a sinusoidal wave
σ_m	frequency in the Fourier transform of a time series
σ_y	standard deviation of time series
σ_z	standard deviation of LVTS
τ	lag between wave parameters for autocorrelation (number of waves)
ϕ	phase of a sinusoidal wave
ϕ_i	phase for MRS constituent
ϕ_m	phase of combined sine and cosine components of the Fourier transform of a time series
ω_i	frequency in MRS analysis of a time series

NONRANDOM BEHAVIOR IN FIELD WAVE SPECTRA AND ITS EFFECT ON GROUPING OF HIGH WAVES

by
Edward F. Thompson

I. INTRODUCTION

1. Hypotheses.

This study is aimed at several basic assertions about the physical characteristics of ocean waves. The study is designed to test the following six hypotheses about the nature of waves:

(a) Spectral components are sometimes discrete and are not smeared over a broad continuous spectrum.

(b) Spectral components are sometimes related in a deterministic, nonrandom way.

(c) The detailed spectral shape may be partially explained by the theory of Benjamin and Feir (1967).

(d) Waves in deep water tend to be organized so that high waves occur in groups.

(e) The modulation period of wave groups is sometimes related to the period and steepness of the waves.

(f) The extent of grouping in each time series and the modulation period are related to certain features of the spectrum.

Most of the hypotheses are in conflict with commonly held conceptions of ocean waves, including the notion of a random wave field represented by a continuous spectrum with random-phase relationships between components.

2. General.

Groups of high ocean waves are an important warning signal to an engineer. Grouped waves represent a more severe condition than ungrouped waves for many coastal and ocean engineering endeavors. Wiegel (1964) observed that "It is the groups of several periodic waves, which are almost always the highest waves in a wave system, that are the most effective in causing structural damage." Groups of high waves may be a major cause of ship capsizing.

The spectacular collapse of part of the massive breakwater at Sines, Portugal, during attack by waves lower than the design condition (Zwamborn, 1979) has recently stimulated interest in the effect of high wave groups on the stability of breakwaters. A laboratory study has shown that groups of high waves are more damaging to a rubble-mound structure than ungrouped waves of the same heights (Johnson, Mansard, and Ploeg, 1978).

Wave groups have considerable engineering importance beyond the implications of several high waves occurring in succession. The existence of groups

introduces a new time scale into the motion of the sea. The new, or modulation, time scale is distinct from and substantially longer than the characteristic time between waves. Modulation time scales can assume values which are compatible with resonant behavior in many floating structures. They can also lead to resonant oscillation of moored ships as well as to resonant oscillation in semienclosed harbors and bays.

High wave groups seem to be a real characteristic of gravity waves as observed in laboratory wind-wave flumes and in a wide variety of field conditions. Evidence reviewed in Section III indicates that groups are more common than would be expected if each wave height were randomly related to the preceding and following wave heights.

Unfortunately, wave grouping characteristics in field records sometimes vary greatly over short time intervals (e.g., Burcharth, 1980). The variations, which are not consistent with present concepts about wave groups, have made it difficult to describe grouping characteristics empirically. It must be concluded that, despite its engineering significance and its demonstrated presence in field records, the phenomenon of wave grouping is poorly understood.

It is often assumed that the sea surface represents a random Gaussian process and that the Fourier transform of a time series of sea-surface elevations represents a continuous spectrum with an infinite number of independent frequency components. Wave groups can be explained as modulations resulting from linear superposition of high-energy components near the peak of a narrow spectrum. This reasoning leads to the supposition that some measure of spectral width may be related to wave grouping characteristics in the time series. However, efforts to identify such a relationship in field data have generally failed.

An alternative approach which has received increasing attention during the last 5 years treats wave groups as a nonlinear phenomenon and rejects the assumption that all spectral components are independent. An obvious case in which spectral components are not independent is a record of steep waves with peaked crests and flat troughs. Wave profiles may be described as a summation of a wave of the fundamental frequency and waves at frequencies which are integral multiples of the fundamental, often called a Stokes wave. The spectrum has peaks at harmonics of the dominant frequency which are phase-bound to the fundamental and are clearly not independent.

Further evidence of nonindependence in the spectrum was published by Benjamin and Feir (1967). Finding that the Stokes wave is unstable to small perturbations in a certain range of frequencies, they showed in the laboratory and in theory that bound spectral components can also be expected at discrete frequencies very near the dominant frequency, much closer than the second harmonic. The bound subharmonic components are evidenced in the time series as strong modulations of the dominant wave.

The Benjamin-Feir (BF) theory, as well as that of Longuet-Higgins (1980), deals only with the growth of instability on an initially nearly uniform wave train in relatively deep water. The theory does not follow the long-term evolution of the wave condition. Also, it does not deal directly with the problem of an actively growing sea state. Despite these restrictions, the BF

theory provides a basis for considering possible existence of nonindependent spectral energy at discrete frequencies near the main peak in a variety of ocean wave conditions.

Field data are conspicuously lacking in the published literature on the question of whether spectral components are really independent. The sparcity of field data is not surprising because field data are notoriously difficult and expensive to acquire, especially in relatively deep water. Also, field data are likely to contain free wave energy in addition to any bound energy. However, several notable field studies by Ramamonjiarisoa and Mollo-Christensen (1979) and Kuo, Mitsuyasu, and Masuda (1979b), and laboratory wind-wave studies by Lake and Yuen (1978) and Mitsuyasu, Kuo, and Masuda (1979) have been published. Among other procedures, these studies made use of spatial gage arrays to evaluate the phase speed of each spectral component. The extent to which phase speed deviates from linear theory and tends toward a constant is an indicator of the nonindependence of the component. These studies have not reached a definitive conclusion, but rather have made the whole question appear more complex and intriguing.

Although the presence of bound frequency components has clear implications for nonrandom-phase relationships between components, this important characteristic of a wave record has apparently never been examined explicitly. Also, the question of whether or not the spectrum has a definite, noncontinuous structure has received very little attention. A review of pertinent literature is given in Section II.

Three samples of field data were selected for analysis in this study. All samples represent relatively deepwater cases in which the spectra were single-peaked, indicating that one wave train was dominating the sea surface. The data samples are described in Section III.

It is contended in this study that previous studies have been self-limiting in the method for computing phase for each spectral component and, in some cases, in the lack of resolution in frequency. This study thus began with the task of developing viable techniques for (a) computing a stable, meaningful value of phase for each important spectral component; and (b) computing spectral components with a resolution in frequency sufficient to identify any detailed structure and yet not have a record so long that the assumption of stationarity becomes suspect. The techniques finally adopted involved the use of high resolution fast Fourier transform (FFT) analysis of a record approximately 15 minutes long, followed by the application of a multiple regression screening (MRS) procedure using a comb of frequencies covering the high-energy part of the spectrum and, in some cases, other parts of the spectrum. This study is believed to represent the first use of a multiple regression screening procedure in conjunction with field wave records. The analysis techniques are described in detail in Section IV.

Wave grouping characteristics in the time series are investigated in this study as a logical and important complement to the detailed study of spectra. However, techniques for investigating wave grouping are not well established. It is necessary to develop and refine techniques for identifying and quantifying wave grouping in a time series. The techniques used in this study are described in Section IV. A new parameter indicative of wave grouping is proposed.

The techniques developed for spectral analysis and wave group analysis were applied to the selected data samples. Results are presented in Section V. In Section VI, the results are discussed and related to the six hypotheses. Evidence from the field data samples supports the validity of each of the six hypotheses.

A summary of this study is given in Section VII.

II. LITERATURE REVIEW

1. Spectra.

Theories of ocean wave development have been based over the last 15 years on one of two general concepts of a wave field. The first approach deals with evolution of a continuous spectrum representing the superposition of an infinite number of independent frequency components. The second approach deals with evolution of an initially uniform train of steep waves. Both approaches were first used in conjunction with deepwater waves, but more recent developments have included shallow-water waves as well. Relevant literature is reviewed in this section, primarily as it relates to deepwater waves.

a. Evolution of Continuous Spectra. Consideration of the spectrum of ocean waves began to appear in the literature in the early 1950's. Examples given by Harris (1974) are Seiwell (1949), Ursell (1950), Pierson (1950), and Neumann (1952). The spectrum is used to describe a sea surface which is generally regarded to have Gaussian-distributed displacements. The Gaussian assumption along with the assumptions of random phase and stationarity led to application of computational procedures developed in other disciplines (e.g., Taylor, 1938; Blackman and Tukey, 1959) to ocean waves. These assumptions have formed the cornerstone of wave spectral analysis techniques, although Harris (1974) pointed out that the development of the fast Fourier transform algorithm (Cooley and Tukey, 1965) obviated the need for many of the restrictive assumptions.

Nonlinear interactions between spectral components have increasingly come to attention in recent years. Second-order interactions have been shown to be of little significance. Third-order interactions, although initially small, sometimes exhibit unbounded growth with time as discovered by Phillips (1960). Subsequent theoretical explorations of this surprising third-order resonant interaction between frequency components include Longuet-Higgins (1962), Benney (1962), and Hasselmann (1962), 1963).

The viability of third-order resonant interactions was demonstrated by laboratory experiments in several special situations (Longuet-Higgins and Smith, 1966; McGoldrick, et al., 1966) before finally being demonstrated for growing wind waves in the laboratory by Mitsuyasu (1968) and later by Wu, Hsu, and Street (1979). Field data showing that nonlinear energy transfer is an important mechanism in explaining fetch-limited wave growth were presented in considerable detail by Hasselmann, et al. (1973). Examples of nonlinear transfer functions computed directly from the field spectra are shown to compare favorably with transfer functions derived from theoretical expressions for the third-order resonant interactions.

The demonstrated importance of nonlinear energy transfer spurred further investigation. Numerical study of the nonlinear interactions for a Pierson-Moskowitz spectrum by Webb (1978) provided new insight. An imaginative approach to computing the strength of nonlinear energy transfer within the peak of a narrow spectrum was given in a paper by Longuet-Higgins (1976) and a companion paper by Fox (1976). Longuet-Higgins made use of the nonlinear Schrodinger equation that describes the envelope of a weekly nonlinear wave train. Both Longuet-Higgins and Fox concluded that nonlinear transfer within the peak is of dominant importance; however, contrary to observations, it tends to broaden the spectral peak and reduce spectral asymmetry.

Although the derivations of Hasselmann (1962, 1963) include finite as well as infinite depth, the finite-depth application had not been explored further until recently (Shemdin, et al., 1978, 1980; Herterich and Hasselmann, 1980). This application appears promising for future investigation.

The stability of a wave spectrum to small oblique perturbations has been considered by Alber (1978), Alber and Saffman (1978), and Crawford, Saffman, and Yuen (1980). A range of conditions giving rise to instability in a Gaussian random surface wave train is identified. Instability is found to exist for a sufficiently narrow spectrum and for sufficiently small perturbation wave angles. The effect of randomness is to reduce the importance of instability. These studies are a counterpart to the deterministic approach of Benjamin and Feir (1967) discussed below.

Most of the above work pertains to random-phase Gaussian sea states. With few exceptions, the descriptions of nonlinear energy transfer represent phase-averaged exchanges.

b. Evolution of Nonlinear Wave Train with Significant Steepness. A deterministic approach to the evolution of a sea state was taken by Benjamin and Feir (1967) and Benjamin (1967). The studies centered on the unexpected discovery of Benjamin and Feir that finite-amplitude, progressive waves in deep water (Stokes-type waves) are unstable to small perturbations at certain frequencies. The instability was found in the laboratory and also shown theoretically.

The BF instability accounts for the unbounded growth of initially small perturbations, and it provides insight on the ultimate disintegration of a coherent wave train.

Another study at about the same time dealt with large, but extremely gradual perturbations in a deepwater wave train (Lighthill, 1965). The study also revealed evidence of instability for a wave packet. However, the solution became singular in finite time and could not predict the ultimate evolution.

The BF analysis shows that the frequency and amplitude dispersion terms required to maintain a steep wave of permanent form give rise to unbounded growth of perturbations with frequency $f_o \pm \delta f_o$, where f_o is the carrier frequency, when δ is in the range

$$0 < \delta \leq \sqrt{2}\ ak \qquad (1)$$

where a and k are the amplitude and wave number of the wave train. The fastest growing instability corresponds to

$$\delta = ak \tag{2}$$

Thus a wave train which initially has significant energy only at frequencies f_o and its higher harmonics ($2f_o$, $3f_o$, etc.) can be expected to develop strong concentrations of energy at sideband frequencies $f_o(1 + ak)$ and $f_o(1 - ak)$. The energy in both sidebands is approximately equal due to their coupled growth.

With well-developed sidebands, the wave train can be considered as a modulated carrier wave. It was noted by Benjamin and Feir (1967) that perturbations corresponding to values of δ near zero in equation (1) represent mainly phase modulation which gradually gives way to pure amplitude modulation as δ is increased to $\sqrt{2}$ ak. For the most unstable mode, given by equation (2), phase and amplitude modulation are equal. The modulation time scale, i.e., the time between wave groups in a wave train with well-developed sidebands, is

$$T_{mod} = \frac{1}{ak\ f_o} \tag{3}$$

Both Benjamin (1967) and Whitham (1967) showed that the instability can occur in finite depth, d, as well, on the condition that

$$kd > 1.363 \tag{4}$$

Contrary to the phase-averaged nonlinear transfer discussed earlier, the BF sideband interactions depend crucially on phase.

The concept of a sea state as a perturbed carrier wave train has stimulated theoretical study of the evolution of the envelope of such a train. Early studies of evolution of the envelope of a train of weakly nonlinear dispersive waves were done by Benney and Newell (1967) and Zakharov (1968). Subsequently, Chu and Mei (1970, 1971) derived envelope equations which overcame the singularity found by Lighthill (1965), but which for other reasons could not be extended to infinite time.

Hasimoto and Ono (1972) derived the nonlinear Schrodinger equation in the context of the envelope of water waves. The equation has been solved exactly by Zakharov and Shabat (1972) for pulselike initial conditions which approach zero sufficiently rapidly. The solution predicts that any initial pulse of waves will eventually disintegrate into a series of wave packets, or solitons, and a dispersive oscillatory tail. Each soliton is a permanent progressive wave solution to the nonlinear Schrodinger equation. The solitons are stable features which can pass through each other with no change of form except possibly a phase shift. Thus the nonlinear Schrodinger equation may be a tool for predicting the ultimate evolution of a sea state.

Laboratory data were given by Yuen and Lake (1975) to show that the nonlinear Schrodinger equation provides a useful quantitative description of the long-term evolution of wave packets.

The experimental investigation was extended to the long-term evolution of an initially uniform wave train by Lake, et al. (1977). When the average value of ak exceeded 0.1, the onset and development of BF sideband instabilities were observed in early stages of evolution, followed by a spread of spectral energy to many frequencies in addition to the carrier and sideband frequencies. Envelope solitons in the "disintegrated" wave train were observed to be consistent with soliton solutions of the nonlinear Schrodinger equation. However, Lake, et al. presented clear evidence that envelope solitons are not the ultimate state of wave-train evolution. They observed that the highly modulated train, characterized by a broad spectrum, actually demodulated and very nearly returned to its initial state as a uniform wave train. A small decrease in carrier frequency was observed in some cases. They suggested that the ultimate evolution of a train of steep waves is a series of periodically recurring states of modulation and demodulation, not a series of stable envelope solitons. They used numerical techniques to solve the nonlinear Schrodinger equation with periodic initial conditions. It was demonstrated that periodically recurring modulated-demodulated states are characteristic of solutions to the nonlinear Schrodinger equation.

Lake and Yuen (1978) extended the investigation further to include wind-generated laboratory waves. They presented strong evidence that a broad wind-wave spectrum is better represented as a coherent collection of bound frequency components than as independent components. They proposed a nonlinear wind-wave model consisting of a single dominant wave frequency with all other spectral energy bound to the dominant wave. It was proposed that free wave energy exists, but the existence is primarily in very short waves generated by local winds and wave breaking, representing a negligible fraction of the total energy. This model is obviously a drastic change from the long-held conception of a spectrum as a random collection of free wave components.

Both Lake, et al. (1977) and Lake and Yuen (1978) reported an important characteristic which cannot be accounted for by the nonlinear Schrodinger equation. When the waves are sufficiently steep, the BF sidebands develop and strong modulation followed by demodulation occurs, but the carrier frequency of the demodulated wave train becomes the frequency of the low-frequency sideband in the original train. Lake and Yuen indicated that discrete shifts such as these may be the primary mechanism by which energy in a developing sea is transferred to lower frequency. Thus the nonlinear Schrodinger equation fails to model a crucial characteristic of developing wind waves.

Modulation frequency was investigated in laboratory wind waves by Lake and Yuen (1978). Identifiable modulations were present with modulation periods on the order of equation (3) but they were generally somewhat longer.

The modulation period given by Benjamin and Feir (eq. 3) applies strictly to small values of wave steepness, ak. An extensive theoretical investigation in which the instabilities of finite-amplitude deepwater waves were calculated over a large range of wave steepness was reported by Longuet-Higgins (1978a, 1978b). Two types of instability were identified--superharmonic instabilities, which are associated with wave breaking, and BF-type subharmonic instabilities. However, as wave steepness increased beyond about 0.346, the BF-type instabilities became stable. A new type of subharmonic instability with a very high growth rate appeared at a wave steepness of about 0.41. The practical significance of this theoretical instability is uncertain.

Longuet-Higgins (1980) extended the analysis of subharmonic instabilities to determine the frequency of the fastest growing instability as a function of wave steepness. His results indicate slightly longer modulation periods than predicted by the BF theory for wave steepness between 0 and 0.3. Longuet-Higgins (1980) showed that his results compare more favorably than the BF results with the laboratory wind-wave data of Lake and Yuen (1978).

An extensive review of the literature relevant to instabilities of deep-water waves is given by Yuen and Lake (1980).

The concept of a perturbed carrier wave train can be reconciled with a broad spectrum of energy only if the assumption of independent spectral components is abandoned. The nonpeak spectral components can be considered as artifacts of the attempt to describe nonlinear waves with a set of linear components. This interpretation has the direct consequences of well-defined relationships between the carrier and other spectral components and a constant phase speed for all components. Higher order harmonics of the carrier have been generally considered to fit this description when wave steepness is high. The most convincing evidence that spectral energy at nonharmonics may also be a result of nonlinear wave shapes has been obtained by computing phase speed for each spectral component between a spatially separated pair of gages.

Early field evidence that the phase speed of spectral components can be higher than expected from the linear dispersion relationship was obtained by Burling (1959), Von Zweck (1969), and Yefimov, Solov'yev, and Khristoforov (1972). Laboratory measurements by Ramamonjiarisoa and Coantic (1976) for wind waves and by Lake and Yuen (1978) for mechanical and wind waves indicate that phase speed for steep wave conditions is essentially constant for frequencies higher than the peak spectral frequency. Additional evidence of deviation from linear theory is given by Rikiishi (1978), Mollo-Christensen and Ramamonjiarisoa (1978), Ramamonjiarisoa and Giovanangeli (1978), and Ramamonjiarisoa and Mollo-Christensen (1979). The latter reference includes field measurements which led the authors to suggest that phase speed at frequencies above the peak can range between the value from linear theory and the phase speed of the peak frequency, depending on the degree of nonlinearity.

The evidence is not conclusively in favor of interpretation of the spectrum for steep waves as a system of bound components. Careful studies indicating the efficacy of linear theory for describing phase speeds of components in a wide frequency range around the peak (but terminating before the second harmonic of the peak) have been reported by Mitsuyasu, Kuo, and Masuda (1978, 1979); Kuo, Mitsuyasu, and Masuda (1979a, 1979b); and Komen (1980).

Although the presence of bound frequency components has clear implications for nonrandom-phase relationships between components, this important aspect of a wave record has apparently never been examined explicitly.

2. Wave Groups.

Increasing recognition of the practical importance of a tendency for high waves to occur in groups has led to numerous studies. Most of the studies deal either with the serial variation in individual wave heights and periods or with characteristics of an envelope of the individual waves.

Most investigators of wave groups seem to prefer dealing with the serial variation in individual wave heights. Rye (1974), Houmb and Overvik (1977), and Arhan and Ezraty (1978) reported autocorrelations between individual wave heights from field records. Autocorrelations averaged between about 0.2 and 0.3, indicating a weak correlation between heights of successive waves. Arhan and Ezraty found essentially no correlation between a wave height and the height of the second or third following wave.

Arhan and Ezraty (1978) also reported evidence from 169 North Sea storm records that the correlation between a wave height and the succeeding wave height depends on the individual wave height. They showed an increasing correlation when the wave height is greater than about 0.75 times the significant height. When the wave height is lower than 0.75 times the significant height, it is uncorrelated with the height of the following wave. Siefert (1976) also observed that the tendency for high waves to occur in succession increases with wave height. These interesting results raise questions about the value of a single autocorrelation between wave heights as a parameter indicative of wave grouping.

Statistics of runs of consecutive waves with heights above some specified level have also indicated a weak tendency for high waves to occur in groups. Literature on the subject includes Goda (1970, 1976), Wilson and Baird (1972), Ewing (1973), Chakrabarti, Snider, and Feldhausen (1974), Rye (1974), and Burcharth (1980).

Nolte and Hsu (1972) studied wave groups by examining statistics of the wave envelope. They found good agreement between their theory and field data. Chou (1978) developed an analytical method for constructing the wave envelope, based on the assumption of a stationary random Gaussian sea state.

Both the serial variation in wave heights and the statistics of the wave envelope are in theory useful approaches to studying wave grouping. However, real ocean wave records typically include numerous small bumps and erratic variations which introduce subjectivity into the definition of individual wave heights and wave envelopes. An appealing alternative has been devised and applied by Sedivy (1978). A wave group is considered to be a short section of wave record which has high variance relative to the variance of the whole record. The local variance is computed throughout the record so as to identify all areas of high local variance (i.e., wave groups). Statistics derived from numerous field records by this approach are given by Sedivy (1978), Nelson (1980), and Thompson and Sedivy (1980).

Sedivy (1978) experimented with various lengths of record for computing the local variance to most clearly identify prominent wave groups. His final choice was two times the peak spectral period for the record. Nelson (1980) confirmed that choice.

Another approach to studying wave grouping involves computing the spectrum of the squared data points in a wave record. The spectrum shows energy from wave groups at very low frequencies while energy at the dominant individual wave frequency appears at about twice the individual wave frequency. Thus, energy and frequencies associated with wave groups can be effectively isolated. This approach is well described and illustrated in Funke and Mansard (1979), and is also discussed in Funke and Mansard (1980).

Funke and Mansard (1979) used the approach to define a single parameter indicative of the extent of wave grouping in a record. Although the Funke-Mansard grouping parameter appears to be effective, a new grouping parameter is proposed in the present study based on Sedivy's (1978) approach to studying wave groups. The grouping parameter proposed in Section IV is similar to the Funke-Mansard parameter in practice but it avoids the need for a rather arbitrary smoothing function included in the Funke-Mansard parameter. It also avoids distortion of the spectrum which may be caused by high frequencies, formed in squaring the record, aliasing into low frequencies.

Attempts to relate the narrowness of the spectrum to wave grouping characteristics in field records have met with limited success. Houmb and Overvik (1977) observed an increase in the autocorrelation between successive wave heights as spectral width decreased. Rye (1974) reported more pronounced wave grouping in a decaying sea. However, Goda (1976) showed inconclusive comparisons of spectral width and wave grouping, and Burcharth (1980) reported no observable relationship. Burcharth also reported considerable short-term variability in wave grouping characteristics. Johnson and Ploeg (1977), Johnson, Mansard, and Ploeg (1978), and Funke and Mansard (1979) discussed the possibility that phase as well as energy of the spectral components may be important in determining wave group characteristics. Rye (1979) concluded after a fairly extensive review that the question of how the spectrum is related to field wave grouping characteristics remains unanswered.

III. FIELD WAVE DATA

Three samples of field wave data were selected for analysis. The following criteria for an ideal data sample were designed to optimize the chance that the hypotheses in Section I would be recognizably true:

(1) Deep water.

(2) Availability of continuous wave records.

(3) Stable or slowly increasing significant wave height.

(4) Relatively high steep waves.

(5) Relatively unidirectional wave field (absence of secondary wave trains from other directions).

(6) Availability of data from at least two sites which are within about 1 kilometer of each other in a line parallel to the direction of wave travel.

(7) Direct measurement of water surface.

Most of these specifications for optimum field wave data were also indicated by Lake and Yuen (1978).

The three gage sites selected are summarized in Table 1, which includes location, gage type, water depth, length of record, interval between records, and time between data points. The gage sites are illustrated in Figures 1, 2, and 3. The history of significant wave height and peak spectral period during the samples is shown in Figures 4, 5, and 6. Peak periods are derived from

Table 1. Location and recording information for wave gages.

Location	Date	Time	Gage type	Coordinates	Water depth (m)	Record length (s)	Time between records (s)	Time between data points (s)
South Haven, Mich.	28 Oct. 76	1700-1800 e.s.t.	Waverider buoy	42°27.5' N. 86°21.2' W.	34.0	Continuous		*0.25
Columbia Light, Wash.	17-18 Oct. 79	1000 P.d.t., 17 Oct. to 0600 P.d.t., 18 Oct.	Waverider buoy	46°11.1' N. 124°11.0' W.	57.9	1,024	2,576	0.50
South Pass, La.	17 Aug. 69	1000-1620 c.d.t.	Baylor staff	29°04.8' N. 88°44.6' W.	103.6	Continuous		0.10

Figure 1. Wave gage location map, South Haven, Michigan.

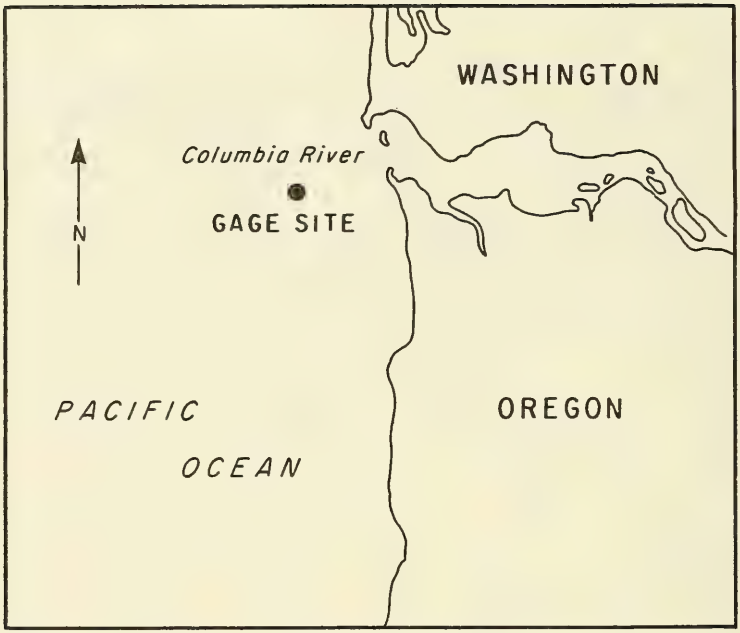

Figure 2. Wave gage location map, Columbia Light, Washington.

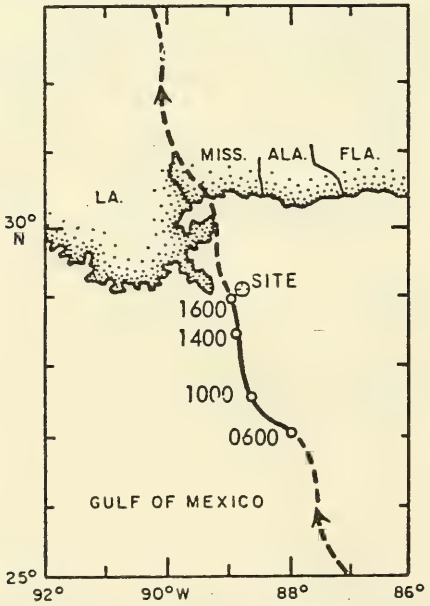

Figure 3. Wave gage location map, South Pass, Louisiana, showing track of Hurricane Camille (from Earle, 1975, copyrighted by the American Geophysical Union).

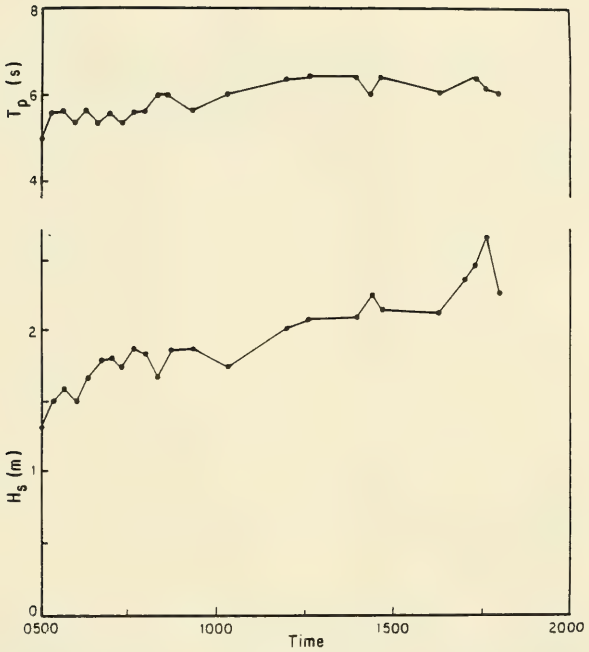

Figure 4. Time history of significant wave height and peak spectral period (from band spectrum with 11 frequencies per band and 0.0107 hertz bandwidth), South Haven, 28 October 1976.

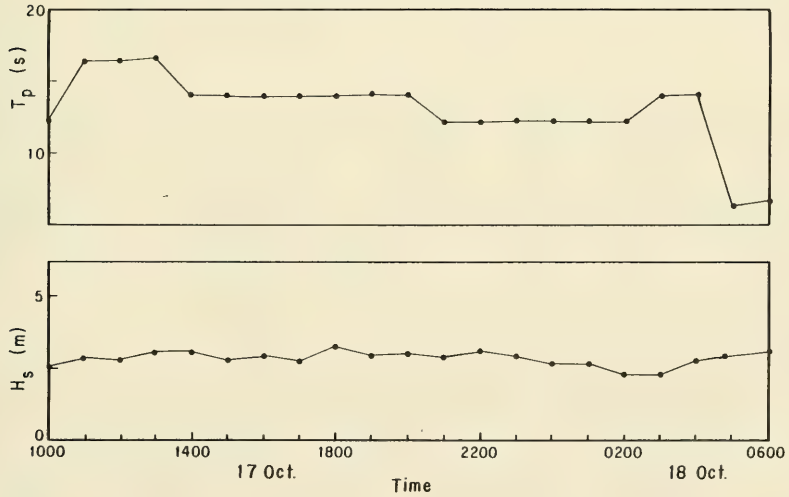

Figure 5. Time history of significant wave height and peak spectral period (from band spectrum with 11 frequencies per band and 0.0107 hertz bandwidth), Columbia Light, 17-18 October 1979.

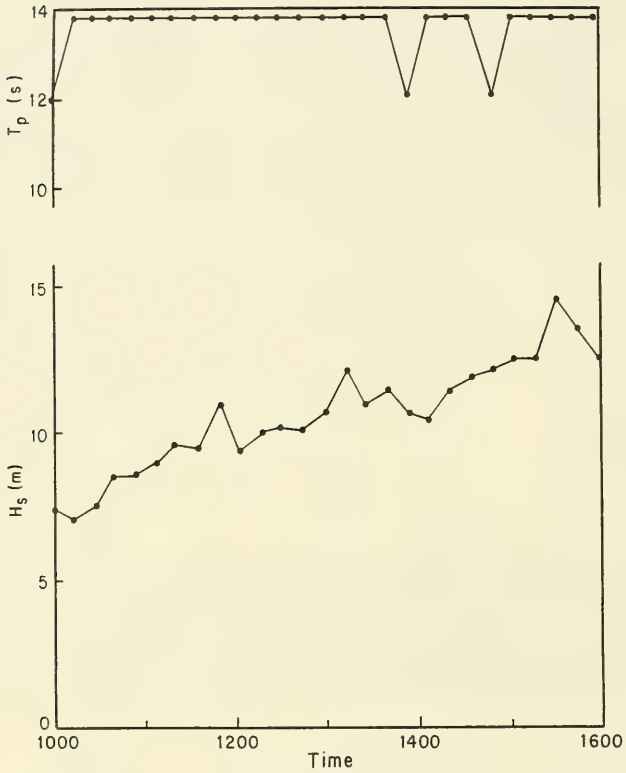

Figure 6. Time history of significant wave height and peak spectral period (from band spectrum with nine frequencies per band and 0.0110 hertz bandwidth), South Pass, 17 August 1969.

band spectra formed by combining variance from a fixed number of adjacent analysis frequencies (see Thompson, 1977, for a more detailed description). Data from Lake Michigan and the Gulf of Mexico fit the above criteria remarkably well, except for criterion (6). The Lake Michigan data also fall short of criterion (7). In fact, it is questionable whether any data sets in the United States meet all specifications.

Meteorological conditions responsible for generating waves in the three samples were quite different. National Oceanic and Atmospheric Administration's (NOAA) Environmental Data and Information Service daily surface weather maps indicated that winds over Lake Michigan on 28 October 1976 were from the south and southwest in response to circulation around a large high-pressure center over Kentucky and southern Illinois (Fig. 7). Although the meteorological condition was not particularly severe, the gage happened to be in a continuous recording mode during the episode. The gage signal had considerable noise contamination during the entire operation at the South Haven site, but a 60-minute sample with relatively little noise was identified for this study.

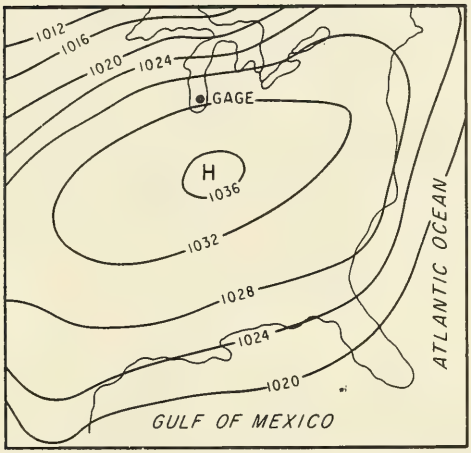

Figure 7. Part of NOAA daily surface weather map, 0700 e.s.t., 28 October 1976.

Winds in the Gulf of Mexico during 17 August 1969 were due to Hurricane Camille which passed almost directly over the gage. The track of the hurricane center is shown in Figure 3. The center was 23 kilometers west of the gage at its nearest point. The data record used in this study was collected on an offshore platform as part of the oil industry's Ocean Data Gathering Program. Patterson (1974) and Earle (1975) have reported on this unique data record. The 60-minute sample selected for detailed analysis in this study represents the highest energy wave conditions, recorded just prior to failure of the gage.

The data sample from the Oregon-Washington coast represents swell generated by circulation around a large low-pressure center located just south of the Aleutian Islands (Fig. 8). The low-pressure center was fairly stationary in this location for several days. Using the known swell period and the distance between the low and the gage (2,400 kilometers), the traveltime between the two points can be estimated coarsely as 60 hours (U.S. Army, Corps of Engineers, Coastal Engineering Research Center, 1977). Thus, the circulation shown in Figure 8 for 1700 P.d.t., 14 October 1979, was almost certainly responsible for generating the swell measured along the U.S. coast on 17 October 1979. Figure 9 shows evidence of a low-pressure system approaching the measurement site but these local winds did not visibly affect waves until after 1600 P.d.t. on 17 October. Many comparable swell episodes are probably available from this gage. This particular episode was selected because it was well documented as a result of another unrelated, unpublished study.

The west coast data sample is least effective of the three field data samples in meeting desired criteria; the data were taken in relatively shallow water compared with the other samples. The data are not continuous, waves are not steep, and criteria (6) and (7) are unfulfilled. However, the waves are expected to be very well focused in direction. The waves have been free from direct wind action for a long time. Any fundamental instability operating on the waves can be expected to have asserted itself after such a long time, a

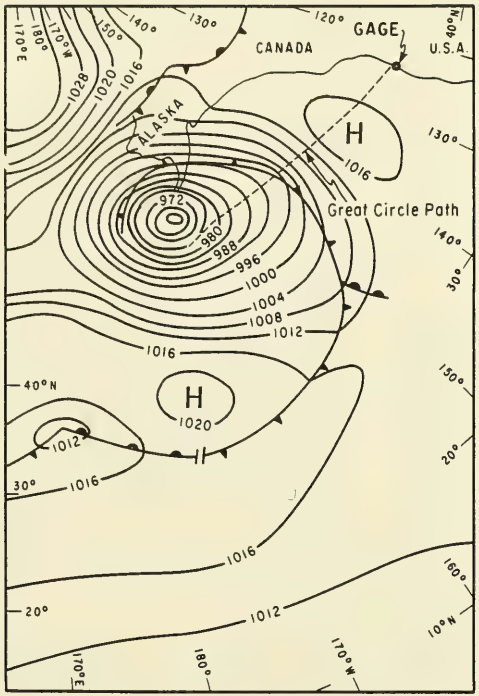

Figure 8. Surface weather map covering northern Pacific Ocean, 1700 P.d.t., 14 October 1979 (from NOAA, National Weather Service).

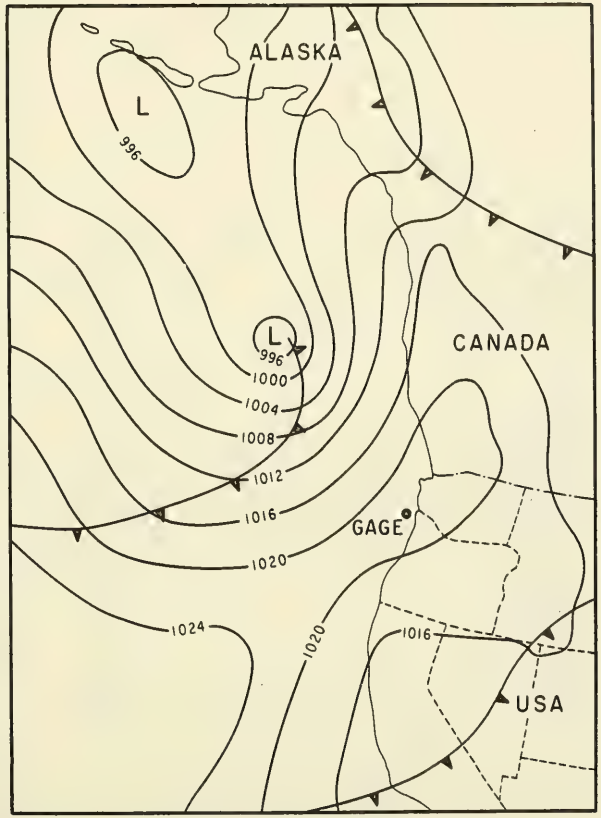

Figure 9. Surface weather map covering northeastern Pacific Ocean, 1400 P.d.t., 17 October 1979 (from NOAA, National Weather Service).

situation which may provide conditions well outside the scope of the BF instability. Similarly, the waves can be expected to be more organized spatially and modulation processes would be operating over relatively long time scales. This reasoning is qualitatively supported by the time series which show evidence of very long modulation periods. The advantage to be gained from such a data sample is that a record with a given length (e.g., 512 seconds) is very likely stationary in terms of any underlying modulation phenomenon. Because the modulation time scale is large, the 40-minute gap between 1,024-second records is not expected to be a severe shortcoming, provided the modulation time scale is short enough to be identifiable in the record. The stationarity of the meteorological system generating the waves also helps to justify this expectation.

IV. ANALYSIS PROCEDURES

1. Data Editing.

The first step in the analysis of field records is editing the data. Although the field records selected for this study were relatively free of signal contamination, past experience has indicated that field records should be checked for data points excessively far from the mean and for large differences between successive data points (Thompson, 1974). These checks identify the electronic contamination occasionally found in field records. Bad data points are defined in this study as points more than 5.0 standard deviations from the mean and successive points which differ by more than 2.5 standard deviations. Bad points are removed from the record and replaced with points obtained by interpolation between good points.

2. Component Frequencies, Amplitudes, and Phases.

a. Background Discussion of Fourier Transform Techniques. Frequency components of a time-series record were initially estimated from a fast Fourier transform (FFT) computer program following the development of Harris (1974). Let the finite time series with zero mean be represented as

$$\begin{aligned} y &= y(n\Delta t) \ , \ n = 1, 2, 3, \ldots, N \\ |y(n\Delta t)| &\leq L \end{aligned} \tag{5}$$

where Δt is the constant time interval between data points, N the number of data points, and L a finite constant. The time series can be represented as a sum of N linearly independent, bounded functions

$$y(n\Delta t) = \sum_{i=1}^{N} c_i f_i(n\Delta t) \tag{6}$$

where c_i is a constant and f_i a known function.

Since ocean waves have a quasi-periodic form, it seems sensible to choose periodic functions for the f_i in equation (6). If the trigonometric functions are used, equation (6) becomes

$$y(n\Delta t) = \sum_{m=1}^{N/2} (a_m \cos \sigma_m n\Delta t + b_m \sin \sigma_m n\Delta t) \tag{7}$$

where a_m and b_m are constants and σ_m a known frequency. It is necessary to pick the frequencies, σ_m, to cover the range of frequencies expected in the wave record. Computational labor may be reduced by choosing frequencies which give rise to orthogonal functions. This set of frequencies is defined as

$$\sigma_m = \frac{2\pi m}{N\Delta t} \tag{8}$$

where $N\Delta t$ is the duration of the record.

The time series is then represented as

$$y(n\Delta t) = \sum_{m=1}^{N/2} \left(a_m \cos \frac{2\pi mn}{N} + b_m \sin \frac{2\pi mn}{N} \right) \tag{9}$$

$$a_m = \left(\frac{2}{N}\right) \sum_{n=1}^{N} y(n\Delta t) \cos\left(\frac{2\pi mn}{N}\right), \quad 1 \le m \le \frac{N}{2}$$

$$b_m = \left(\frac{2}{N}\right) \sum_{n=1}^{N} y(n\Delta t) \sin\left(\frac{2\pi mn}{N}\right), \quad 1 \le m \le \left(\frac{N}{2} - 1\right) \tag{10}$$

It is noted in the above that a constant a_o could be defined as

$$a_o = \left(\frac{1}{N}\right) \sum_{n=1}^{N} y(n\Delta t) \tag{11}$$

which is simply the mean value of the time series, taken as zero in this analysis. Also, the value of $b_{N/2}$ is undefined because $\sin 2\pi mn/N$ is identically equal to zero when m is equal to $N/2$.

The set of coefficients a_m and b_m is called the Fourier transform of the time series $y(n\Delta t)$, $n = 1, 2, 3, \ldots, N$. Trigonometric identities can be used to express equation (9) in the form

$$y(n\Delta t) = \sum_{m=1}^{N/2} A_m \cos\left(\frac{2\pi mn}{N} - \phi_m\right) \tag{12}$$

where

$$A_m = \sqrt{a_m^2 + b_m^2}$$

$$\phi_m = \tan^{-1} \frac{b_m}{a_m} \tag{13}$$

When the time series represents sea-surface elevations, the coefficients A_m are fundamentally related to the potential energy in the sea surface as shown by Harris (1974). Hence, the Fourier transform represented in equation (12) is a method for partitioning energy in the sea surface among $N/2$ discrete frequencies.

Harris (1974) applied the Fourier transform in equations (9) and (10) to a simple sinusoidal wave given by

$$y(n\Delta t) = H \cos(\sigma n\Delta t - \phi) \tag{14}$$

where σ is an arbitrary frequency. σ can be expressed in a form comparable to equation (8) as

$$\sigma = \frac{2\pi(\hat{m} + \delta)}{N\Delta t} \quad , \quad -\frac{1}{2} < \delta \leq \frac{1}{2} \tag{15}$$

where $\hat{m}$ and δ are arbitrary constants defining the frequency of the sinusoidal wave. Then the coefficients are given by

$$\begin{aligned} a_m &= \frac{H \sin \pi\delta \cos(\pi\delta - \phi)}{N} \left\{ \frac{1}{\tan[\pi(\hat{m} - m + \delta)/N]} + \frac{1}{\tan[\pi(\hat{m} + m + \delta)/N]} \right\} \\ b_m &= \frac{H \sin \pi\delta \sin(\pi\delta - \phi)}{N} \left\{ \frac{1}{\tan[\pi(\hat{m} - m + \delta)/N]} - \frac{1}{\tan[\pi(\hat{m} + m + \delta)/N]} \right\} \end{aligned} \tag{16}$$

If it is further specified that $\hat{m}$ is not near zero or $N/2$, the expression for a_m and b_m for analysis frequencies near the true frequency can be simplified to

$$\begin{aligned} a_m &\approx \frac{H \sin \pi\delta \cos(\pi\delta - \phi)}{N} \left\{ \frac{1}{\tan[\pi(\hat{m} - m + \delta)/N]} \right\} \\ b_m &\approx \frac{H \sin \pi\delta \sin(\pi\delta - \phi)}{N} \left\{ \frac{1}{\tan[\pi(\hat{m} - m + \delta)/N]} \right\} \end{aligned} \tag{17}$$

It is evident in both equations (16) and (17) that if $\delta \neq 0$, a part of the wave energy will be assigned to all analysis frequencies. Steps can be taken to concentrate this spillover in a narrow band of frequencies containing the true frequency as follows. The function $\tilde{y}(n\Delta t)$ is obtained from the time series as

$$\tilde{y}(n\Delta t) = w(n\Delta t)\, y(n\Delta t) \tag{18}$$

where

$$w(n\Delta t) = \frac{1}{2}\left(1 - \cos\frac{2\pi n}{N}\right) \tag{19}$$

The data window in equation (19) is often called the Tukey window or cosine bell data window. Harris (1974) and others have shown that the spillover is reduced considerably when the function $\tilde{y}(n\Delta t)$ in equations (18) and (19) is analyzed instead of $y(n\Delta t)$.

Substitution of equations (14), (15), and (19) into equation (18) gives

$$\begin{aligned} \tilde{y}(n\Delta t) = \frac{H}{4} \Bigg\{ & 2 \cos\left[\frac{2\pi(\hat{m} + \delta)\, n}{N} - \phi\right] - \cos\left[\frac{2\pi(\hat{m} - 1 + \delta)\, n}{N} - \phi\right] \\ & - \cos\left[\frac{2\pi(\hat{m} + 1 + \delta)\, n}{N} - \phi\right] \Bigg\} \end{aligned} \tag{20}$$

From equation (20) it is clear that the function $\tilde{y}(n\Delta t)$ actually represents a sum of three sinusoidal waves with frequencies differing by one frequency increment $2\pi n/N$. Thus, the partitioning of wave energy in a very narrow band around the true frequency must be less clearly refined when the cosine bell data window is used.

b. Application of Fourier Transform Techniques to Field Data. A computer program based on the FFT algorithm was used to estimate A_m^2 and ϕ_m in equation (13) from field data. The program was applied in the preliminary study of the South Haven data to a 1,024-second record both with and without the cosine bell data window.

The preliminary South Haven analysis indicated that a resolution of at least 0.001 hertz would be needed to resolve detailed concentrations of spectral energy with confidence. It also indicated that detailed spectral characteristics can change considerably over time intervals of less than 5 minutes. The frequency resolution of the FFT analysis is limited by record length, as shown in equation (8), so it is impossible to identify frequencies corresponding to major energy concentrations to an accuracy of 0.001 hertz with a 5-minute record using a direct application of the FFT. An alternative analysis approach is needed.

Two approaches for artificially increasing the length of a short record were explored. Although the actual frequency resolution must depend on the length of the data time series, it appeared that the nominally greater resolution produced with an artificially lengthened record might permit a better definition of major peak frequencies. One approach is to pad the record symmetrically with zeros to create a 1,024-second record which contains a much shorter length of actual data.

$$\hat{y}(n\Delta t) = \begin{cases} 0 \ , \ 1 \le n \le \dfrac{M-N}{2} \ , \ \dfrac{M+N}{2} < n \le M \\ y(n\Delta t) \ , \ \dfrac{M-N}{2} < n \le \dfrac{M+N}{2} \end{cases} \tag{21}$$

where M is the total number of points in padded time series; in this case, M = 1,024. In equation (21), n can range from 1 to M where M is greater than N.

Another approach is to periodically repeat the short data record as many times as necessary to create a 1,024-second record.

$$\hat{\hat{y}}(n\Delta t) = y[(n - IN)\,\Delta t] \ , \ IN < n \le (I + 1)\,N \tag{22}$$

where I is an integer. Care was taken in this approach to reasonably match the elevation, $y(\Delta t)$ and $y(N\Delta t)$, and slope, $dy(\Delta t)/dt$ and $dy(N\Delta t)/dt$, at both ends of the short record. However, both the approaches for artificially lengthening the record are capable of generating potentially troublesome spurious peaks in the spectrum and were abandoned.

Another approach to this problem is to compute spectra from partially overlapped time series defined as

$$
\begin{aligned}
y_1(n\Delta t) &= y(n\Delta t) \\
y_2(n\Delta t) &= y[(n + J)\ \Delta t] \\
&\vdots \qquad\qquad \vdots \\
y_i(n\Delta t) &= y\{[n + (i - 1)\ J]\ \Delta t\}\ ,\ J < N
\end{aligned}
\tag{23}
$$

Differences between successive spectra computed by this approach can be attributed to the nonoverlapped sections of record; hence, frequency constituents of a short section of record can be inferred. The approach produced inconsistent results and was abandoned.

Another difficulty identified in preliminary FFT analysis was the variability of spectral phases, ϕ_m in equation (13), between adjacent frequencies which appeared in the amplitude spectrum to be part of a single spectral peak. Phase relationships in the spectrum certainly cannot be studied unless an unambiguous phase value can be assigned to each concentration of energy in the detailed spectrum. Tests with sinusoidal waves were analyzed to more clearly identify what was happening to phases. Tests with a single sinusoidal component indicated a gradual variation of phase up to the spectral peak, a jump in phase of π radians at the peak, and a gradual variation on the other side of the peak.

The same behavior can be demonstrated analytically from equation (17) for a single sinusoidal wave. δ, ϕ, and $\hat{m}$ in equation (17) are fixed for a given sinusoidal time series. Hence, a_m and b_m can change only in response to changes in $\tan \pi(\hat{m} - m + \delta)/N$ as m varies. However, $\tan \pi(\hat{m} - m + \delta)/N$ changes gradually with m over the entire range $1 \leq m \leq N$. As m approaches $\hat{m}$ from below, $\tan \pi(\hat{m} - m + \delta)/N$ is positive but approaches zero. If $0 < \delta \leq 1/2$, $\tan \pi(\hat{m} - m + \delta)/N$ becomes less than zero when $m = \hat{m} + 1$, although it is still very small in magnitude. If $-1/2 < \delta < 0$, the change of sign in the tangent function occurs when $m = \hat{m}$. Thus, both a_m and b_m in equation (17) change sign when $m = \hat{m}$ or $m = \hat{m} + 1$, depending on the value of δ. When ϕ_m in equation (13) is computed over an interval of 2π, the change in sign of both a_m and b_m near the spectral peak appears as an abrupt phase shift of π.

More insight on spectral phase can be obtained by substituting equation (17) into equation (13) to get

$$
\phi_m = \pi\delta - \phi \tag{24}
$$

which is correct only for values of m very close to $\hat{m}$. Since $-1/2 < \delta \leq 1/2$, the phase estimates returned by the FFT analysis at the spectral peak can differ from the correct value ϕ by as much as $\pi/2$. This behavior is illustrated in Figure 10 for an artificial signal composed of three sinusoidal waves. It is clear that the FFT phase estimate is determined by equation (24), and it can differ greatly from the actual phase of the component waves.

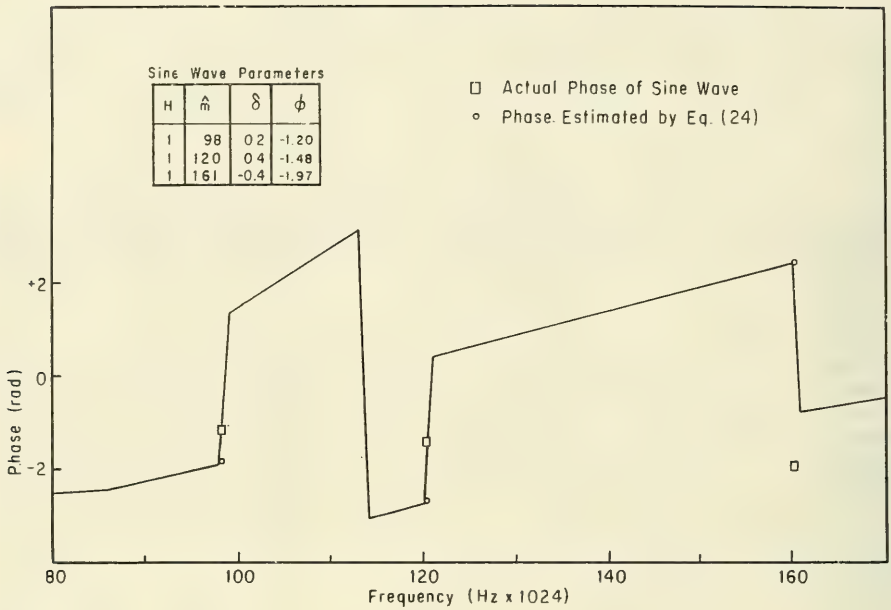

Figure 10. Phase versus frequency from FFT analysis of artificial signal composed of three sinusoidal waves, with N = 4,096 and Δt = 0.25 second.

The phase variations which can be induced by FFT analysis are thus considerable. Spectral phases calculated when the cosine bell data window is used are equally if not more variable. Harris' (1974) analysis for a single sinusoidal wave indicates three successive phase shifts of π radians at three adjacent analysis frequencies surrounding the true peak when the cosine bell window is used. If phases are constrained to an interval of π radians, phases very near the peak are given by equation (24).

These difficulties in producing a reasonably accurate estimate of spectral phase and in getting high resolution in frequency for relatively short records may have been a major factor in leading previous investigators to conclude that spectral components are independent and their phases are random. An essential step in this study was to devise a method for estimating prominent frequencies, amplitudes, and phases, a method free of the above limitations.

c. Multiple Regression Screening Analysis. A technique which appears to give consistent phase information and avoids the direct resolution versus record length trade-off inherent in the FFT is the MRS. Although the MRS has apparently never been applied to ocean wave record analysis, it appears to have real advantages over the FFT analysis for the purposes of this study.

The MRS analysis fits, in the least squares sense, a sum of sinusoids with preassigned frequencies to a given data record. The analysis identifies and

ranks the selected frequencies which explain the maximum amount of variance in the data time series. The first frequency is the one most highly correlated with the data time series. The second frequency, together with the first frequency, explains the maximum amount of variance in the data time series. The third frequency, along with the first and second frequencies, is selected to make the maximum improvement. The selection process is continued until a desired number of frequencies have been selected or until a desired fraction of the variance has been explained. Amplitudes and phases for each selected frequency are recomputed each time a new frequency is selected.

The development of systemmatic screening procedures and application to meteorological problems are briefly reviewed by Harris (1962). The procedures have been adapted for use with ocean wave records (D.L. Harris, Research Scientist, University of Florida, personal communication). A detailed description of the technique used in this study is given in Appendix A.

The MRS technique is well suited for use with a high-speed digital computer. However, the extensive manipulations and memory requirements involved in MRS make it impractical to specify more than about 100 different frequencies. This number is far short of the number of frequencies necessary to obtain a detailed resolution in a field data record of unknown frequency composition.

For this study, field wave records can be efficiently analyzed by using a combination of both MRS and FFT techniques. The FFT analysis with no data window is applied first to a record approximately 15 minutes long to identify the general range of frequencies encompassing the high-energy concentrations. Then the MRS analysis is used with a coarse-toothed comb of 88 equispaced frequencies covering the high-energy range. This configuration was modified slightly for analysis of the Columbia Light records in that only 60 equispaced frequencies were used to span the high-energy range and the additional 28 frequencies were used to cover a range at twice the frequency of the high-energy range. The frequency spacing ranged from 0.0004 hertz for Columbia Light to 0.002 hertz for South Pass. A second MRS analysis used a series of fine-toothed combs centered on the frequencies ranked highest in the first MRS analysis. A third MRS analysis was used when needed to obtain an accuracy of between 0.0001 and 0.0002 hertz. The MRS was applied to a 1,024-second record at South Haven, a 512-second record at Columbia Light, and a 600-second record at South Pass, although the analysis procedures impose no inherent restrictions on record length.

The MRS program is set up to print a summary of selected constituents at each step in the analysis. Thus, each time a new frequency constituent, ω_i, is selected and the corresponding β_i and α_i in equation (A-13) in Appendix A have been computed, a printed display of A_i and ϕ_i in equation (A-14) and ω_i is provided for all ω_i selected thus far. The display was used to subjectively decide how many constituents should be retained from each analysis, as follows. In the initial part of each run the amplitude and phase of each selected constituent changed very little as constituents were added. However, eventually a constituent was added which was nearly identical in

frequency to one previously selected. This usually resulted in an unreasonably large increase in amplitude and a large phase change for the previously selected constituent as an interference pattern was set up between the two frequencies. Such occurrences are considered an artifact of the attempt to fit a particular field record. Since they destroy amplitude and phase information for previously selected constituents, it is expected that they can only obscure any meaningful physical processes. Therefore, the constituent which gave rise to the first such occurrence and all subsequently selected constituents were ignored.

Between 10 and 21 constituents were retained in each MRS analysis which, in the final run, accounted for between 53 and 81 percent of the variance in the field data. Figure 11 illustrates how the explained variance increases as more constituents are added for one South Haven record. The figure also illustrates the improved effectiveness of the constituents as their frequencies are tuned in successive MRS runs. Figure 12 shows similar results for one Columbia Light record.

The veracity of constituents returned by the MRS was tested by analyzing an artificial 512-second record made up of three fundamental frequencies and their second and third harmonics (Table 2). Frequencies used in the first MRS run were intentionally offset from the true frequencies. The second MRS run included frequencies nearly identical to the true frequencies. The MRS analysis returned excellent estimates of both amplitude and frequency for the three fundamentals (Fig. 13). In all three cases the MRS points plotted closest to the actual constituents were from the second MRS run. Second harmonic frequencies were also included in the MRS and were successfully identified for two of the three frequencies, as indicated in the figure. The frequency line spacing from the standard FFT analysis of a 512-second record (Fig. 13) clearly indicates that MRS allows a frequency resolution superior to FFT analysis.

The absence of MRS constituents near the second harmonic of the middle actual frequency in Figure 13 bears further discussion. This second harmonic has the smallest amplitude of the three included in the artificial record. MRS eventually selected a constituent appropriate to this second harmonic, but the selection occurred after the normal termination point. Similarly, it is expected that the MRS analysis of field records will omit some constituents which may be important in identifying structure in the records. However, it also seems clear that dominant constituents will be properly identified and retained.

Phases returned from MRS analysis of the artificial record were within 4° of the actual phases of the fundamentals (Fig. 14). The ability to identify a meaningful phase, demonstrated in the figure, is a vast improvement over the uncertainty in phase obtained in FFT analysis.

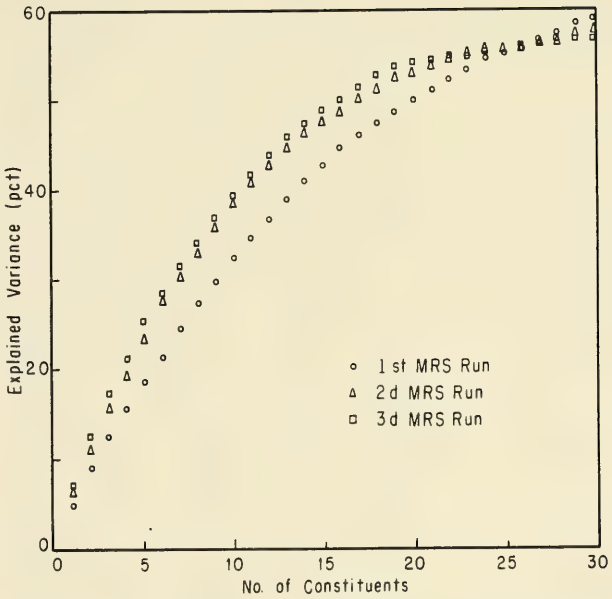

Figure 11. Variance as a function of number of constituents from MRS analysis, South Haven, 1,024-second record starting at 1700 e.s.t., 28 October 1976.

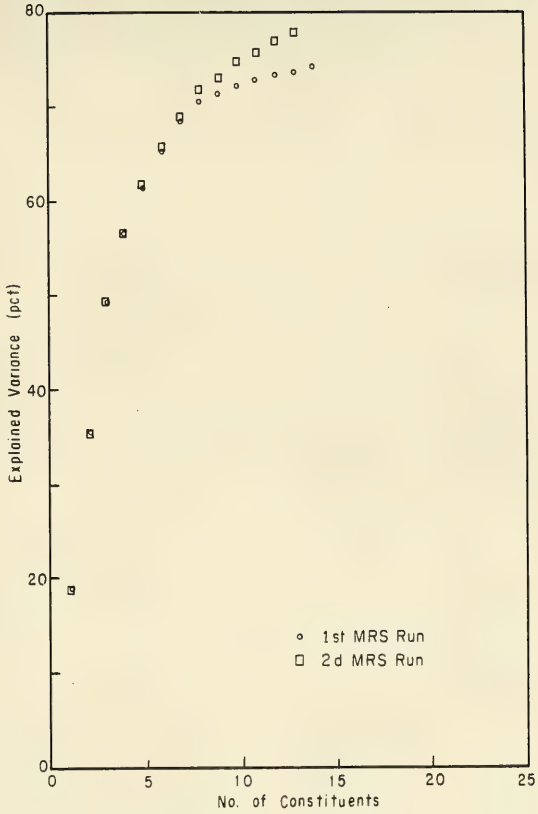

Figure 12. Variance as a function of number of constituents from MRS analysis, Columbia Light, 512-second record starting at 1300 P.d.t., 17 October 1979.

Table 2. Constituents used in creating artificial record.

Amplitude (cm)	Frequency (Hz)	Phase (°)
41	0.0607	331°
13	0.1215	331°
4	0.1822	331°
32	0.0633	103°
10	0.1267	103°
3	0.1900	103°
58	0.0661	19°
16	0.1323	19°
5	0.1984	19°

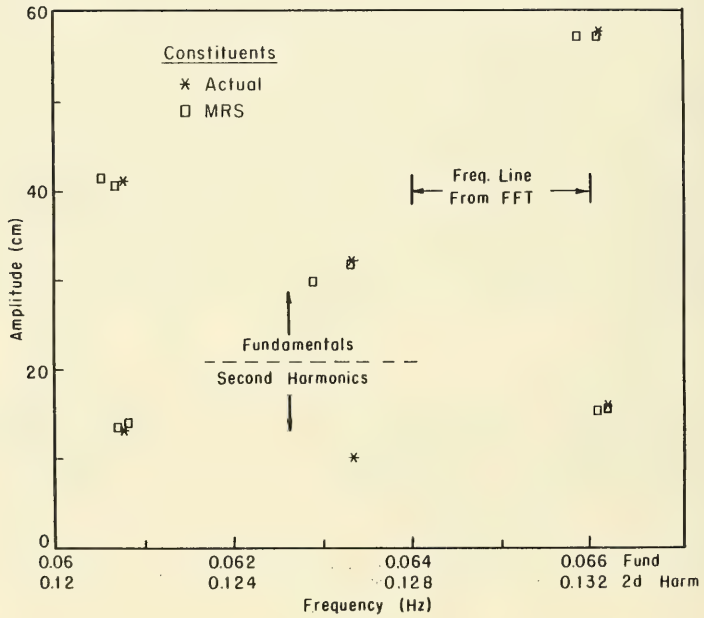

Figure 13. Amplitude versus frequency of constituents from MRS analysis of artificial signal with nine sinusoidal components (see Table 2); the artificial signal represented a 512-second record with points at 0.5-second intervals.

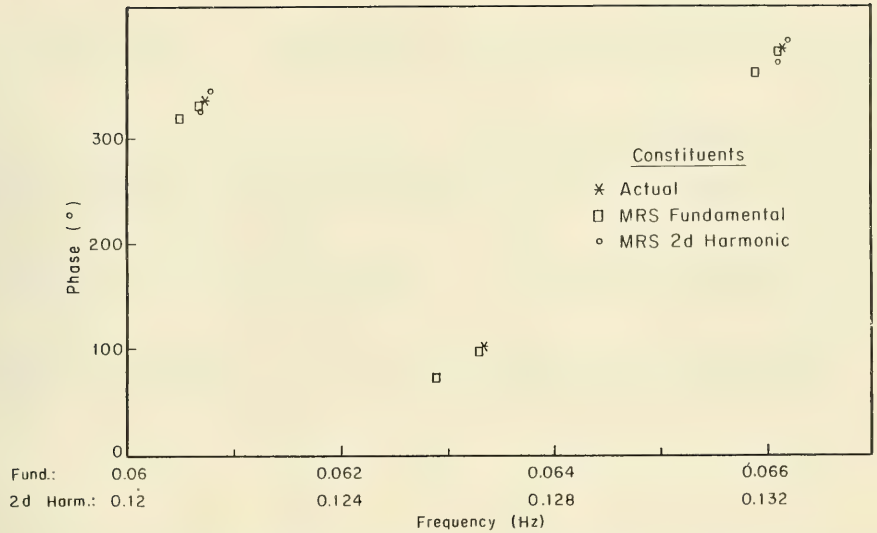

Figure 14. Phase versus frequency of constituents in Figure 13.

A further test of MRS analysis applied to actual field records was obtained by recombining constituents to create a synthesized time series. If the MRS constituents are faithful indicators of major components of the field record, the synthesized time series must resemble the field data time series. Plots of actual and synthesized time series are given in Appendix B.

It is concluded that MRS analysis is indeed a useful tool for identifying and quantifying major constituents in a field wave record.

3. Wave Groups.

The MRS technique described previously provides information on the specific frequency constituents which most effectively represent a data time series. A crucial part of this study is to relate this information to wave grouping characteristics of the time series. Since there is no completely satisfactory technique currently available for identifying field wave grouping characteristics, three different techniques were used. All three techniques were set up as well-defined but quasi-objective procedures.

The first technique is based on the concept of a wave group as a small area of sea surface containing relatively high energy. Groups are identified in a time-series record as sections of the record in which the local variance is high relative to the variance of the whole record. Fluctuations in local variance can provide information on both the intensity and the time scale of wave grouping in the time series.

Another simple statistic indicative of wave grouping is obtained by defining heights and periods for individual waves in the time series. The autocorrelation between successive wave heights is indicative of any tendency for

both high waves and low waves to occur in succession. The autocorrelation between wave periods can be helpful in identifying a tendency for the grouping of periods.

A third technique used previously by some investigators to identify modulation characteristics in a time series involves a spectral analysis of the squared time series. The spectrum shows strong modulation frequencies explicitly if they exist. It can also provide an indication of the strength of modulation.

The three techniques used to investigate field wave grouping characteristics are described in more detail in the following paragraphs.

a. Local Variance Time Series. The basic starting point in this analysis is a time series of sea-surface elevations as given in equation (5). The first point in a new time series is created by computing the variance of the first I points in the original time series,

$$Z(\Delta t) = \frac{1}{I} \sum_{i=1}^{I} y^2(i\Delta t) - \left[\frac{1}{I} \sum_{i=1}^{I} y(i\Delta t)\right]^2 , \quad I < N \tag{25}$$

The second point in the new time series is the variance of the second through the (I + 1)'th original points. The n'th point in the new time series is

$$Z(n\Delta t) = \frac{1}{I} \sum_{i=n}^{I+n} y^2(i\Delta t) - \left[\frac{1}{I} \sum_{i=n}^{I+n} y(i\Delta t)\right]^2 , \quad I + n \leq N \tag{26}$$

where $Z(n\Delta t)$ is the new time series and I a constant. $Z(n\Delta t)$, n = 1, 2 ..., (N - I) represents the time variation of local variance and will be referred to as the Local Variance Time Series (LVTS).

The constant I must be chosen so wave groups will be evident in the LVTS. If I is too small, the LVTS fluctuates erratically with a period on the order of the period of large waves in the original time series. If I is too large, high wave groups are smeared out in the LVTS. After some experimentation, a value of I was chosen to approximate the number of data points in two repetitions of the peak spectral period from the original time series, $y(n\Delta t)$. Sedivy's (1978) and Nelson's (1980) studies of statistical properties of wave groups used the same LVTS approach including the same criteria for choosing I. Both investigators used a systemmatic approach to determine that the optimum I is twice the peak spectral period.

The LVTS is processed by computer procedures developed for use with time series of sea-surface elevation. The mean is removed

$$z(n\Delta t) = Z(n\Delta t) - \frac{1}{N - I} \sum_{i=1}^{N-I} Z(i\Delta t) \tag{27}$$

where $z(n\Delta t)$ is the LVTS with mean removed. The standard deviation is computed

$$\sigma_z^2 = \frac{1}{N - I} \sum_{n=1}^{N-I} z^2(n\Delta t) \tag{28}$$

where σ_z is the standard deviation of LVTS. All peaks and valleys in the LVTS are identified and their positions in time are retained. Small, inconsequential peaks and valleys are then deleted with a computer algorithm described in Appendix C and in Thompson (1980). Peaks and valleys smaller than one standard deviation, σ_z, are deleted. The remaining peaks and valleys are useful indicators of the occurrence of wave groups, although even these must be reviewed in conjunction with the original time series, $y(n\Delta t)$, to best identify groups of high waves.

The LVTS can be used to define a simple parameter which is indicative of the extent of wave grouping in a record. The dimensionless parameter

$$G = \frac{\sigma_z}{\sigma_y^2} \tag{29}$$

where G is grouping parameter, σ_y^2 the variance of $y(n\Delta t)$; n = 1, 2, ..., N, represents the ratio of the standard deviation of the LVTS (which is in units of length squared) to the variance of the original time series (which also is in units of length squared). G is small for a record of reasonably high, uniform waves and relatively large for a record containing well-defined groups of high waves. The grouping parameter defined in equation (29) is believed to be similar in practice to a parameter defined by Funke and Mansard (1979), but equation (29) is preferred in this study for reasons discussed in Section II.

b. Autocorrelation. The use of autocorrelation requires the definition of individual waves in the original time series. The computer algorithm (see App. C) is used to identify meaningful crests and troughs in the original time series, $y(n\Delta t)$. Wave height is defined as the difference in elevation between a crest and preceding trough. Wave period is defined as the time difference between successive troughs. The autocorrelation between wave heights is computed as

$$R_H^2(\tau) = \frac{\left[\sum_{j=\tau+1}^{J} H(j)\, H(j-\tau)\right]^2}{\sum_{j=\tau+1}^{J} H^2(j) \sum_{j=1}^{J-\tau} H^2(j)} \tag{30}$$

where

$R_H(\tau)$ = autocorrelation between wave heights

τ = lag between wave heights (number of waves)

$H(j)$ = difference between height of j'th wave and the mean wave height for the record

J = number of waves in record

Similarly, the autocorrelation between wave periods is

$$R_T^2(\tau) = \frac{\left[\sum_{j=\tau+1}^{J} T(j)\, T(j-\tau)\right]^2}{\sum_{j=\tau+1}^{J} T^2(j) \sum_{j=1}^{J-\tau} T^2(j)} \tag{31}$$

where $R_T(\tau)$ is the autocorrelation between wave periods and $T(j)$ the difference between period of the j'th wave and the mean period for the record.

Wave amplitude is defined as the absolute value of the elevation difference between a crest or trough and the mean elevation for the record. An autocorrelation between amplitude can also be computed as

$$R_A^2(\tau) = \frac{\left[\sum_{j=\tau+1}^{2J} A(j)\, A(j-\tau)\right]^2}{\sum_{j=\tau+1}^{2J} A^2(j) \sum_{j=1}^{2J-\tau} A^2(j)} \tag{32}$$

where $R_A(\tau)$ is the autocorrelation between wave amplitudes and $A(j)$ the difference between j'th amplitude and the mean amplitude for the record.

c. Squared Time Series. Another approach to the study of wave grouping involves the analysis of the squared time series

$$\overset{o}{y}(n\Delta t) = y^2(n\Delta t) \quad , \; n = 1, 2, 3, \ldots, N \tag{33}$$

The squared time series, $\overset{o}{y}(n\Delta t)$, can be subjected to the standard FFT analysis with no data window. The spectrum obtained from $\overset{o}{y}(n\Delta t)$ for a Columbia Light record is shown in Figure 15. Wave groups, produced by interference between nearby frequencies in the original time series, appear as very low frequency energy in the spectrum of the squared time series. A potential difficulty with this approach arises because higher apparent frequencies are created in squaring the time series. Energy at very high frequencies can, through aliasing, distort the low-frequency part of the spectrum of the squared time series.

A better definition of important very low frequencies and their associated amplitudes and phases can be obtained by MRS analysis. This approach was used for added insight in one case.

V. RESULTS

1. Component Amplitudes and Phases.

The MRS analysis has been applied to selected time series from the three field sites. A summary of the analyses is given in Table 3, including record length, number of constituents retained from MRS analysis, percent variance in the time series explained by the constituents, percent variance explained by the first 10 constituents, and number of constituents at second harmonic frequencies. The MRS was more effective at explaining variance in the Columbia Light and South Pass records than in the South Haven records. At least one second harmonic constituent was selected in every Columbia Light analysis.

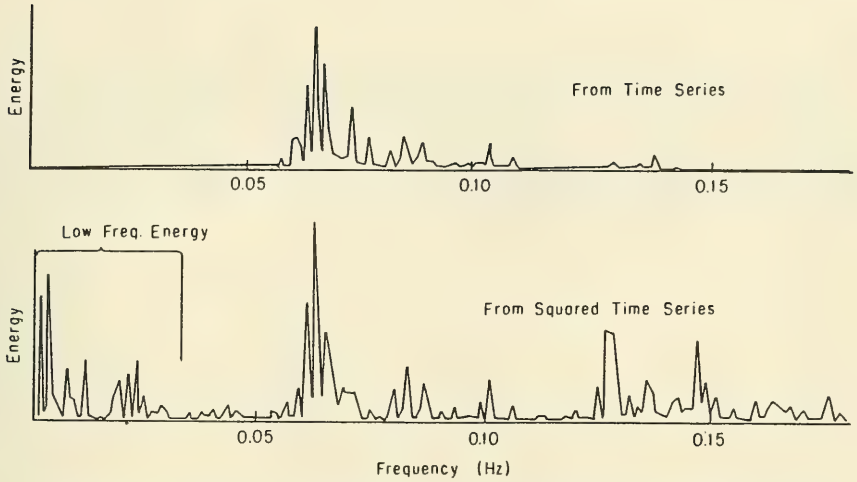

Figure 15. Spectra computed from time series and squared time series, Columbia Light, 1,024-second record starting at 1300 P.d.t., 17 October 1979.

Table 3. Summary of MRS analysis from three field sites.

Starting time			Record length	No. of constituents	Pct variance explained	Pct variance explained by 1st 10 constituents	No. of constituents at 2d harmonic frequency
(hr)	(min)	(s)	(s)				
South Haven (28 October 1976)							
17	00	00	1,024	19	53.9	39.5	-[1]
17	20	00	1,024	21	58.3	41.4	-[1]
17	40	00	1,024	18	53.3	39.8	-[1]
Columbia Light (17 October 1979)							
13	00	00	512	13	78.2	75.0	4
13	08	32	512	17	79.7	71.3	3
14	00	00	512	--[2]	----[2]	----[2]	-[2]
14	08	32	512	15	81.0	74.8	5
15	00	00	512	17	78.6	67.2	5
15	08	32	512	14	74.9	69.0	4
13	00	00	1,024	18	71.8	59.4	1
South Pass (17 August 1969)							
15	00	00	600	19	75.8	59.2	3
15	10	00	600	18	79.5	69.2	3
15	20	00	600	18	74.5	60.3	3
15	30	00	600	12	67.7	64.5	0
15	40	00	600	10	68.0	68.0	0
15	50	00	600	19	80.9	61.6	4

[1] No second harmonic frequencies used in these MRS runs.

[2] Analysis not completed due to difficulties in computer runs.

To display the MRS constituents in detail, the constituent amplitudes for each record were squared to be representative of wave energy. They were then normalized by the total of all squared amplitudes in the record and plotted as a function of frequency (Figs. 16 to 29). The band spectrum, computed with cosine bell data window which best matches the times for MRS analysis, is also shown in each figure. The band spectrum is formed by combining variance from a fixed number of adjacent analysis frequencies.

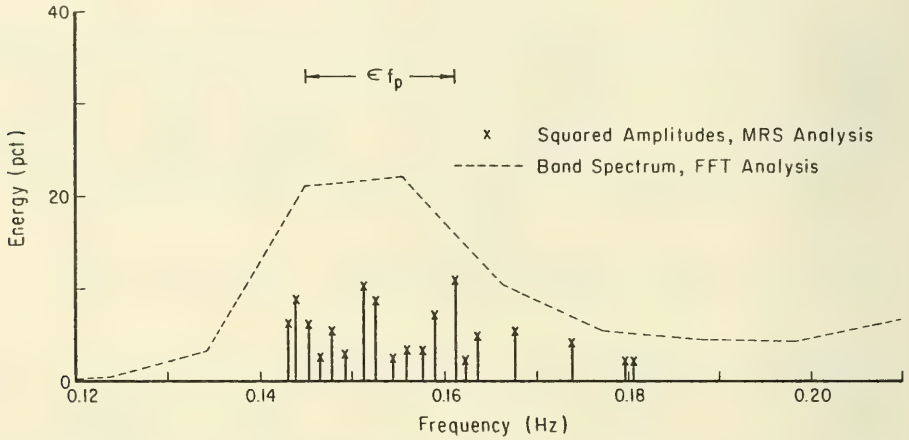

Figure 16. Energy versus frequency for South Haven, 1,024-second record starting at 1700 e.s.t. σ_y = 57.91 centimeters, f_p = 0.1514 hertz, ε = 0.107, εf_p = 0.0162 hertz.

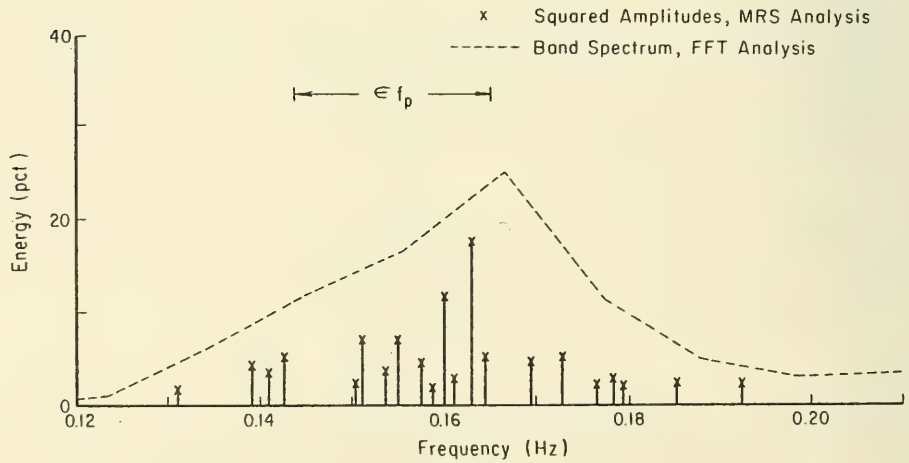

Figure 17. Energy versus frequency for South Haven, 1,024-second record starting at 1720 e.s.t. σ_y = 61.27 centimeters, f_p = 0.1631 hertz, ε = 0.131, εf_p = 0.0214 hertz.

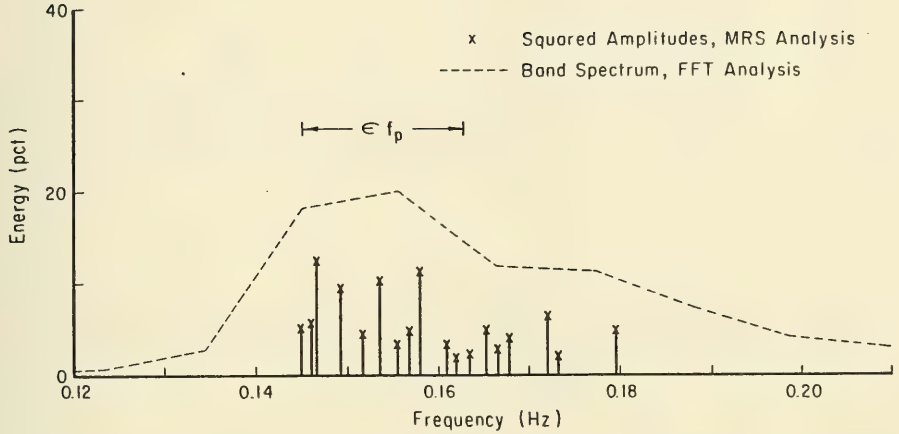

Figure 18. Energy versus frequency for South Haven, 1,024-second record starting at 1740 e.s.t. σ_y = 66.14 centimeters, f_p = 0.1494 hertz, ϵ = 0.119, ϵf_p = 0.0178 hertz.

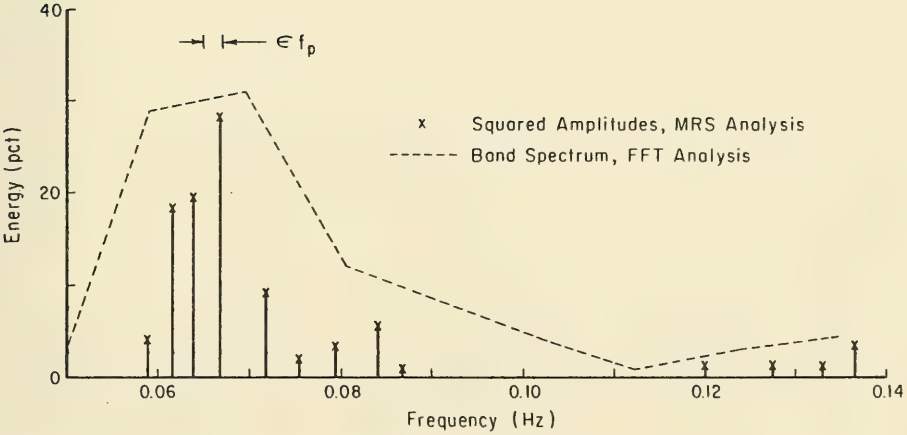

Figure 19. Energy versus frequency for Columbia Light, MRS analysis of 512-second record starting at 1300 P.d.t., and FFT analysis of 1,024-second record starting at 1300 P.d.t. σ_y = 75.25 centimeters, f_p = 0.0635 hertz, ϵ = 0.030, ϵf_p = 0.0019 hertz.

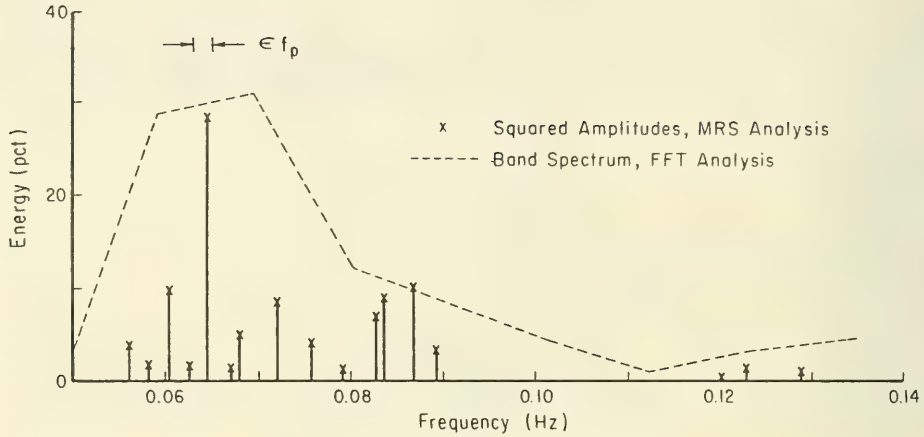

Figure 20. Energy versus frequency for Columbia Light, MRS analysis of 512-second record starting at 1308.5 P.d.t., and FFT analysis of 1,024-second record starting at 1300 P.d.t. σ_y = 75.25 centimeters, f_p = 0.0635 hertz, ε = 0.030, εf_p = 0.0019 hertz.

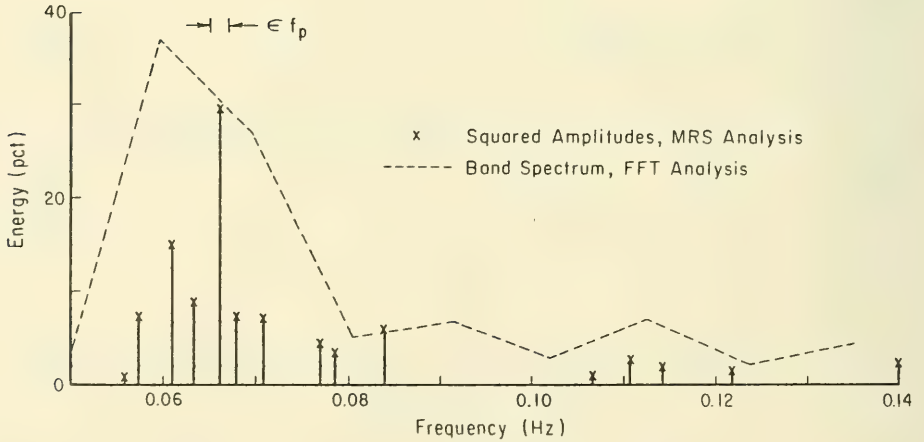

Figure 21. Energy versus frequency for Columbia Light, MRS analysis of 512-second record starting at 1408.5 P.d.t., and FFT analysis of 1,024-second record starting at 1400 P.d.t. σ_y = 75.25 centimeters, f_p = 0.0654 hertz, ε = 0.031, εf_p = 0.0020 hertz.

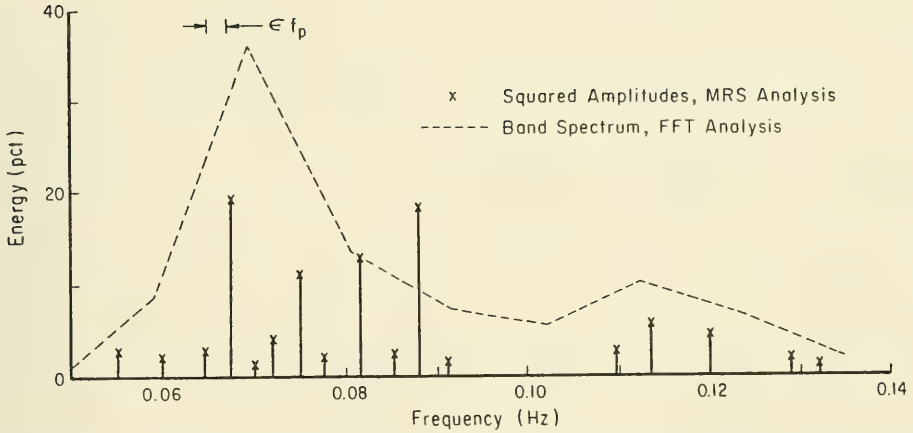

Figure 22. Energy versus frequency for Columbia Light, MRS analysis of 512-second record starting at 1500 P.d.t., and FFT analysis of 1,024-second record starting at 1500 P.d.t. σ_y = 68.50 centimeters, f_p = 0.0684 hertz, ε = 0.030, εf_p = 0.0021 hertz.

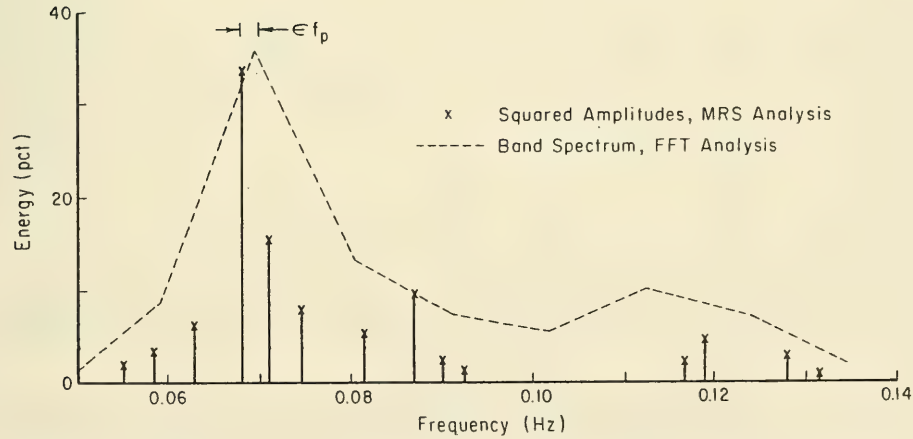

Figure 23. Energy versus frequency for Columbia Light, MRS analysis of 512-second record starting at 1508.5 P.d.t., and FFT analysis of 1,024-second record starting at 1500 P.d.t. σ_y = 68.50 centimeters, f_p = 0.0684 hertz, ε = 0.030, εf_p = 0.0021 hertz.

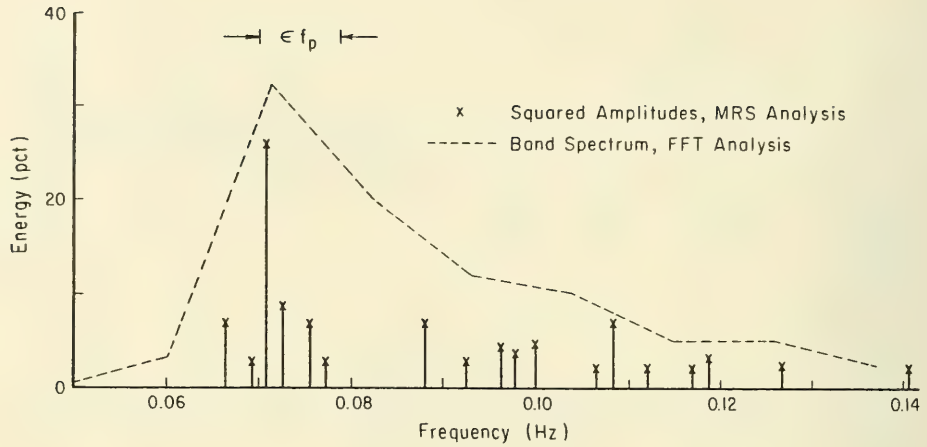

Figure 24. Energy versus frequency for South Pass, MRS analysis of 600-second record starting at 1500 c.d.t., and FFT analysis of 819-second record starting at 1503.3 c.d.t. σ_y = 303.3 centimeters, f_p = 0.0708 hertz, ε = 0.122, εf_p = 0.0087 hertz.

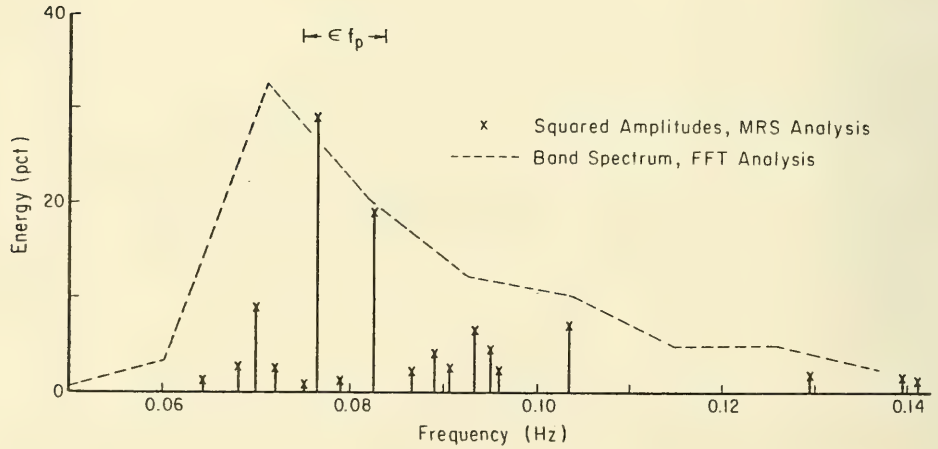

Figure 25. Energy versus frequency for South Pass, MRS analysis of 600-second record starting at 1510 c.d.t., and FFT analysis of 819-second record starting at 1503.3 c.d.t. σ_y = 303.3 centimeters, f_p = 0.0708 hertz, ε = 0.122, εf_p = 0.0087 hertz.

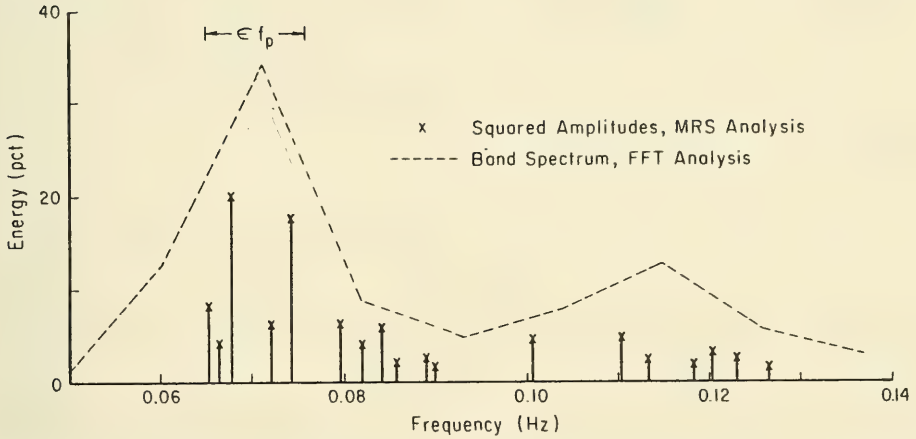

Figure 26. Energy versus frequency for South Pass, MRS analysis of 600-second record starting at 1520 c.d.t., and FFT analysis of 819-second record starting at 1517 c.d.t. σ_y = 324.0 centimeters, f_p = 0.0745 hertz, ε = 0.145, εf_p = 0.0108 hertz.

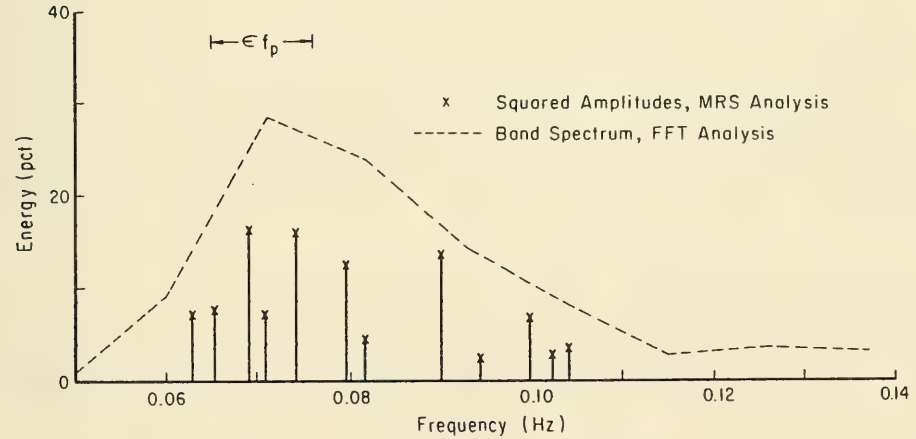

Figure 27. Energy versus frequency for South Pass, MRS analysis of 600-second record starting at 1530 c.d.t., and FFT analysis of 819-second record starting at 1530.7 c.d.t. σ_y = 324.0 centimeters, f_p = 0.0745 hertz, ε = 0.145, εf_p = 0.0108 hertz.

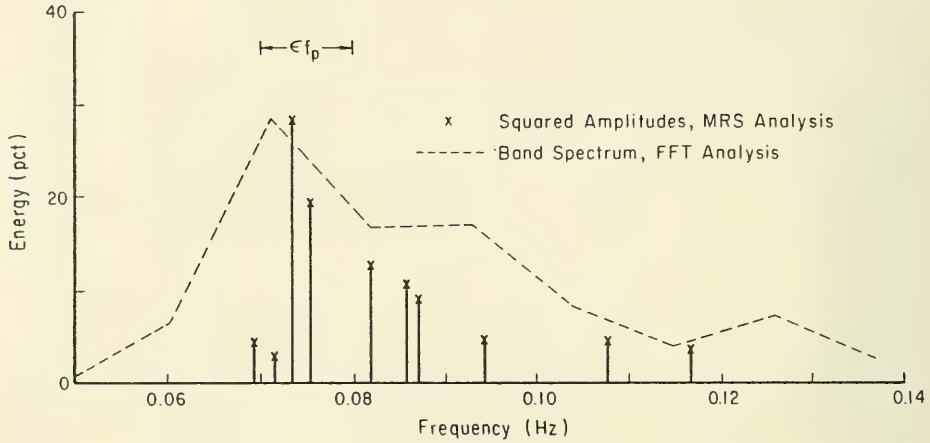

Figure 28. Energy versus frequency for South Pass, MRS analysis of 600-second record starting at 1540 c.d.t., and FFT analysis of 819-second record starting at 1544.4 c.d.t. σ_y = 346.8 centimeters, f_p = 0.0720 hertz, ε = 0.145, εf_p = 0.0104 hertz.

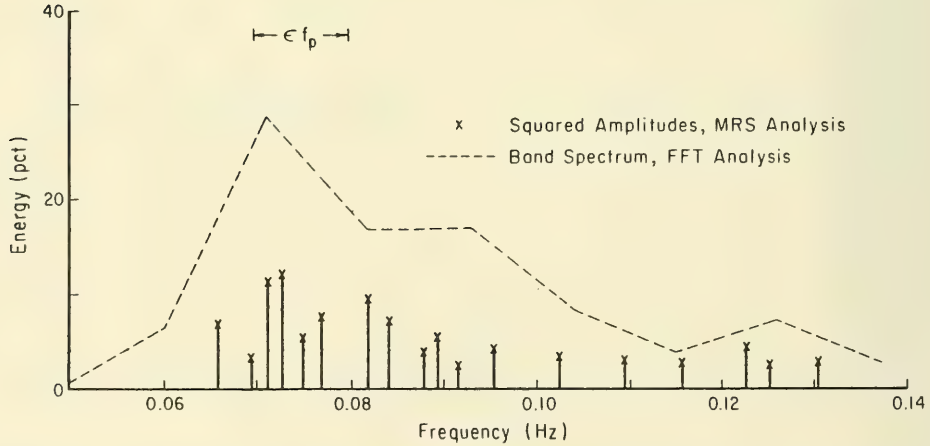

Figure 29. Energy versus frequency for South Pass, MRS analysis of 600-second record starting at 1550 c.d.t., and FFT analysis of 819-second record starting at 1544.4 c.d.t. σ_y = 346.8 centimeters, f_p = 0.0720 hertz, ε = 0.145, εf_p = 0.0104 hertz.

The range of frequencies considered in the initial MRS analysis of each record is generally comparable to the plotted frequency range. The range is 0.131 to 0.214 hertz for South Haven, 0.054 to 0.090 hertz and 0.112 to 0.139 hertz for Columbia Light, and 0.052 to 0.226 hertz for South Pass. The spacing between analysis frequencies in the initial MRS run was 0.00096 hertz (South Haven), 0.0006 hertz (Columbia Light), and 0.002 hertz (South Pass).

Deepwater wave steepness, ε, can be estimated by using

$$\begin{aligned} \varepsilon &= ak_o \\ a &= 2\sigma_y \end{aligned} \tag{34}$$

and the dispersion relation governing waves of small steepness

$$k_o = \frac{(2\pi)^2}{g} f_p^2$$

where

a = significant wave amplitude

f_p = peak spectral frequency

k_o = deepwater wave number corresponding to peak frequency f_p

g = acceleration due to gravity

Wave steepness was estimated for each record using a value of f_p corresponding to the highest peak of harmonics (not grouped into bands) of the FFT spectrum which best matches the times for MRS analysis. FFT spectra are computed from 1,024-second records for South Haven and Columbia Light and 819.2-second records for South Pass. Values of ε were estimated by equation (34) for South Haven and South Pass. A similar procedure was used to estimate ε for Columbia Light except that linear theory was used to estimate shallow-water wave number, k, in place of k_o in the equation. Although the waves at South Pass are not strictly in deep water, the error induced by using the deepwater wave number is a maximum of about 3 percent.

Values of σ_y, f_p, ε, and εf_p are given with each figure (Figs. 16 to 29). The range of frequency covered by εf_p is positioned graphically in each figure above some high-amplitude constituents. εf_p is a rough indicator of the frequency spacing between constituents for Columbia Light. For the other two locations, εf_p spans a large range relative to the frequency spacing between constituents.

A plot of phase (App. A, A-14) versus frequency for each constituent from the South Haven data shows strong evidence of a trend for decreasing phase with increasing frequency (App. D, Fig. D-1). The phase axis in the figure is stretched to cover several cycles of 360°. This stretching was suggested quite clearly in the data as can be seen by the numerous points included in each 360° cycle. The amplitudes of the constituents were ranked from highest to lowest and the rank is noted beside each point in the figure. Much of the

scatter in the figure is due to the lower amplitude constituents. There is also a surprising consistency in slope among the three records analyzed.

Similar plots of phase versus frequency for Columbia Light are shown in Appendix D, Figures D-2 to D-7. Phases associated with second harmonic frequencies are indicated by an x and a double-valued horizontal scale is used. The figures give evidence of a trend for slow decrease in phase with increasing frequency.

Plots of phase versus frequency for South Pass are shown in Appendix D, Figures D-8 to D-13. Most of the figures indicate a coarse trend for decreasing phase with increasing frequency over the main energy-containing frequencies (0.06 to 0.11 hertz); however, two figures (Figs. D-8 and D-13) indicate the opposite trend.

Most of the phase versus frequency plots for all three sites indicate a general trend for decreasing phase with increasing frequency. However, a comparison of initial and final MRS analyses for each record reveals a strong tendency for increasing phase with increasing frequency over very small frequency intervals. This tendency is shown in Figure 30 for one Columbia Light record. The dashline in the figure has a large positive slope between the two square symbols nearest the points labeled 6, 3, 2, 1, 4, 8, 5, 10, and 12. The same tendency is evident in Figure 14 for a synthesized record.

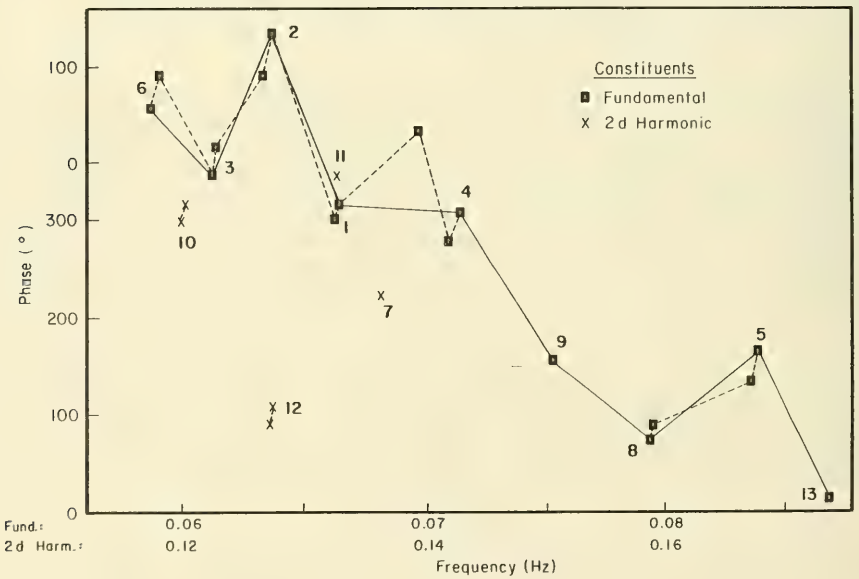

Figure 30. Phase change with frequency in successive MRS analyses at Columbia Light, 1300 to 1308.5 P.d.t., 512-second record analyzed. Numbers indicate amplitude rank for constituents.

Plots of each field data time series analyzed with the MRS program and the synthesized time series obtained by recombining the constituents are included in Appendix B. Each field record with the corresponding synthesized record is shown together on a single page for a visual comparison. The vertical elevation scale is meaningful for relative elevations in a record but not in an absolute or mean sense.

2. Wave Groups.

The LVTS (eq. 26), described previously, was computed and processed for records from the three sites. The record lengths used are 1,024 seconds for Columbia Light and 1,200 seconds for South Haven and South Pass. Major peaks and valleys from the LVTS are plotted versus time in Appendix E. The magnitude of the peaks and the time between peaks are erratic. The modulation period

$$T_{mod} = \frac{1}{\varepsilon f_p} \tag{35}$$

and the variance of the original time series, σ_y^2, are shown to scale on each plot for reference.

The grouping parameter, G (eq. 29) is listed with each plot in Appendix E. The range of grouping parameters is comparable at all three sites. Grouping parameters are also given in Table 4, including G values from a larger sample of data from Columbia Light and South Pass.

Individual wave heights were estimated by the procedures described in the previous section for all three sites, using 1,024-second records for Columbia Light and 1,200-second records for South Haven and South Pass. The autocorrelation between heights (eq. 30) is given in Table 5 for up to three lags. Autocorrelations are generally greater than zero at the first lag and are in most cases highest for South Haven. Very few of the records show any evidence of positive autocorrelation beyond the first lag. The autocorrelations between periods (eq. 31) and between amplitudes (eq. 32) are given in Tables 6 and 7 for the three sites. There is little evidence of autocorrelation between wave periods.

The height of the highest single wave in each Columbia Light record is plotted in Figure 31 as a function of grouping parameter, G (see eq. 29). Each height is scaled by the significant height for the record, estimated as $4\sigma_y$. The largest height, about twice the significant height, coincides with a high value of G. To provide perspective in the figure, the ratio of highest wave height to significant wave height was calculated from the Rayleigh distribution for the exceedance probability 1/N, where N is the number of waves in the record. N was estimated in two ways for each record: (a) the number of individual waves identified, and (b) the record length divided by peak spectral period. The highest and lowest values of N from all records by either of the two estimates are used in the figure to indicate the range of ratios expected from the Rayleigh distribution. Similar plots for the second and third highest wave heights in each record are given in Figures 32 and 33.

Table 4. Grouping parameter at three field sites.

Date	Time	G
South Haven		
28 Oct. 1976	1700	0.63
	1720	0.79
	1740	0.69
Columbia Light		
17 Oct. 1979	1300	0.67
	1400	0.50
	1500	0.59
	1600	0.54
	1700	0.68
	1800	0.68
	1900	0.65
	2000	0.59
	2100	0.79
	2200	0.56
	2300	0.53
18 Oct. 1979	0000	0.52
	0100	0.65
	0200	0.74
	0300	0.41
	0400	0.42
	0500	0.46
	0600	0.34
South Pass		
17 Aug. 1969	1000	0.55
	1020	0.45
	1040	0.59
	1100	0.57
	1120	0.50
	1140	0.89
	1200	0.53
	1220	0.63
	1240	0.62
	1300	0.68
	1320	0.76
	1340	0.63
	1400	0.48
	1420	0.51
	1440	0.52
	1500	0.60
	1520	0.59
	1540	0.66

Table 5. Autocorrelations between wave heights at three field sites.

Date	Time	Autocorrelation 1 lag	2 lags	3 lags
South Haven				
28 Oct. 1976	1700	0.49	0.09	-0.07
	1720	0.54	0.19	0.01
	1740	0.51	0.20	0.01
Columbia Light				
17 Oct. 1979	1300	0.55	0.34	0.26
	1400	0.21	-0.08	0.06
	1500	0.45	0.14	0.01
	1600	0.09	-0.06	0.18
	1700	0.24	0.04	0.08
	1800	0.47	0.28	0.26
	1900	0.38	0.11	0.06
	2000	0.27	0.00	-0.21
	2100	0.38	-0.12	-0.20
	2200	0.31	-0.12	-0.07
	2300	0.32	-0.01	-0.11
18 Oct. 1979	0000	0.24	-0.04	0.01
	0100	0.41	0.11	0.06
	0200	0.28	0.18	-0.02
	0300	-0.09	0.12	-0.02
	0400	-0.08	0.02	0.01
	0500	-0.03	0.16	-0.09
	0600	-0.07	0.06	-0.14
South Pass				
17 Aug. 1969	1000	0.08	0.04	0.21
	1020	0.08	-0.14	0.16
	1040	0.22	0.09	-0.15
	1100	0.38	0.28	0.12
	1120	0.29	-0.05	-0.16
	1140	0.34	0.06	-0.14
	1200	0.25	-0.07	-0.04
	1220	0.31	0.14	-0.03
	1240	0.35	0.05	-0.15
	1300	0.33	0.07	0.07
	1320	0.49	0.25	0.18
	1340	0.42	0.07	-0.02
	1400	0.19	-0.05	0.01
	1420	0.16	-0.11	-0.21
	1440	0.24	-0.02	-0.03
	1500	0.29	0.11	0.10
	1520	0.21	-0.02	-0.07
	1540	0.37	0.16	-0.01

Table 6. Autocorrelations between wave periods at three field sites.

Date	Time	Autocorrelation 1 lag	2 lags
	South Haven		
28 Oct. 1976	1700	0.11	0.08
	1720	-0.02	-0.01
	1740	-0.01	0.06
	Columbia Light		
17 Oct. 1979	1300	-0.02	-0.02
	1400	0.19	0.14
	1500	0.18	0.12
	1600	0.12	0.02
	1700	0.09	-0.05
	1800	0.12	-0.01
	1900	0.28	0.06
	2000	0.08	0.12
	2100	0.01	-0.05
	2200	0.05	-0.08
	2300	0.01	-0.07
18 Oct. 1979	0000	0.26	-0.02
	0100	0.14	0.03
	0200	0.17	0.02
	0300	-0.06	-0.02
	0400	0.06	-0.08
	0500	0.01	-0.16
	0600	-0.06	0.06
	South Pass		
17 Aug. 1969	1000	0.10	-0.04
	1020	0.14	0.12
	1040	0.20	-0.02
	1100	0.07	0.06
	1120	0.23	-0.01
	1140	-0.10	0.03
	1200	0.17	0.10
	1220	0.01	-0.17
	1240	0.15	0.01
	1300	0.07	-0.17
	1320	0.13	0.08
	1340	0.21	-0.01
	1400	0.08	0.05
	1420	0.04	0.14
	1440	0.11	-0.01
	1500	0.09	0.12
	1520	-0.01	0.14
	1540	0.11	-0.02

Table 7. Autocorrelations between amplitudes at three field sites.

Date	Time	Autocorrelation 1 lag	2 lags	3 lags
	South Haven			
28 Oct. 1976	1700	0.53	0.38	0.15
	1720	0.59	0.39	0.24
	1740	0.37	0.46	0.09
	Columbia Light			
17 Oct. 1979	1300	0.63	0.37	0.29
	1400	0.46	0.12	-0.01
	1500	0.54	0.26	0.16
	1600	0.43	-0.02	-0.15
	1700	0.53	0.16	0.11
	1800	0.56	0.35	0.32
	1900	0.49	0.20	0.18
	2000	0.50	0.20	0.03
	2100	0.57	0.24	0.04
	2200	0.50	0.12	0.01
	2300	0.42	0.18	0.10
18 Oct. 1979	0000	0.52	0.12	0.01
	0100	0.55	0.24	0.16
	0200	0.42	0.15	0.20
	0300	0.10	-0.16	0.11
	0400	0.13	-0.20	0.11
	0500	0.26	-0.20	0.03
	0600	0.29	-0.18	-0.03
	South Pass			
17 Aug. 1969	1000	0.41	0.01	-0.09
	1020	0.41	0.00	-0.18
	1040	0.42	0.07	0.14
	1100	0.45	0.24	0.18
	1120	0.44	0.11	0.01
	1140	0.55	0.24	0.05
	1200	0.46	0.19	0.10
	1220	0.50	0.14	0.11
	1240	0.50	0.24	0.08
	1300	0.49	0.17	0.11
	1320	0.59	0.39	0.24
	1340	0.46	0.26	0.13
	1400	0.39	0.11	-0.06
	1420	0.37	0.09	-0.08
	1440	0.41	0.08	-0.08
	1500	0.41	0.20	0.05
	1520	0.42	0.12	-0.09
	1540	0.50	0.29	0.09

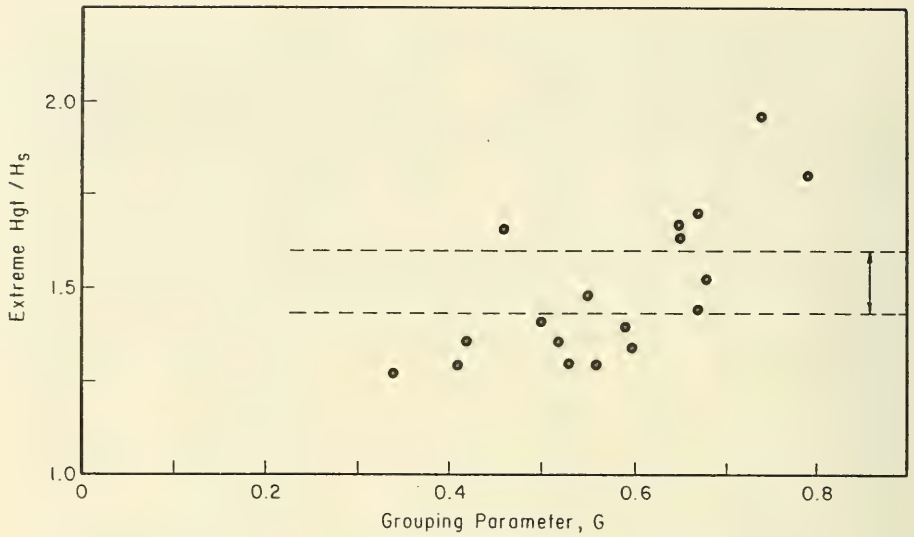

Figure 31. Ratio of highest wave height to significant height versus grouping parameter at Columbia Light, 1300 P.d.t, 17 October to 0600 P.d.t., 18 October 1979; 1,024-second records analyzed for 18 cases. Dashlines indicate range expected from Rayleigh distribution.

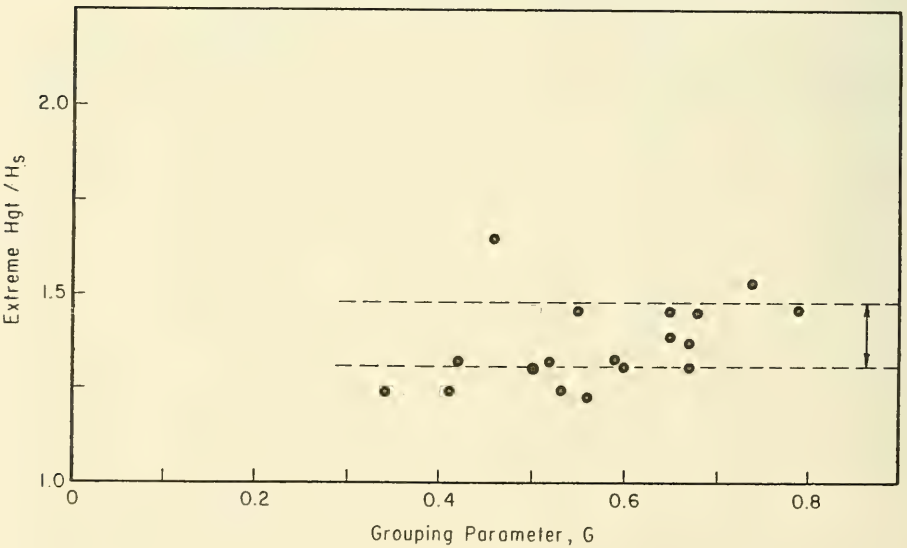

Figure 32. Ratio of second highest wave height to significant height versus grouping parameter at Columbia Light. Dashlines indicate range expected from Rayleigh distribution.

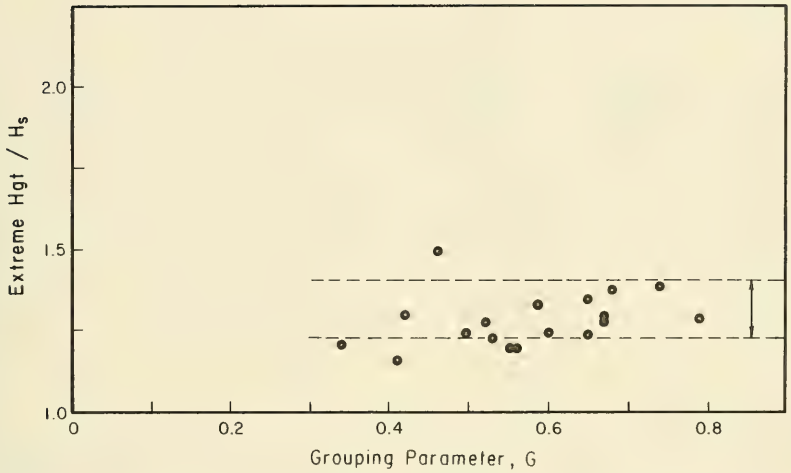

Figure 33. Ratio of third highest wave height to significant height versus grouping parameter at Columbia Light. Dashlines indicate range expected from Rayleigh distribution.

The highest wave height in each South Pass record, scaled by significant height, also shows a tendency to increase with increasing values of G (Fig. 34). The highest height, equal to 2.1 times the significant height, coincides with the highest value of G. Plots of extreme wave height versus G for the second and third highest waves in each South Pass record are given in Figures 35 and 36.

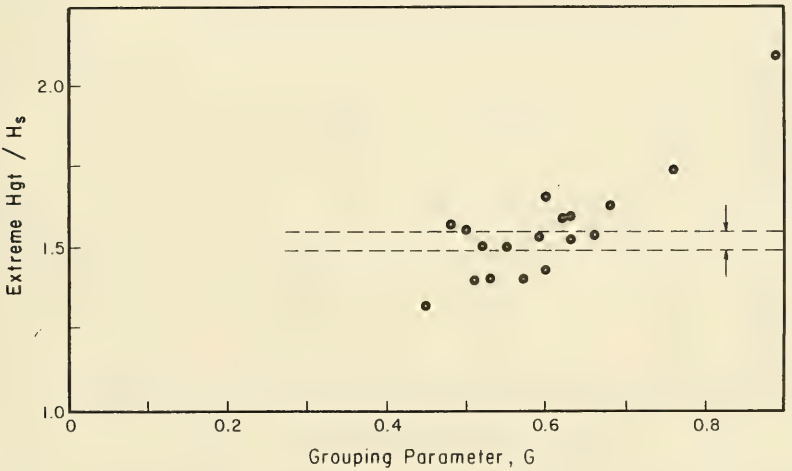

Figure 34. Ratio of highest wave height to significant height versus grouping parameter at South Pass, 1000 to 1600 c.d.t., 17 August 1969; 1,200-second records analyzed for 18 cases. Dashlines indicate range expected from Rayleigh distribution.

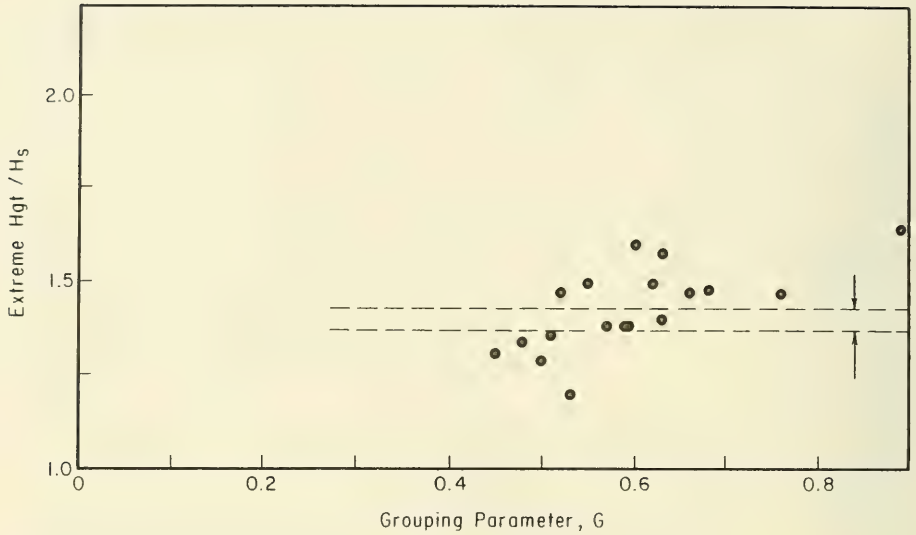

Figure 35. Ratio of second highest wave height to significant height versus grouping parameter at South Pass. Dashlines indicate range expected from Rayleigh distribution.

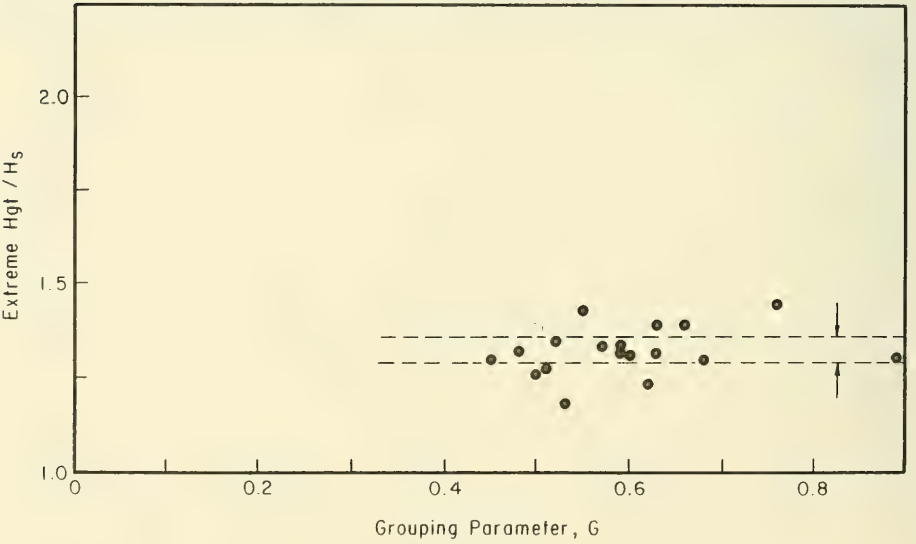

Figure 36. Ratio of third highest wave height to significant height versus grouping parameter at South Pass. Dashlines indicate range expected from Rayleigh distribution.

MRS analysis of the squared time series (eq. 33) was done for one Columbia Light record. The spectrum from the FFT analysis (Fig. 15) shows substantial energy at very low frequencies. The MRS analysis, covering only the very low frequencies, returned the amplitudes and frequencies plotted in Figure 37. The constituents accounted for 29.0 percent of the variance in the squared time series. Phase versus frequency for the squared time series is plotted in Figure 38. The synthesized time series, created by recombining the square roots of the MRS constituents (Fig. 39,a and b), shows clear peaks for times at which the original time series contains groups of high waves.

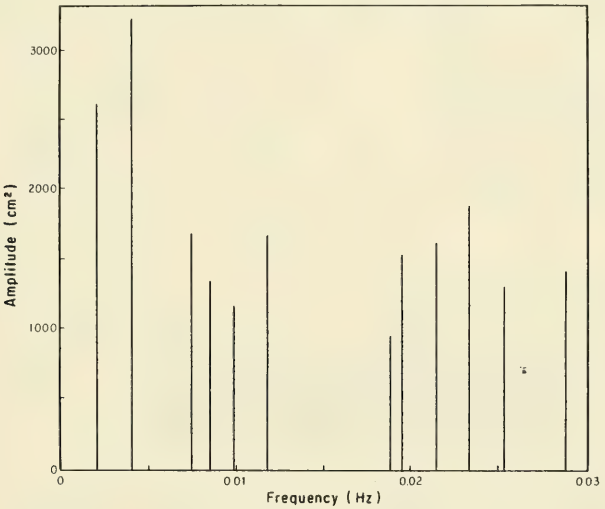

Figure 37. Amplitude versus frequency from MRS analysis of low frequencies in squared time series at Columbia Light, 1300 to 1317 P.d.t., 17 October 1979; 1,024-second record used. Range of frequencies in initial MRS run was 0.0006 to 0.0528 hertz.

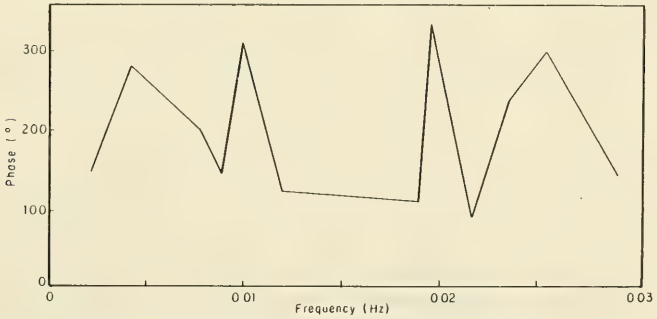

Figure 38. Phase versus frequency from MRS analysis of low frequencies in squared time series at Columbia Light, 1300 to 1317 P.d.t., 17 October 1979; 1,024-second record used.

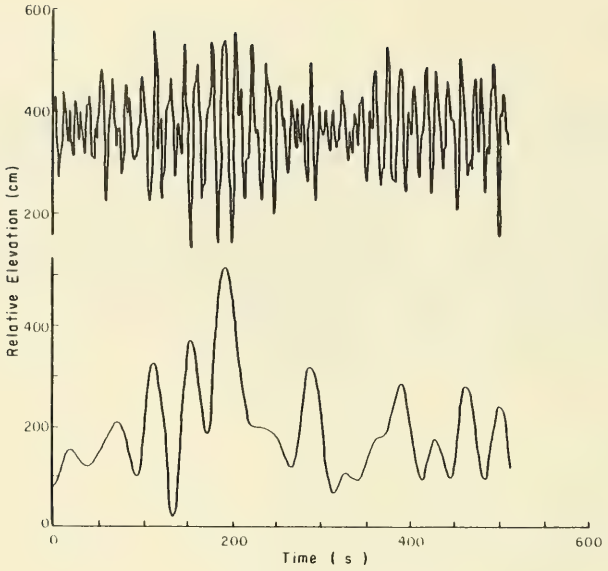

a. 1300 to 1308.5 P.d.t.

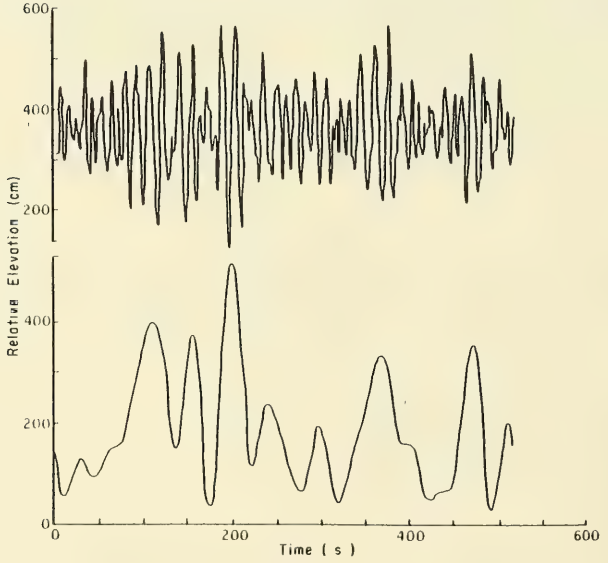

b. 1308.5 to 1317 P.d.t.

Figure 39. Comparison of Columbia Light field data time series (top) with time series synthesized from low-frequency MRS constituents (bottom) for (a) 1300 to 1308.5 P.d.t. and (b) 1308.5 to 1317 P.d.t., 17 October 1979; 1,024-second record used.

VI. INTERPRETATION

Several analyses related to wave grouping characteristics and detailed spectral structure of field wave records were presented in the previous section. The objective of this section is to interpret the analyses, using the six hypotheses in Section I.

The wave data analyzed were taken at sites in three different water bodies: Lake Michigan (South Haven), Pacific Ocean (Columbia Light), and Gulf of Mexico (South Pass). The data represent moderate to high wave conditions with unimodal spectra and reasonably constant significant height and peak spectral period. The data represent actively growing waves at two sites (South Haven and South Pass) and old swell at the third site (Columbia Light). These similarities and differences affect interpretation of the analyses.

Many of the time series selected for analysis show evidence that high waves tend to occur in groups, e.g., the time series for 1720 to 1737 at South Haven, 1300 to 1308.5 at Columbia Light, and 1510 to 1520 at South Pass (App. B). However, there are several notable exceptions in which the high waves do not appear in clear groups, e.g., the time series for 1408.5 to 1417 at Columbia Light and 1500 to 1510 at South Pass. Thus, both grouped and ungrouped time series are considered in the analysis.

The field data time-series plots from South Haven and Columbia Light (App. B) appear to have a few unusually low wave troughs. The tendency for very low troughs may be exaggerated relative to the South Pass time series. There is a possibility that low, sharp troughs result from imperfect response of the Waverider buoy gage to high waves. Since low troughs seem to coincide with groups of high waves, the troughs are not a deterrent to a study of wave groups. However, they may exaggerate the appearance of existing groups.

One procedure presented earlier to aid in identifying wave groups in a time series was the Local Variance Time Series (LVTS) analysis. A comparison of the LVTS in Appendix E with the field data time series in Appendix B for 1300 to 1317 at Columbia Light (a well-grouped record) shows that the peaks of the LVTS effectively indicate the presence of six high wave groups and their location in the time series. Note that each time series plot covers 512 seconds while each LVTS plot covers 1,024 seconds. Similarly, the LVTS peaks for 1540 to 1600 at South Pass (another well-grouped record) indicate the presence and location of high wave groups in the corresponding time series. Both the Columbia Light and South Pass records also gave high values of G and R_H, the two parameters considered indicative of grouping (see Tables 4 and 5).

By contrast, the LVTS for 1400 to 1417 at Columbia Light (a poorly grouped record) indicates few peaks which are high relative to the variance of the original time series. There is also a lack of low valleys in the last half of the LVTS, which indicates that groups are not well separated by low variance sections of record. Values of G and R_H are relatively low for the record. The LVTS for 1500 to 1510 at South Pass (another poorly grouped record) shows an absence of peaks which are high relative to the time-series variance. Values of G and R_H for this record were computed for a 20-minute record which includes some well-grouped waves, so they are not particularly helpful in this case.

Consideration of the above examples leads to the generalization that the LVTS effectively identifies prominent wave groups when they exist in a record. However, the original time series should be checked to verify the existence of the groups, especially if the LVTS shows an absence of peaks which are large relative to the time-series variance. The parameters G and R_H are of some use in identifying the extent of high wave grouping in a record.

To further use the LVTS it is useful to subjectively identify each analyzed field data time series with some evidence of wave groups. A review of Appendix B indicates that all the records suffice except for 1408.5 to 1417 at Columbia Light and 1500 to 1510 at South Pass. Thus attention is focused on Appendix E, Figures E-1 to E-4, E-6, E-7 (the last half), E-8, and E-9. The time between major wave groups is represented by the time between prominent peaks in the LVTS. This time has a clear tendency to be longest in the Columbia Light records and shortest in the South Haven records. The figures indicate considerable variability in this time, but T_{mod}, computed by equation (35) and shown in each figure, is a plausible estimate of a modulation time scale.

Quantitative estimates of modulation time scale for wave groups were extracted from Appendix E by measuring the time between successive peaks in the LVTS, to be referred to as T_{LVTS}. Since small LVTS peaks may not be relevant to dominant modulation processes in a record, they were ignored in estimating T_{LVTS} if the difference in amplitude between a peak and either adjacent trough is less than about 1.5 times the time series variance, σ_y^2.

A plot of T_{LVTS} versus T_{mod} from equation (35) shows considerable scatter (Fig. 40). The South Haven and South Pass data points show evidence of a small tendency for T_{LVTS} to increase with T_{mod}. Further, some of the data points closest to the line for which T_{LVTS} and T_{mod} are equal represent time differences between the larger LVTS peaks. For example, of the six T_{LVTS} values obtained by considering only the two highest peaks of Figure E-8 and the six highest peaks of Figure E-9, four values are within 15 percent of T_{mod}.

T_{LVTS} values for Columbia Light are all less than T_{mod}, although they show a small tendency to be higher than T_{LVTS} values for the other locations. One obvious difficulty in dealing with the Columbia Light data is the magnitude of T_{mod}. If 500-second modulations are truly present, there are only two repetitions in the 1,024-second record. Records continuous more than at least 1 hour are needed to adequately examine the evidence supporting 500-second modulations. The plots in Appendix E certainly do not preclude the existence of 500-second modulations. Of the three T_{LVTS} values obtained by considering only the two highest peaks in Figure E-4 and the three highest peaks in Figure E-6, two values are within 2.5 percent of T_{mod}.

Wave modulation information was summarized by Lake and Yuen (1978) and Longuet-Higgins (1980) as a plot of dimensionless modulation frequency versus wave steepness. A comparable plot using dimensionless T_{LVTS} values determined by the wave period corresponding to peak spectral frequency is given in

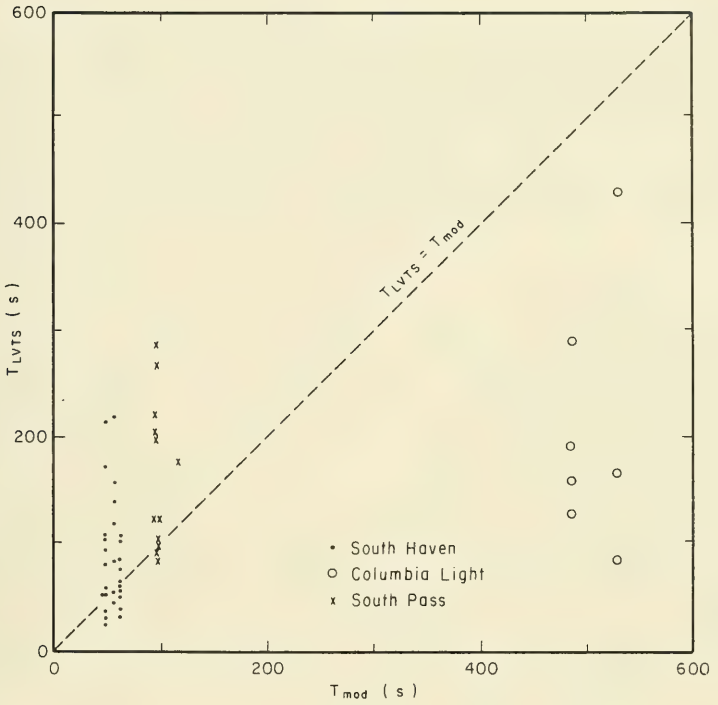

Figure 40. Comparison of modulation period estimated from LVTS and from wave steepness.

Figure 41. The relationships predicted by the BF theory and by Longuet-Higgins (1980) are also shown. Scatter in the field data is greater than in Lake and Yuen's laboratory data. A more definitive comparison of field data and theory is obtained by computing a mean dimensionless modulation frequency for each field record which has five or more T_{LVTS} values. The comparison (Fig. 42) indicates that the field data correspond more closely with the Longuet-Higgins (1980) prediction of modulation frequency than with the BF prediction.

Constituents obtained by MRS analysis of the squared time series for Columbia Light, 1300 to 1317, were presented in Figure 37. Two constituents have considerably higher amplitude than the others. They occur at frequencies to 0.0021 and 0.0042 hertz, corresponding to periods of 476 and 238 seconds. These periods are expected to be indicative of modulation periods in the time series. In fact, the 476-second period is only 10 percent less than T_{mod} from equation (35).

Thus, field evidence from all three locations indicates that waves in deep water sometimes tend to be organized so that high waves occur in groups (Sec. I, hypothesis d) and the modulation period of wave groups is related to wave period and steepness (hypothesis e).

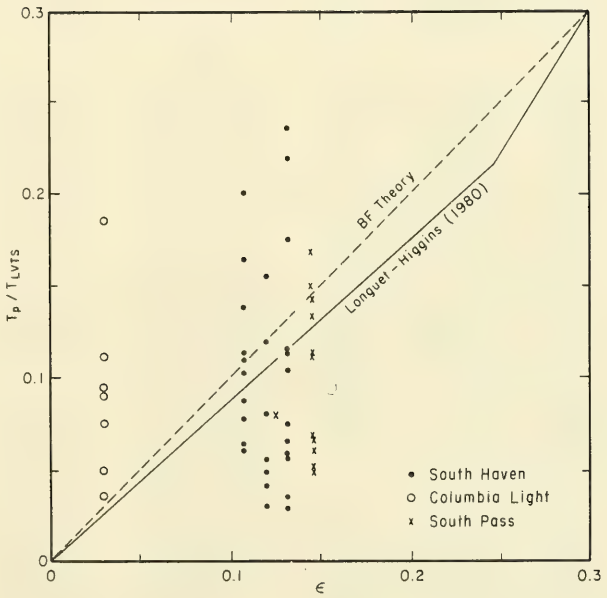

Figure 41. Dimensionless modulation frequency versus wave steepness.

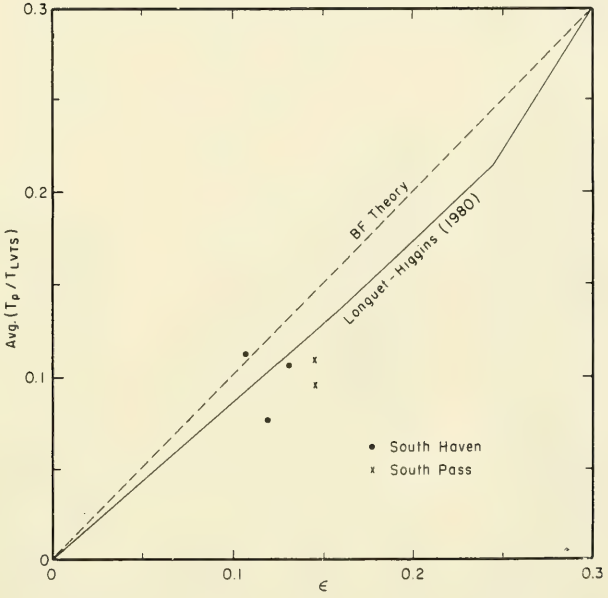

Figure 42. Average dimensionless modulation frequency versus wave steepness; each average was computed from at least five estimates in a single record.

The remaining hypotheses (a, b, c, and f) pertain to the frequency constituents in each field record. The first of two approaches to estimating the constituents was an FFT analysis to produce a band spectrum with 0.011-hertz bandwidth. This procedure is typical of routine field data analysis procedures in use. The second approach was MRS analysis to identify prominent constituents to an accurancy of about 0.0002 hertz. Contrary to FFT analysis, the MRS analysis provides a meaningful phase as well as amplitude for each constituent. A visual comparison of field data time series with time series synthesized from MRS constituents (App. B) indicates that prominent wave grouping characteristics of the field record are also present in the synthesized record.

Figures 16 to 29 indicate how wave grouping is represented in the MRS constituents. In keeping with earlier discussion, Figures 21 and 24 are considered poorly grouped cases. All but two (Figs. 20 and 29) of the remaining figures for Columbia Light and South Pass, considered as reasonably well grouped cases, have two or more prominent constituents which extend well above the 10 percent level. Individual constituents for South Haven are less dominating, so those that extend above the 10 percent level are considered prominent. Frequency spacings, Δf_{MRS}, between each adjacent pair of prominent constituents are tabulated (Table 8). A modulation period, T_{MRS}, can be defined from the MRS analysis as the reciprocal of Δf_{MRS}. T_{MRS} values are also given in the table along with εf_p and T_{mod} (eq. 35). A plot of T_{MRS} versus T_{mod} (Fig. 43), despite considerable scatter, gives some evidence of a relationship between T_{mod} and the spacing between frequency constituents. From Figures 40 and 43, it is evident that T_{MRS} derived from the frequency spacing between constituents is comparable to T_{LVTS}. Figure 43 also indicates a tendency for T_{MRS} to be longer than T_{mod} for actively growing waves.

Table 8. Frequency spacing between prominent constituents from MRS analysis.

Site	Starting time for MRS analysis	Δf_{MRS} (Hz)	εf_p (Hz)	T_{MRS} (s)	T_{mod} (s)
South Haven	1700	0.0100	0.0162	100	62
South Haven	1720	0.0029	0.0214	342	47
South Haven	1740	0.0071	0.0178	141	56
South Haven	1740	0.0044	0.0178	227	56
Columbia Light	1300	0.0024	0.0019	417	527
Columbia Light	1300	0.0028	0.0019	357	527
Columbia Light	1500	0.0074	0.0021	135	485
Columbia Light	1500	0.0068	0.0021	147	485
Columbia Light	1500	0.0064	0.0021	156	485
Columbia Light	1508.5	0.0028	0.0021	357	485
South Pass	1510	0.0062	0.0087	161	115
South Pass	1520	0.0065	0.0108	154	93
South Pass	1530	0.0050	0.0108	200	93
South Pass	1530	0.0055	0.0108	182	93
South Pass	1530	0.0103	0.0108	97	93
South Pass	1540	0.0018	0.0104	556	96
South Pass	1540	0.0066	0.0104	152	96

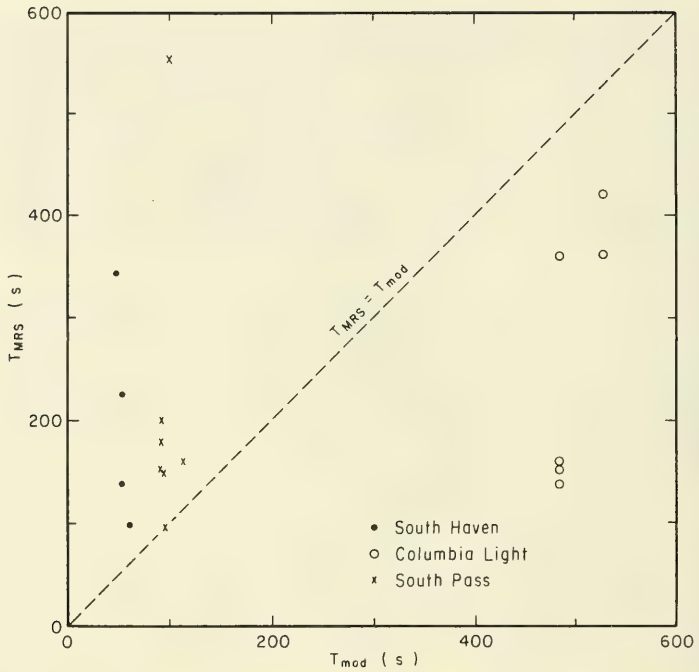

Figure 43. Comparison of modulation period estimated from spacing between MRS constituents and from wave steepness.

The three Columbia Light data points in Figure 43, which fall closest to the 45° line, are from the 1300- and 1508.5-hour records. The corresponding field data time series show evidence of the approximate 400-second modulation indicated by T_{MRS}. The three Columbia Light data points with T_{MRS} approximately equal to 150 seconds are from the 1500-hour record. The corresponding field data time series shows clear evidence of this modulation time scale and no evidence of 400-second modulation. However, the 1508.5-hour record has some evidence of 150-second modulation. Values of T_{MRS} from South Pass are consistently between about 100 and 200 seconds, with one exception. This modulation time scale is consistent with prominent groups in the field data time series. Similarly, T_{MRS} values from South Haven are reasonably consistent with prominent groups in the field data time series.

From an examination of cases in which wave grouping is most clear, it is evident that the MRS analysis represents prominent modulational time scales by identifying two or more high-amplitude constituents separated by a frequency equal to the reciprocal of modulation period. Thus, the extent of wave grouping and the modulation period are related to the energy content and frequency spacing of dominant frequency constituents in a record. The evidence supports hypothesis (e), with the provision that spectral resolution is sufficient to identify constituents involved in the modulation process. Figures 16 to 29 show clearly that a 0.011-hertz bandwidth spectrum masks information on modulation time scales.

Band spectra from Columbia Light and South Pass (Figs. 19 to 29) are quite similar in shape and peak frequency. They are consistent with the standard concept of a smooth, continuous spectrum. However, the significant differences in modulation time scale between the Columbia Light and South Pass records cannot be identified in the smooth spectral curves. Thus, hypothesis (a) must be true, which is that spectral components are sometimes discrete and are not smeared over a broad, continuous spectrum.

It was noted earlier that wave grouping characteristics change over 10-minute intervals in some of the field records. The changes include the appearance and disappearance of noticeable groupings as well as in one case, a large change in modulation time scale. The MRS analyses provide definitive data for comparing the structure of successive time-series records.

The procedure used for comparison was to match prominent constituents in each of the records used in estimating T_{MRS} values (Figs. 16 to 19, 22, 23, and 25 to 28) with constituents in records immediately preceding or following. Constituents for which the frequencies were within about 0.001 hertz of each other were considered matched. Thus, the 1300- to 1308.5-hour and 1308.5- to 1317-hour Columbia Light analyses (Figs. 19 and 20) were compared. Constituents were identified in the second record at about the same frequencies as the three prominent constituents in the first record, and vice versa. Similarly, the Columbia Light MRS analyses in Figures 22 and 23 were compared and matched constituents were identified when they occurred. The South Haven and South Pass MRS analyses were also compared. Most of the prominent constituents could be matched with constituents in preceding or following records. However, the matching constituent is often much lower in amplitude.

It is expected that all the field records contain independent frequency constituents. However, it is also anticipated that they contain some nonindependent constituents which are bound together and are nondispersive. Although both bound and free constituents may be represented in Figures 16 to 29, the process used to select the records and constituents used in estimating T_{MRS} values has favored those constituents which contribute to wave grouping. It is suggested that these constituents are nonindependent.

Phases from MRS analysis associated with constituents matched between records, as discussed above, are plotted in Figure 44. Although the phase of each constituent clearly varies between records, there is a strong indication that phases of the constituents *relative to each other* do not vary between records. In fact, there is evidence in the figure that the relative phases of constituents with similar frequency at South Pass do not vary during the entire 60-minute recording interval. A step further, comparing constituents in the 1300- to 1308.5-hour and the 1508.5- to 1517-hour Columbia Light analyses, reveals additional constituent matches. Relative phases for these constituents from records a full 2 hours apart show an amazing consistency (Fig. 45). Phases for matched constituents from the 1308.5- to 1317-hour analysis are also reasonably consistent, as shown in the figure. The same conclusion is reached from a comparison of relative phase for frequency-matched constituents in the first and last South Haven and South Pass records (Figs. 46 and 47). Since, by chance, the first and last South Pass records were not well grouped, phases for constituents in the 1510- to 1520-hour record which matched constituents in the other two records are also plotted to give further credence to the pattern. This evidence strongly supports the hypothesis that frequency components are sometimes related in a deterministic, nonrandom way (hypothesis b).

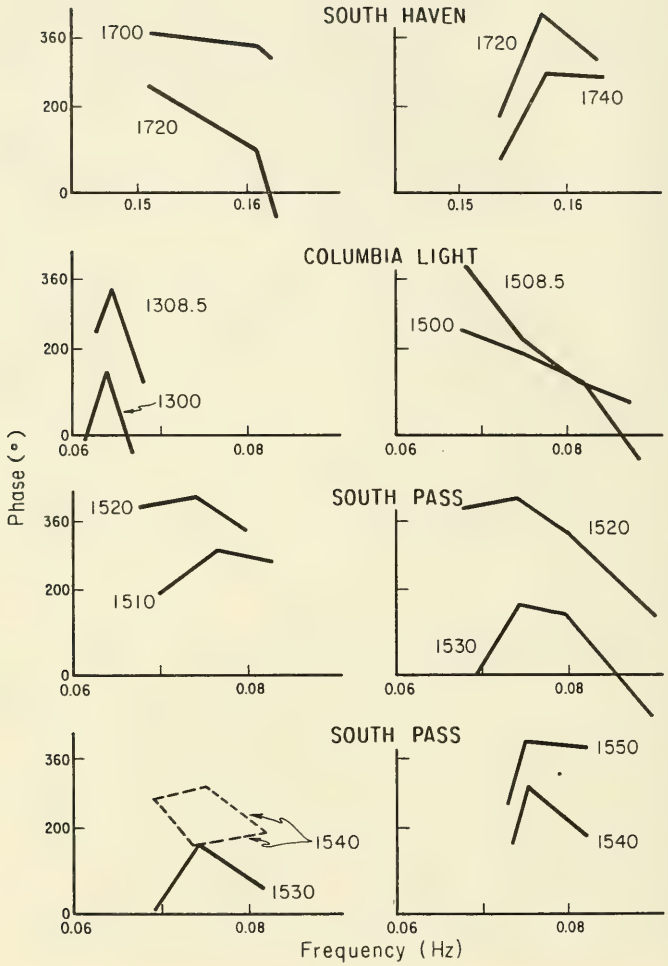

Figure 44. Comparison of phase for frequency-matched high-amplitude MRS constituents from different records; starting time of record is noted beside each curve. Dashed curves indicate an ambiguous case in which two constituents from one record could be matched with one constituent in the other record.

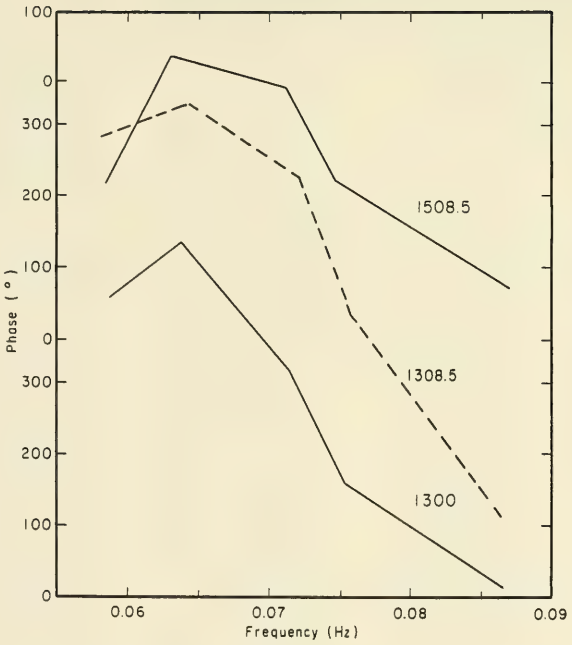

Figure 45. Comparison of phase for all frequency-matched MRS constituents from three Columbia Light records; starting time of record is noted beside each curve.

Figure 46. Comparison of phase for all frequency-matched MRS constituents from two South Haven records; starting time of record is noted beside each curve.

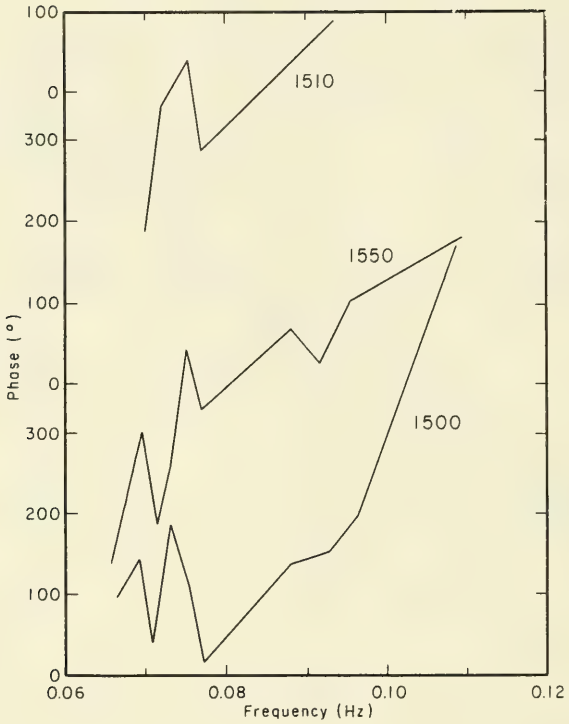

Figure 47. Comparison of phase for frequency-matched MRS constituents from three South Pass records. Uppermost curve represents constituents which match paired constituents from the other two records; starting time of record is noted beside each curve.

The preceding discussion invites some solid speculation. It is suggested that each of the field records examined contains energy at a set of approximately 10, possibly more, discrete frequencies. These well-defined frequency constituents are not independent, but are closely bound together in such a way that their phase relationships relative to each other are nearly invariant in time. The possibility of independent frequency constituents coexisting with bound constituents is not precluded, but the bound system clearly appears to be the major feature, accounting for most of the energy in the field records.

The energy in each of the bound constituents varies tremendously over short time intervals, as evidenced in the records of waves passing fixed gages. The large and rapid variation is associated with striking variations of wave grouping characteristics observed in the time series, variations which have thwarted past attempts to establish empirical relationships for wave grouping in field records.

Because the MRS analysis technique identifies only those constituents containing substantial energy, it can never identify all constituents in the bound set from analysis of one particular record. Some information about important frequencies in the set can be obtained by matching constituents in MRS analyses of successive records, a technique already used to advantage in this study. Although a detailed analysis of available information about the set does not seem warranted, the possibility of a characteristic frequency spacing between bound constituents merits further consideration.

It is assumed that many of the bound constituents in the high energy part of the spectrum are identified in each MRS analysis. The distribution of frequency spacing between successive MRS constituents was estimated from all analyses for each of the three sites (Fig. 48). The range of εf_p values computed for each site is indicated in the figure. The peak of the distribution curve indicates a preferred frequency spacing of about 0.0012 hertz for South Haven, 0.0028 hertz for Columbia Light, and 0.0022 hertz for South Pass.

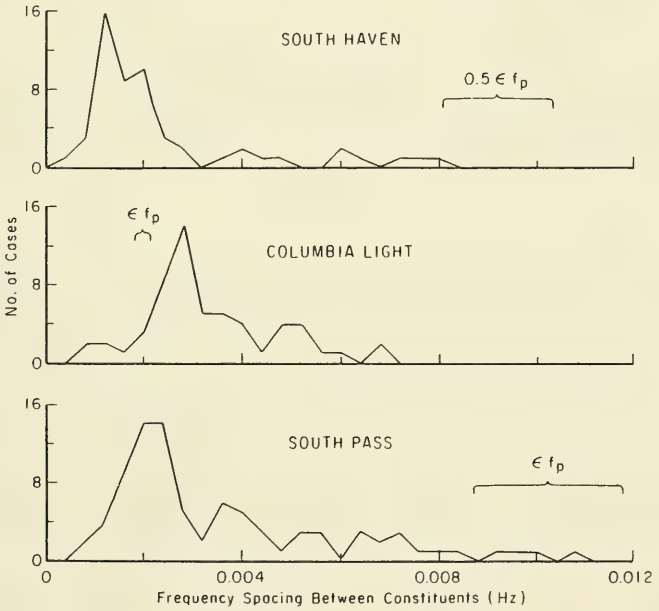

Figure 48. Distribution of frequency spacing between MRS constituents.

The BF-type instability would be expected to lead to frequency spacings of εf_p. εf_p for the Columbia Light records is approximately 0.0020 hertz which is within 30 percent of the modal frequency spacing between constituents. Thus, the BF instability is a possible explanation for the frequency structure of constituents in the Columbia Light records.

Values of εf_p for the South Haven and South Pass records are an order of magnitude larger than the modal frequency spacing between constituents. For these records, $2\ \varepsilon f_p$ is a better indicator of the range of frequency covered by the high energy part of the spectrum. However, these records represent actively growing waves. The BF instability operates over a range of frequencies to a separation $\sqrt{2}\ \varepsilon f_p$ on either side of the carrier frequency, f_p. It is possible that the observed constituents in the field records are participating in resonant exchange of energy fueled by a BF-type instability of the carrier. Since the waves are actively growing, it is quite possible that the instability is being observed in an early stage, before the most unstable mode has dominated as prominent sidebands spaced εf_p on either side of the carrier.

Well-developed BF-type sidebands should certainly be present in the Columbia Light swell records if the mechanism is operating. Although the frequency structure is fairly consistent with expectations, the amplitude structure is not. The mechanism does not account for the observed large and rapid shifts in energy between constituents.

Although the field data do not clearly follow all aspects of BF theory, the preceding discussion and the modulation information shown in Figures 40 to 43 provide evidence that BF theory gives useful insight on the characteristics of some field records. It is submitted that the evidence is more than circumstantial and that detailed spectral shape may be partially explained by the BF theory (hypothesis c).

VII. SUMMARY

Wave measurements are examined from three relatively deepwater field sites in Lake Michigan, the Pacific Ocean, and the Gulf of Mexico. Approximately 1 hour of data representing high waves, unimodal spectra, and nearly constant significant height and peak spectral period was selected for each site. The data represent actively growing waves at two sites and swell at the third site. Record lengths for analysis vary from 512 to 1,200 seconds.

Analysis is done in both the frequency and the time domain. The FFT spectral analysis procedure is shown to possess limitations for resolving details of the distribution of energy as a function of frequency and for identifying correct phase values for each frequency component. Phases returned by FFT procedures are shown to be subject to erratic variations. These variations are believed to have led previous investigators to conclude that phases are random.

Shortcomings of the FFT spectral analysis procedures are circumvented by using a MRS technique to identify major frequency constituents. The MRS technique has been used in published meteorological studies and in at least one unpublished laboratory wave study; however, the current study is believed to be the first in which the MRS technique is applied to field wave records.

Time domain analyses of the field records are focused on extracting wave grouping information directly from the time series. A wave group is conceptualized as a small area of sea surface containing relatively high energy. Groups are identified as sections of the time series in which the local variance is high relative to the variance of the whole record. Fluctuations

in local variance, referred to as the LVTS, provide information on both the intensity and the time scale of wave grouping. The LVTS is used to define a new parameter which is indicative of wave grouping. Autocorrelation between individual wave heights is also considered as an indicator of wave grouping.

Analyses of the selected data from the three sites are used to test six hypotheses about the nature of ocean waves. The hypotheses and the evidence obtained in this study for or against them are as follows:

(1) Spectral components are sometimes discrete and are not smeared over a broad continuous spectrum. MRS analysis is used to identify evidence of a fine structure in the spectral representation of ocean wave records. The structure is sufficiently detailed to be transparent to most spectral analysis procedures applied to field records. Thus, the continuous spectra often reported in field studies may be generated by analysis procedures rather than by physical processes. Evidence is also found that the amplitude of MRS constituents defining the structure is highly variable in time.

(2) Spectral components are sometimes related in a deterministic, nonrandom way. MRS constituents with about the same frequency are matched between records from each site. Phases of matched constituents show strong evidence of nonrandom behavior. These records provide evidence that the phase relationship among constituents is relatively invariant.

(3) The detailed spectral shape may be partially explained by Benjamin and Feir's (1967) theory, which provided a theoretical basis for expecting discrete, detailed structure in a spectrum. Frequency spacings between MRS constituents in the swell data are shown to be reasonably consistent with BF theory. The frequency range covered by constituents in the sea data is reasonably consistent with expectations from the BF theory. The amplitude structure is not clearly consistent with BF theory. Also, the variability of amplitude structure between records is not predicted by BF theory.

(4) Waves in deep water tend to organize so that high waves occur in groups. An investigation of the time series, autocorrelation between individual wave heights and the LVTS, along with a review of the literature, indicates high waves often tend to occur in groups. Evidence also indicates that grouping characteristics can be highly variable over short time intervals.

(5) The modulation period of wave groups is sometimes related to the period and steepness of the waves. The LVTS is used to show that a modulation period computed from the peak frequency and steepness of the waves is comparable to the time between wave groups, despite considerable scatter. Modulation frequency computed by Benjamin and Feir (1967) and by Longuet-Higgins (1980) is shown to compare favorably with field data, though closer agreement is indicated with the more refined stability criteria established through a higher order of approximation by Longuet-Higgins.

(6) The extent of grouping in each time series and the modulation period are related to certain features of the spectrum. Evidence is presented that the MRS analysis represents grouped wave records by identifying two or more high-amplitude constituents separated by a frequency which approximates the modulation period. Thus, grouping characteristics are related to the detailed spectrum but may not be related to a spectrum computed by more conventional techniques.

This study is based on a small sample of field data, so a sweeping generalization of the results is not appropriate. However, evidence supporting the six hypotheses leads to the conclusion that some commonly held conceptions of ocean waves, including the notion of a random wave field represented by a continuous random-phase spectrum, are open to serious question.

LITERATURE CITED

ALBER, I.E., "The Effects of Randomness on the Stability of Two-Dimensional Surface Wavetrains," *Proceedings of the Royal Society of London*, Series A, 363, No. 1715, 1978, pp. 525-546.

ALBER, I.E., and SAFFMAN, P.G., "Stability of Random Nonlinear Deep Water Waves with Finite Bandwidth Spectra," Report No. 31326-6035-RU-00, TRW, Redondo Beach, Calif., Oct. 1978.

ARHAN, M., and EZRATY, R., "Statistical Relations Between Successive Wave Heights," *Oceanologica Acta*, Vol. 1, No. 2, 1978, pp. 151-158.

AUBERT, E.J., LUND, I.A., and THOMASELL, A., Jr., "Some Objective Six-Hour Predictions Prepared by Statistical Methods," *Journal of Meteorology*, Vol. 16, 1959, pp. 436-446.

BENJAMIN, T.B., "Instability of Periodic Wavetrains in Nonlinear Dispersive Systems," *Proceedings of the Royal Society of London*, Series A, 299, No. 1456, 1967, pp. 59-75.

BENJAMIN, T.B., and FEIR, J.E., "The Disintegration of Wave Trains on Deep Water, Part 1, Theory," *Journal of Fluid Mechanics*, Vol. 27, Part 3, Feb. 1967, pp. 417-430.

BENNEY, D.J., "Non-Linear Gravity Wave Interactions," *Journal of Fluid Mechanics*, Vol. 14, Part 4, Dec. 1962, pp. 577-584.

BENNEY, D.J., and NEWELL, A.C., "The Propagation of Nonlinear Wave Envelopes," *Journal of Mathematics and Physics*, Vol. 46, 1967, pp. 133-139.

BLACKMAN, R.B., and TUKEY, J.W., *The Measurement of Power Spectra*, Dover Publications, Inc., New York, 1959.

BURCHARTH, H.F., "A Comparison of Nature Waves and Model Waves with Special Reference to Wave Grouping," *Proceedings of the 17th International Conference on Coastal Engineering*, American Society of Civil Engineers, Vol. 3, 1980, pp. 2992-3009.

BURLING, R.W., "The Phase Velocity of Wave-Components Under the Action of Wind," *New Zealand Journal on Geological Geophysics*, Vol. 2, No. 1, Feb. 1959, pp. 66-87.

CHAKRABARTI, S.K., SNIDER, R.H., and FELDHAUSEN, P.H., "Mean Length of Runs of Ocean Waves," *Journal of Geophysical Research*, Vol. 79, No. 36, Dec. 1974, pp. 5665-5667.

CHOU, S.J., "Selection of Optimum Wave Conditions for Time-Domain Simulation of Non-linear Phenomena," Ph.D. Dissertation, University of California, Berkeley, Calif., 1978.

CHU, V.H., and MEI, C.C., "On Slowly-Varying Stokes Waves," *Journal of Fluid Mechanics*, Vol. 41, Part 4, May 1970, pp. 873-887.

CHU, V.H. and MEI, C.C., "The Non-linear Evolution of Stokes Waves in Deep Water," *Journal of Fluid Mechanics*, Vol. 47, Part 2, May 1971, pp. 337-351.

COOLEY, J.W., and TUKEY, J.W., "The Fast Fourier Transform," *Institute of Electrical and Electronic Engineers Spectrum*, Vol. 4, 1965, pp. 63-70.

CRAWFORD, D.R., SAFFMAN, P.G., and YUEN, H.C., "Evolution of a Random Inhomogeneous Field of Nonlinear Deep-water Gravity Waves," *Wave Motion*, Vol. 2, No. 1, 1980, pp. 1-16.

EARLE, M.D., "Extreme Wave Conditions During Hurricane Camille," *Journal of Geophysical Research*, Vol. 80, No. 3, Jan. 1975, pp. 377-379.

EWING, J.A., "Mean Length of Runs of High Waves," *Journal of Geophysical Research*, Vol. 78, No. 12, Apr. 1973, pp. 1933-1936.

FOX, M.J.H., "On the Nonlinear Transfer of Energy in the Peak of a Gravity-Wave Spectrum," *Proceedings of the Royal Society of London*, Series A, 348, 1976, pp. 467-483.

FUNKE, E.R., and MANSARD, E.P.D., "On the Synthesis of Realistic Sea States in a Laboratory Flume," Report No. LTR-HY-66, National Research Council, Mechanical Engineering, Hydraulics Laboratory, Canada, Aug. 1979.

FUNKE, E.R., and MANSARD, E.P.D., "On the Synthesis of Realistic Sea States," *Proceedings of the 17th International Conference on Coastal Engineering*, American Society of Civil Engineers, Vol. 3, 1980, pp. 2974-2991.

GODA, Y., "Numerical Experiments on Wave Statistics with Spectral Simulation," *Report of the Port and Harbour Research Institute*, Vol. 9, No. 3, Sept. 1970, pp. 3-57.

GODA, Y., "On Wave Groups," *Proceedings of the First International Conference on Behavior of Offshore Structures*, Norwegian Institute of Technology, Vol. 1, 1976, pp. 115-128.

HARRIS, D.L., "The Equivalence Between Certain Statistical Prediction Methods and Linearized Dynamical Methods," *Monthly Weather Review*, Aug. 1962, pp. 331-340.

HARRIS, D.L., "Finite Spectrum Analyses of Wave Records," *Proceedings of the International Symposium on Ocean Wave Measurement and Analysis*, American Society of Civil Engineers, Vol. 1, 1974, pp. 107-123 (also Reprint 6-74, U.S. Army, Corps of Engineers, Coastal Engineering Research Center, Fort Belvoir, Va., NTIS A002 113).

HASIMOTO, H., and ONO, H., "Nonlinear Modulation of Gravity Waves," *Journal of the Physical Society of Japan*, Vol. 33, No. 3, Sept. 1972, pp. 805-811.

HASSELMANN, K., "On the Nonlinear Energy Transfer in a Gravity Wave Spectrum, Part 1," *Journal of Fluid Mechanics*, Vol. 12, Part 4, Apr. 1962, pp. 481-500.

HASSELMANN, K., "On the Nonlinear Energy Transfer in a Gravity Wave Spectrum," *Journal of Fluid Mechanics*, Vol. 15, Part 2, Feb. 1963, pp. 273-281.

HASSELMANN, K., et al., "Measurements of Wind-Wave Growth and Swell Decay During the Joint North Sea Wave Project (JONSWAP)," *Deutschen Hydrograph, Zeits*, Supplement A8, No. 12, 1973.

HERTERICH, K., and HASSELMANN, K., "A Similarity Relation for the Nonlinear Energy Transfer in a Finite-Depth Gravity-Wave Spectrum," *Journal of Fluid Mechanics*, Vol. 97, Part 1, Mar. 1980, pp. 215-224.

HOUMB, O.G., and OVERVIK, T., "On the Statistical Properties of 115 Wave Records from the Norwegian Continental Shelf," Norwegian Institute of Technology, University of Trondheim, Trondheim, Norway, Jan. 1977.

JOHNSON, R.R., MANSARD, E.P.D., and PLOEG, J., "Effects of Wave Grouping on Breakwater Stability," *Proceedings of the 16th Conference on Coastal Engineering*, American Society of Civil Engineers, Vol. 3, 1978, pp. 2228-2243.

JOHNSON, R.R., and PLOEG, J., "The Problem of Defining Design Wave Conditions," *Proceedings of the Ports '77 Fourth Annual Symposium of the Waterway, Port, Coastal, and Ocean Division*, American Society of Civil Engineers, 1977, pp. 413-415.

KOMEN, G.J., "Nonlinear Contributions to the Frequency Spectrum of Wind-Generated Water Waves," *Journal of Physical Oceanography*, Vol. 10, No. 5, May 1980, pp. 779-790.

KUO, Y.Y., MITSUYASU, H., and MASUDA, A., "Experimental Study on the Phase Velocity of Wind Waves, Part 1, Laboratory Wind Waves," *Reports of Research Institute for Applied Mechancis*, Vol. XXVII, No. 83, Kyushu University, Fukuoka, Japan, July 1979a, pp. 1-19.

KUO, Y.Y., MITSUYASU, H., and MASUDA, A., "Experimental Study on the Phase Velocity of Wind Waves, Part 2, Ocean Waves," *Reports of Research Institute for Applied Mechanics*, Vol. XXVII, No. 84, Kyushu University, Fukuoka, Japan, Sept. 1979b, pp. 47-66.

LAKE, B.M., and YUEN, H.C., "A New Model for Nonlinear Wind Waves, Part 1, Physical Model and Experimental Evidence," *Journal of Fluid Mechanics*, Vol. 88, Sept. 1978, pp. 33-62.

LAKE, B.M., et al., "Nonlinear Deep-water Waves: Theory and Experiment, Part 2, Evolution of a Continuous Wave Train," *Journal of Fluid Mechanics*, Vol. 83, Part 1, Nov. 1977, pp. 49-74.

LIGHTHILL, M.J., "Contributions to the Theory of Waves in Nonlinear Dispersive Systems," *Journal of the Institute of Mathematical Applications*, Vol. 1, 1965, pp. 269-307.

LONGUET-HIGGINS, M.S., "Resonant Interactions Between Two Trains of Gravity Waves," *Journal of Fluid Mechanics*, Vol. 12, Part 3, Mar. 1962, pp. 321-332.

LONGUET-HIGGINS, M.S., "On the Nonlinear Transfer of Energy in the Peak of a Gravity-Wave Spectrum: A Simplified Model," *Proceedings of the Royal Society of London*, Series A, 347, 1976, pp. 311-328.

LONGUET-HIGGINS, M.S., "The Instabilities of Gravity Waves of Finite Amplitude in Deep Water, I. Superharmonics," *Proceedings of the Royal Society of London*, Series A, 360, 1978a, pp. 471-488.

LONGUET-HIGGINS, M.S., "The Instabilities of Gravity Waves of Finite Amplitude in Deep Water, II. Subharmonics," *Proceedings of the Royal Society of London*, Series A, 360, 1978b, pp. 489-505.

LONGUET-HIGGINS, M.S., "Modulation of the Amplitude of Steep Wind Waves," *Journal of Fluid Mechanics*, Vol. 99, Part 4, Aug. 1980, pp. 705-713.

LONGUET-HIGGINS, M.S., and SMITH, N.D., "An Experiment on Third Order Resonant Wave Interactions," *Journal of Fluid Mechanics*, Vol. 25, Part 3, July 1966, pp. 417-435.

McGOLDRICK, L.F., et al., "Measurements on Resonant Wave Interactions," *Journal of Fluid Mechanics*, Vol. 25, Part 3, July 1966, pp. 437-456.

MITSUYASU, H., "A Note on the Nonlinear Energy Transfer in the Spectrum of Wind-Generated Waves," *Reports of Research Institute for Applied Mechanics*, Vol. XVI, No. 54, Kyushu University, Fukuoka, Japan, 1968, pp. 251-264.

MITSUYASU, H., KUO, Y.Y., and MASUDA, A., "The Dispersion Relation for Wind Waves in Decay Area," *Turbulent Fluxes Through the Sea Surface, Wave Dynamics, and Prediction*, Plenum Press, New York, 1978, pp. 221-232.

MITSUYASU, H., KUO, Y.Y., and MASUDA, A., "On the Dispersion Relation of Random Gravity Waves, Part 2, An Experiment," *Journal of Fluid Mechanics*, Vol. 92, Part 4, 1979, pp. 731-749.

MOLLO-CHRISTENSEN, E., and RAMAMONJIARISOA, A., "Modeling the Presence of Wave Groups in a Random Wave Field," *Journal of Geophysical Research*, Vol. 83, No. C8, Aug. 1978, pp. 4117-4122.

NELSON, A.R., "Statistical Properties of Ocean Wave Groups," M.S. Thesis, Naval Postgraduate School, Monterey, Calif., 1980.

NEUMANN, G., "On Wind Generated Ocean Waves with Special Reference to the Problem of Wave Forecasting," New York University, Department of Meteorology and Oceanography, New York, 1952.

NOLTE, K.G., and HSU, F.H., "Statistics of Ocean Wave Groups," *Proceedings of the Fourth Annual Offshore Technology Conference*, Vol. II, 1972, pp. 637-644.

PATTERSON, M.M., "Oceanographic Data from Hurricane Camille," *Proceedings of the Sixth Annual Offshore Technology Conference*, Vol. II, 1974, pp. 781-790.

PHILLIPS, O.M., "On the Dynamics of Unsteady Gravity Waves of Finite Amplitude, Part 1, The Elementary Interactions," *Journal of Fluid Mechanics*, Vol. 9, Part 2, Oct. 1960, pp. 193-217.

PIERSON, W.J., Jr., "The Interpretation of Crossed Orthogonals in Wave Refraction Phenomena," TM-21, U.S. Army, Corps of Engineers, Beach Erosion Board, Washington, D.C., Nov. 1950.

RAMAMONJIARISOA, A., and COANTIC, M., "Loi Experimentale de Dispersion des Vagues Produites par le Vent sur une Faible Longueur d'Action," Vol. B282, C.R. Academy of Science, Paris, France, Feb. 1976, pp. 111-114.

RAMAMONJIARISOA, A., and GIOVANANGELI, J.P., "Observations de la Vitesse de Propagation des Vagues Engendrees par le Vent au Large," Vol. B287, C.R. Academy of Science, Paris, France, Sept. 1978, pp. 133-136.

RAMAMONJIARISOA, A., and MOLLO-CHRISTENSEN, E., "Modulation Characteristics of Sea Surface Waves," *Journal of Geophysical Research*, Vol. 84, No. C12, Dec. 1979, pp. 7769-7775.

RIKIISHI, K., "A New Method for Measuring the Directional Wave Spectrum, Part II, Measurement of the Directional Spectrum and Phase Velocity of Laboratory Wind Waves," *Journal of Physical Oceanography*, Vol. 8, No. 3, May 1978, pp. 518-529.

RYE, H., "Wave Group Formation Among Storm Waves," *Proceedings of the 14th Conference on Coastal Engineering*, American Society of Civil Engineers, Vol. 1, 1974, pp. 164-183.

RYE, H., "Wave Parameter Studies and Wave Groups," *Proceedings of the International Conference on Sea Climatology*, Paris, France, 1979.

SEDIVY, D.G., "Ocean Wave Group Analysis," Report No. NPS-68 Se Th 78091, Naval Postgraduate School, Monterey, Calif., Sept. 1978.

SEIWELL, H.R., "The Principles of Time Series Analyses Applied to Ocean Wave Data," *Proceedings of the National Academy of Sciences*, Vol. 35, No. 9, 1949, pp. 518-528.

SHEMDIN, O.H., et al., "Nonlinear and Linear Bottom Interaction Effects in Shallow Water," *Turbulent Fluxes Through the Sea Surface, Wave Dynamics, and Prediction*, Plenum Press, New York, 1978, pp. 347-372.

SHEMDIN, O.H., et al., "Mechanisms of Wave Transformation in Finite-Depth Water," *Journal of Geophysical Research*, Vol. 85, No. C9, Sept. 1980, pp. 5012-5018.

SIEFERT, W., "Consecutive High Waves in Coastal Waters," *Proceedings of the 15th Conference on Coastal Engineering*, American Society of Civil Engineers, Vol. 1, 1976, pp. 171-182.

TAYLOR, G.I., "The Spectrum of Turbulence," *Proceedings of the Royal Society of London*, Series A, 164, 1938, pp. 476-490.

THOMPSON, E.F., "Results from the CERC Wave Measurement Program," *Proceedings of the International Symposium on Ocean Wave Measurement and Analysis*, American Society of Civil Engineers, Vol. 1, 1974, pp. 836-855 (also Reprint 7-74, U.S. Army, Corps of Engineers, Coastal Engineering Research Center, Fort Belvoir, Va., NTIS A002 114).

THOMPSON, E.F., "Wave Climate at Selected Locations Along U.S. Coasts," TR 77-1, U.S. Army, Corps of Engineers, Coastal Engineering Research Center, Fort Belvoir, Va., Jan. 1977.

THOMPSON, E.F., "Energy Spectra in Shallow U.S. Coastal Waters," TP 80-2, U.S. Army, Corps of Engineers, Coastal Engineering Research Center, Fort Belvoir, Va., Feb. 1980.

THOMPSON, E.F., "Nonrandom Behavior in Field Wave Spectra and Its Effect on Grouping of High Waves," D.Sc. Dissertation, George Washington University, Washington, D.C., 1981.

THOMPSON, W.C., and SEDIVY, D.G., "Statistical Characteristics of Ocean Wave Groups," *Proceedings of the 17th International Conference on Coastal Engineering*, The Institute of Engineers, 1980, pp. 163-164.

U.S. ARMY, CORPS OF ENGINEERS, COASTAL ENGINEERING RESEARCH CENTER, *Shore Protection Manual*, 3d ed., Vols. I, II, and III, Stock No. 008-022-00113-1, U.S. Government Printing Office, Washington, D.C., 1977, 1,262 pp.

URSELL, F., "On the Application of Harmonic Analysis to Ocean Wave Research, *Science*, Vol. III, No. 2286, 1950, pp. 445-446.

VON ZWECK, O., "Observations of Propagation Characteristics of a Wind Driven Sea," Report No. 69-4, Department of Meteorology, Massachusetts Institute of Technology, Cambridge, Mass., 1969.

WEBB, D.J., "Non-linear Transfers Between Sea Waves," *Deep-Sea Research*, Vol. 25, 1978, pp. 279-298.

WHITHAM, G.B., "Variational Methods and Applications to Water Waves," *Proceedings of the Royal Society of London*, Series A, 299, 1967, pp. 6-25.

WIEGEL, R.L., *Oceanographical Engineering*, Prentice Hall, Inc., Englewood Cliffs, New Jersey, 1964.

WILSON, J.R., and BAIRD, W.F., "A Discussion of Some Measured Wave Data," *Proceedings of the 13th Conference on Coastal Engineering*, American Society of Civil Engineers, Vol. 1, 1972, pp. 113-130.

WU, H.Y., HSU, E.Y., and STREET, R.L., "Experimental Study of Nonlinear Wave-Wave Interaction and White-Cap Dissipation of Wind-Generated Waves," *Dynamics of Atmospheres and Oceans*, Vol. 3, 1979, pp. 55-78.

YEFIMOV, V.V., SOLOV'YEV, Y.P., and KHRISTOFOROV, G.N., "Observational Determination of the Phase Velocities of Spectral Components of Wind Waves," *Izv. Academy of Science, USSR Atmospheric Oceanic Physics*, Vol. 8, No. 4, 1972.

YUEN, H.C., and LAKE, B.M., "Nonlinear Deep Water Waves: Theory and Experiment," *Physics of Fluids*, Vol. 18, No. 8, Aug. 1975, pp. 956-960.

YUEN, H.C., and LAKE, B.M., "Instabilities of Waves on Deep Water," *Annual Review Fluid Mechanics*, Vol. 12, 1980, pp. 303-334.

ZAKHAROV, V.E., "Stability of Periodic Waves of Finite Amplitude on the Surface of a Deep Fluid," *Journal of Applied Mechanics and Technical Physics*, Vol. 9, No. 2, 1968, pp. 190-194.

ZAKHAROV, V.E., and SHABAT, A.B., "Exact Theory of Two-Dimensional Self-Focusing and One-Dimensional Self-Modulation of Waves in Nonlinear Media," Translated in *Soviet Physics, JETP*, Vol. 34, No. 1, Jan. 1972, pp. 62-69.

ZWAMBORN, J.A., "Analysis of Causes of Damage to Sines Breakwater," *Proceedings of Coastal Structures '79*, American Society of Civil Engineers, Vol. 1, 1979, pp. 422-441.

APPENDIX A

BACKGROUND DISCUSSION OF MULTIPLE REGRESSION SCREENING (MRS) TECHNIQUE

The MRS analysis fits, in the least squares sense, a sum of sinusoids with preassigned frequencies to a given data record.

It is desired to obtain an estimate of the time series in the form

$$y_e(n\Delta t) = d_0 + d_1X_1(n\Delta t) + d_2X_2(n\Delta t) + \ldots + d_pX_p(n\Delta t) \quad p < N \tag{A-1}$$

where d_i are constants and X_i the selected known functions of time. It is assumed that the mean of the time series is zero so equation (A-1) can be rewritten

$$y_e(n\Delta t) = d_1x_1(n\Delta t) + d_2x_2(n\Delta t) + \ldots + d_px_p(n\Delta t) \tag{A-2}$$

where x_i are selected known functions of time with mean removed.

The constants d_i are selected to minimize the sum of the squared differences between actual and estimated values in the time series

$$\sum_{n=1}^{N} [y(n\Delta t) - y_e(n\Delta t)]^2 \tag{A-3}$$

By combining equations (A-2) and (A-3), the sum of squared differences can be written as

$$\sum_{n=1}^{N} [y(n\Delta t) - d_1x_1(n\Delta t) - d_2x_2(n\Delta t) - \ldots - d_px_p(n\Delta t)]^2 \tag{A-4}$$

By using the method of least squares, the optimum values of $d_1, d_2, \ldots, d_p$ can be obtained as the solution to p simultaneous equations

$$\begin{aligned}
d_1 \sum_{n=1}^{N} x_1^2 + d_2 \sum_{n=1}^{N} x_1x_2 + \ldots + d_p \sum_{n=1}^{N} x_1x_p &= \sum_{n=1}^{N} x_1y \\
d_1 \sum_{n=1}^{N} x_2x_1 + d_2 \sum_{n=1}^{N} x_2^2 + \ldots + d_p \sum_{n=1}^{N} x_2x_p &= \sum_{n=1}^{N} x_2y \\
&\vdots \\
d_1 \sum_{n=1}^{N} x_px_1 + d_2 \sum_{n=1}^{N} x_px_2 + \ldots + d_p \sum_{n=1}^{N} x_p^2 &= \sum_{n=1}^{N} x_py
\end{aligned} \tag{A-5}$$

These equations are often called the normal equations.

Equations (A-5) can be solved by forming the augmented matrix

$$\begin{bmatrix} \sum x_1^2 & \sum x_1x_2 & \cdots & \sum x_1x_p & \sum x_1y \\ \sum x_2x_1 & \sum x_2^2 & \cdots & \sum x_2x_p & \sum x_2y \\ & \vdots & & & \\ \sum x_px_1 & \sum x_px_2 & \cdots & \sum x_p^2 & \sum x_py \end{bmatrix} \tag{A-6}$$

The solution is further simplified by adding a (p + 1)'th row to equation (A-6) so that the matrix is square and symmetric.

$$\begin{bmatrix} \sum x_1^2 & \sum x_1x_2 & \cdots & \sum x_1x_p & \sum x_1y \\ \sum x_2x_1 & \sum x_2^2 & \cdots & \sum x_2x_p & \sum x_2y \\ & \vdots & & & \\ \sum x_px_1 & \sum x_px_2 & \cdots & \sum x_p^2 & \sum x_py \\ \sum x_1y & \sum x_2y & \cdots & \sum x_py & \sum y^2 \end{bmatrix} \tag{A-7}$$

The solution is obtained by inverting equation (A-7).

In using a relationship of the form of equation (A-2) to approximate an ocean wave record, it can be expected that some of the functions x_i will be important constituents of the field record and other x_i will be of little significance. The goal of the analysis is to identify and quantify only the major constituents. The most important constituent, x_i, in equation (A-2) is defined as the one which has the highest correlation with the time series

$$R^2_{x_iy} = \frac{(\sum x_iy)^2}{\sum x_i^2 \sum y^2} \tag{A-8}$$

where $R^2_{x_iy}$ is the square of the correlation between x_i and y. If x_K is the constituent for which equation (A-8) is largest, columns 1 and K in equation (A-7) are switched to give

$$\begin{bmatrix} \sum x_1x_K & \sum x_1x_2 & \cdots & \sum x_1x_{K-1} & \sum x_1^2 & \sum x_1x_{K+1} & \cdots & \sum x_1x_p & \sum x_1y \\ \sum x_2x_K & \sum x_2^2 & \cdots & \sum x_2x_{K-1} & \sum x_2x_1 & \sum x_2x_{K+1} & \cdots & \sum x_2x_p & \sum x_2y \\ & \vdots & & & & & & & \\ \sum x_{K-1}x_K & \sum x_{K-1}x_2 & & & & & & & \\ \sum x_K^2 & \sum x_Kx_2 & & & & & & & \\ \sum x_{K+1}x_K & \sum x_{K+1}x_2 & & & & & & & \\ & \vdots & & & & & & & \\ \sum x_px_K & \sum x_px_2 & \cdots & \sum x_px_{K-1} & \sum x_px_1 & \sum x_px_{K+1} & \cdots & \sum x_p^2 & \sum x_py \\ \sum x_Ky & \sum x_2y & \cdots & \sum x_{K-1}y & \sum x_1y & \sum x_{K+1}y & \cdots & \sum x_py & \sum y^2 \end{bmatrix} \tag{A-9}$$

Rows 1 and K in equation (A-9) are then switched to give

$$\begin{bmatrix}
\sum x_K^2 & \sum x_K x_2 & \cdots & \sum x_K x_{K-1} & \sum x_K x_1 & \sum x_K x_{K+1} & \cdots & \sum x_K x_p & \sum x_K y \\
\sum x_2 x_K & \sum x_2^2 & \cdots & \sum x_2 x_{K-1} & \sum x_2 x_1 & \sum x_2 x_{K+1} & \cdots & \sum x_2 x_p & \sum x_2 y \\
\vdots & & & & & & & & \\
\sum x_{K-1} x_K & \sum x_{K-1} x_2 & \cdots & \sum x_{K-1}^2 & \sum x_{K-1} x_1 & \sum x_{K-1} x_{K+1} & \cdots & \sum x_{K-1} x_p & \sum x_{K-1} y \\
\sum x_1 x_K & \sum x_1 x_2 & \cdots & \sum x_1 x_{K-1} & \sum x_1^2 & \sum x_1 x_{K+1} & \cdots & \sum x_1 x_p & \sum x_1 y \\
\sum x_{K+1} x_K & \sum x_{K+1} x_2 & \cdots & \sum x_{K+1} x_{K-1} & \sum x_{K+1} x_1 & \sum x_{K+1}^2 & \cdots & \sum x_{K+1} x_p & \sum x_{K+1} y \\
\vdots & & & & & & & & \\
\sum x_p x_K & \sum x_p x_2 & \cdots & \sum x_p x_{K-1} & \sum x_p x_1 & \sum x_p x_{K+1} & \cdots & \sum x_p^2 & \sum x_p y \\
\sum x_K y & \sum x_2 y & \cdots & \sum x_{K-1} y & \sum x_1 y & \sum x_{K+1} y & \cdots & \sum x_p y & \sum y^2
\end{bmatrix} \qquad \text{(A-10)}$$

Techniques are available for partially solving equation (A-10) to obtain d_K in equation (A-2) (e.g., Aubert, Lund, and Thomasell, 1959). The techniques require manipulation of equation (A-10) to convert the first element in the first column to one and other elements to zero. The remaining columns are then orthogonalized with respect to the first column. Correlations between the remaining columns and the time series are computed to identify the most important remaining constituent. Suppose it is in column 1. Columns and rows are then switched to position the selected constituent in the second row and column. The remaining columns (p - 1) are again orthogonalized with respect to the first two columns. This procedure actually gives a recomputed d_K as well as solving for d_L.

The procedure is repeated for as many steps as desired up to a maximum of p steps. At each step another x_i is selected and the values of the d coefficient are computed for the newly selected x_i and all previously selected x_i so as to explain the maximum amount of variance in the field data time series.

Because of the quasi-periodic nature of ocean waves, it is desirable to choose periodic functions for the x_i. Thus, it is convenient to choose

$$\begin{aligned} x_{2i-1} &= \cos(\omega_i n\Delta t) \\ x_{2i} &= \sin(\omega_i n\Delta t) \end{aligned} \qquad \text{(A-11)}$$

where ω_i is the set of selected frequencies. Substitution of equation (A-11) into equation (A-2) gives

$$y_e(n\Delta t) = \sum_{i=1}^{p/2} [d_{2i-1} \cos(\omega_i n\Delta t) + d_{2i} \sin(\omega_i n\Delta t)] \qquad \text{(A-12)}$$

or, defining $\beta_i = d_{2i-1}$, $\alpha_i = d_{2i}$

$$y_e(n\Delta t) = \sum_{i=1}^{p/2} [\beta_i \cos(\omega_i n\Delta t) + \alpha_i \sin(\omega_i n\Delta t)] \qquad \text{(A-13)}$$

Equation (A-13) is comparable in form to equation (7) in the text but has the important difference that the frequencies are arbitrary. They are no longer tied to the record length, but the convenience of orthogonality is generally lost. Amplitude and phase for each frequency constituent are defined by

$$A_i = \sqrt{\beta_i^2 + \alpha_i^2}$$
$$\phi_i = \tan^{-1} \frac{\alpha_i}{\beta_i} \tag{A-14}$$

which are comparable to equation (13) in the text.

It is desirable to consider the x_i's specified in equation (A-11) in pairs in the MRS analysis. This requires only minor modifications in the procedure. Constituents are judged in pairs on the basis of a multiple correlation with the time series defined as

$$R^2_{x_{2i-1}x_{2i}y} = \left[\frac{(\sum x_{2i-1}y)^2}{\sum x^2_{2i-1} \sum y^2} + \frac{(\sum x_{2i}y)^2}{\sum x^2_{2i} \sum y^2} - \frac{2 \sum x_{2i-1}y \sum x_{2i}y \sum x_{2i-1}x_{2i}}{\sum x^2_{2i-1} \sum x^2_{2i} \sum y^2} \right] \left[1 - \frac{(\sum x_{2i-1}x_{2i})^2}{\sum x^2_{2i-1} \sum x^2_{2i}} \right]^{-1} \tag{A-15}$$

The switching of columns and the switching of rows, shown in equations (A-9) and (A-10), are done in pairs rather than singly. The solution of a column and orthogonalization of remaining columns is done twice in succession to solve for both β and α of the selected frequency. Then equation (A-15) is computed for all remaining constituents to again identify the maximum. The procedure is continued for as many steps as desired.

APPENDIX B

TIME SERIES PLOTS FOR FIELD DATA AND RECOMBINED MRS CONSTITUENTS

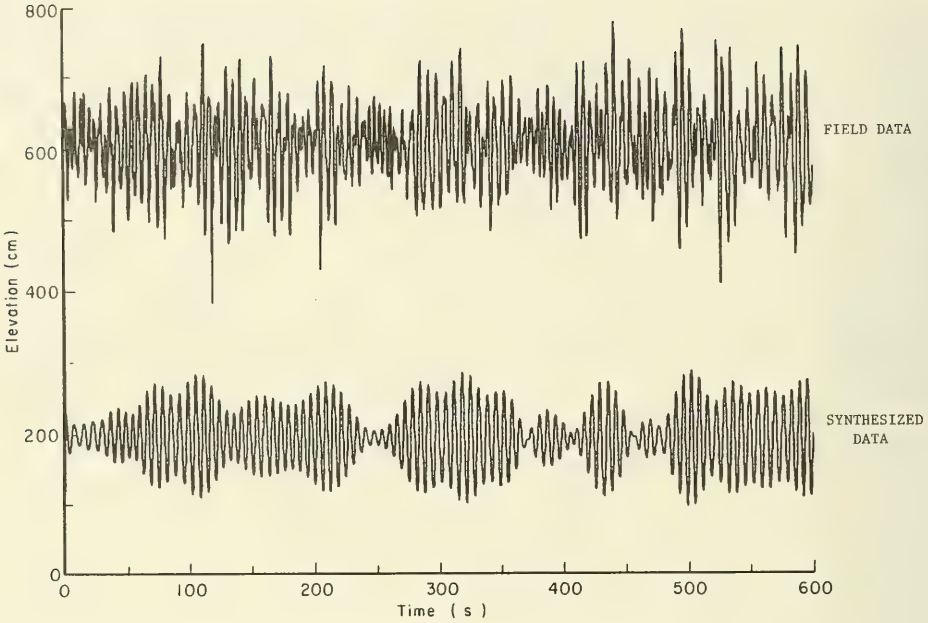

Figure B-1. South Haven, 1700 to 1710 e.s.t.

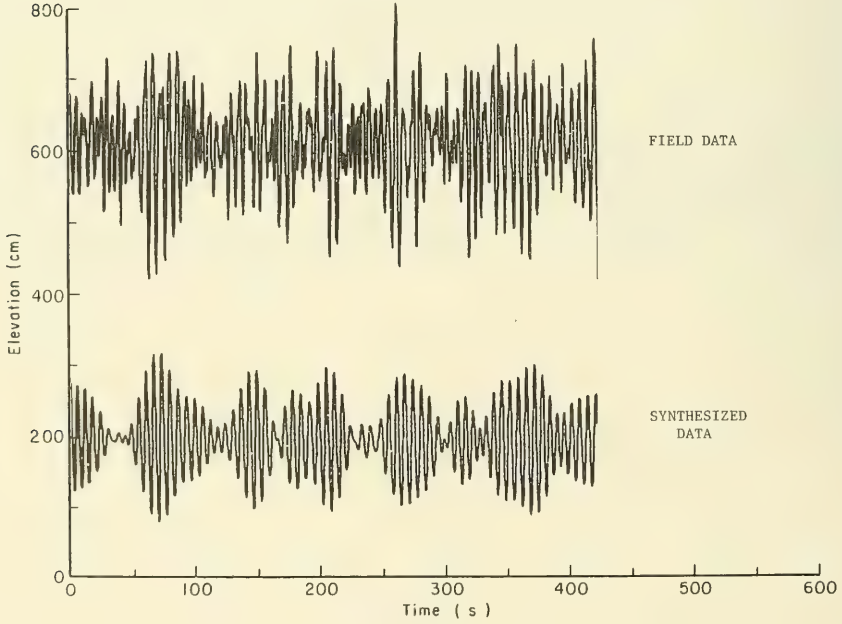

Figure B-2. South Haven, 1710 to 1717 e.s.t.

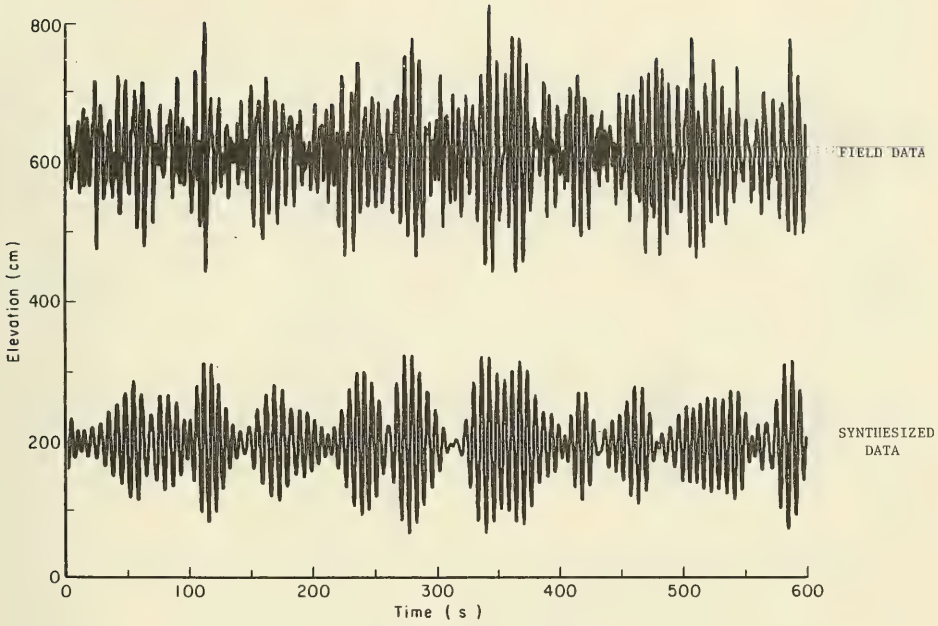

Figure B-3. South Haven, 1720 to 1730 e.s.t.

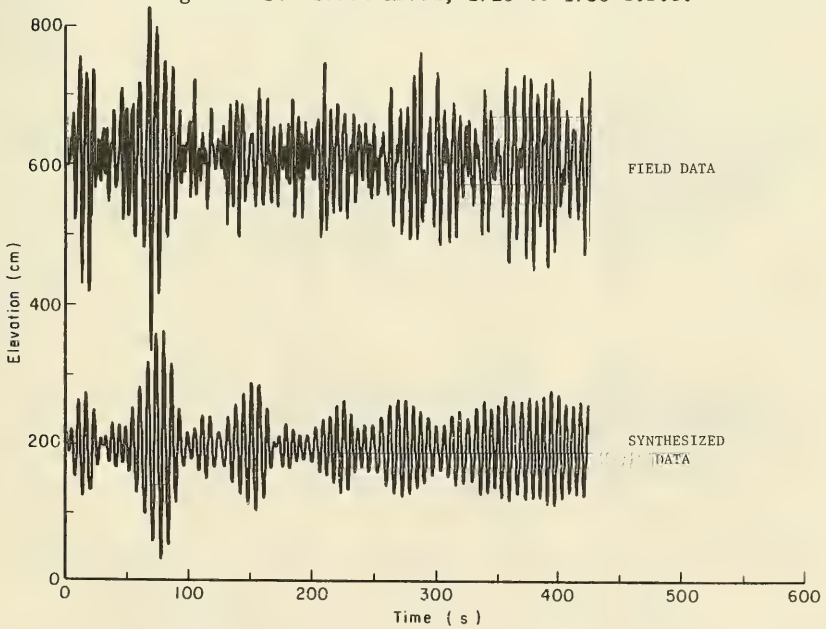

Figure B-4. South Haven, 1730 to 1737 e.s.t.

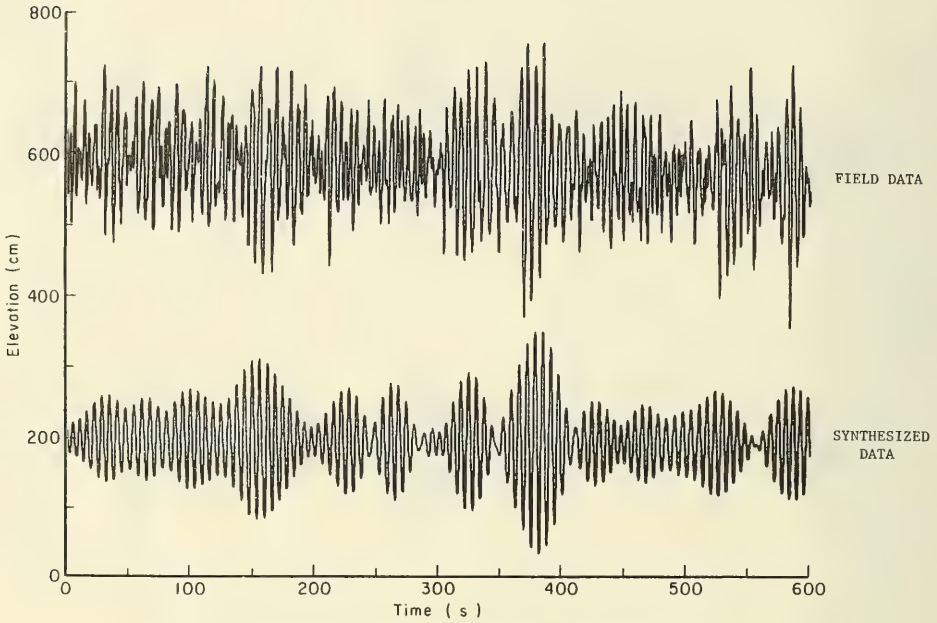

Figure B-5. South Haven, 1740 to 1750 e.s.t.

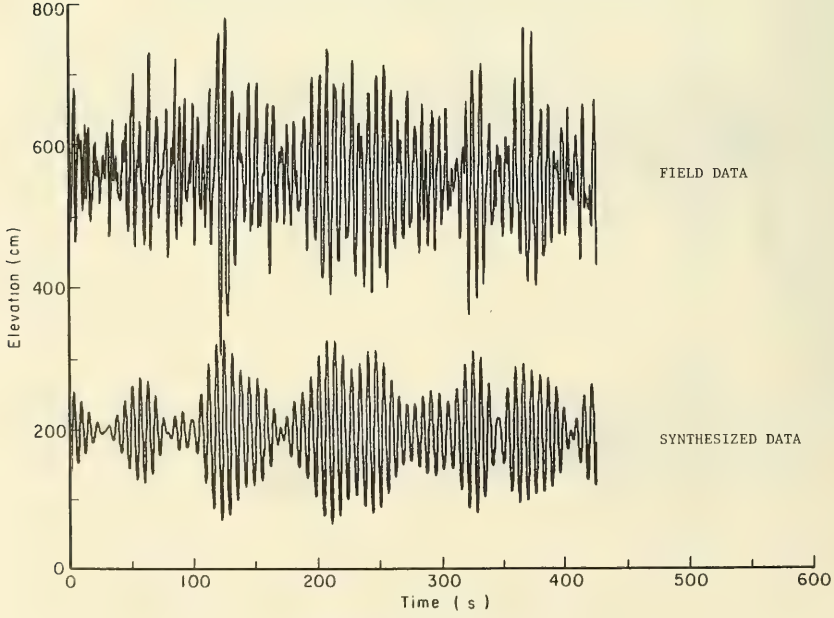

Figure B-6. South Haven, 1750 to 1757 e.s.t.

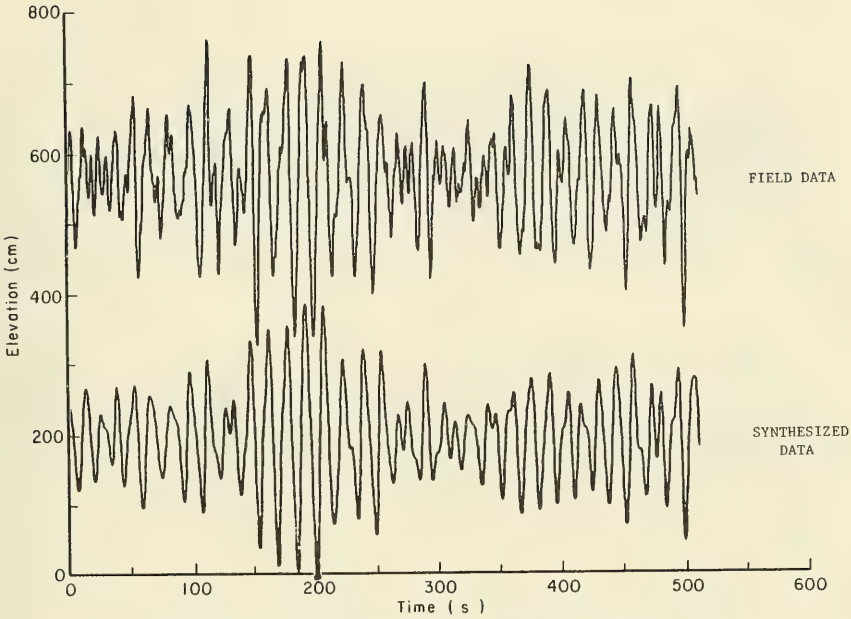

Figure B-7. Columbia Light, 1300 to 1308.5 P.d.t.

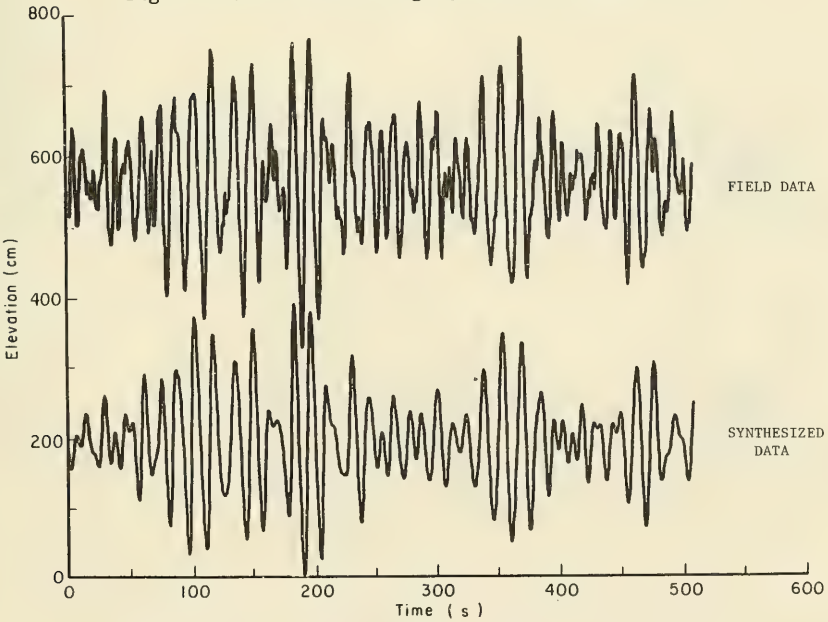

Figure B-8. Columbia Light, 1308.5 to 1317 P.d.t.

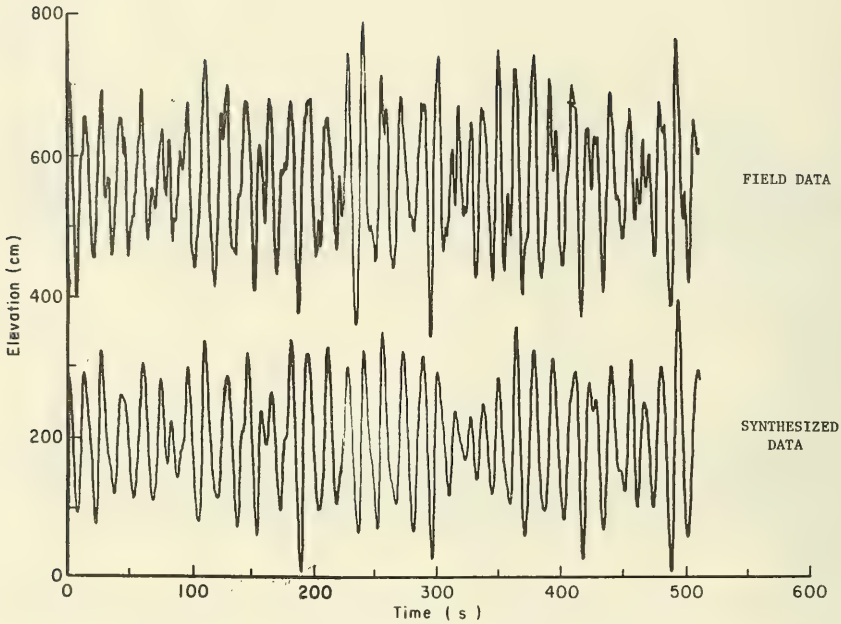

Figure B-9. Columbia Light, 1408.5 to 1417 P.d.t.

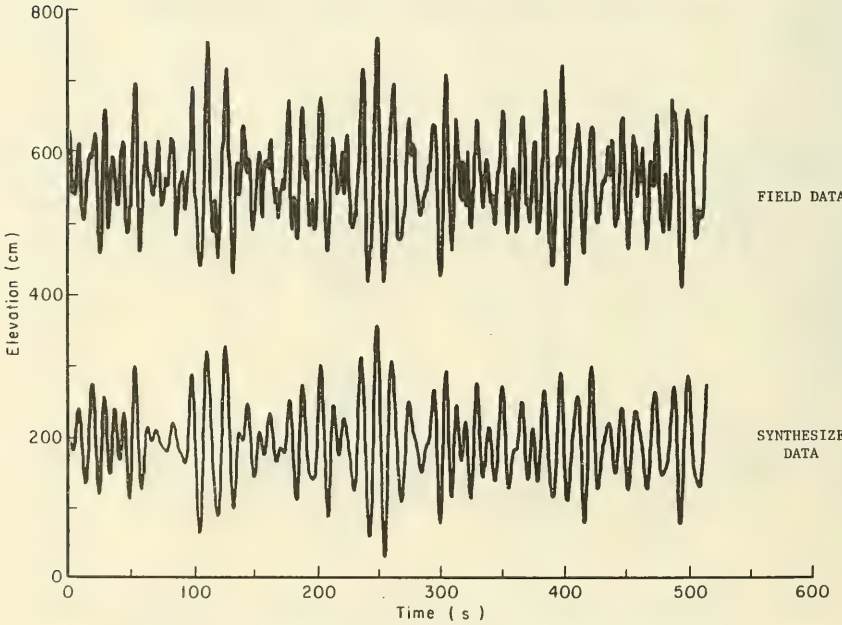

Figure B-10. Columbia Light, 1500 to 1508.5 P.d.t.

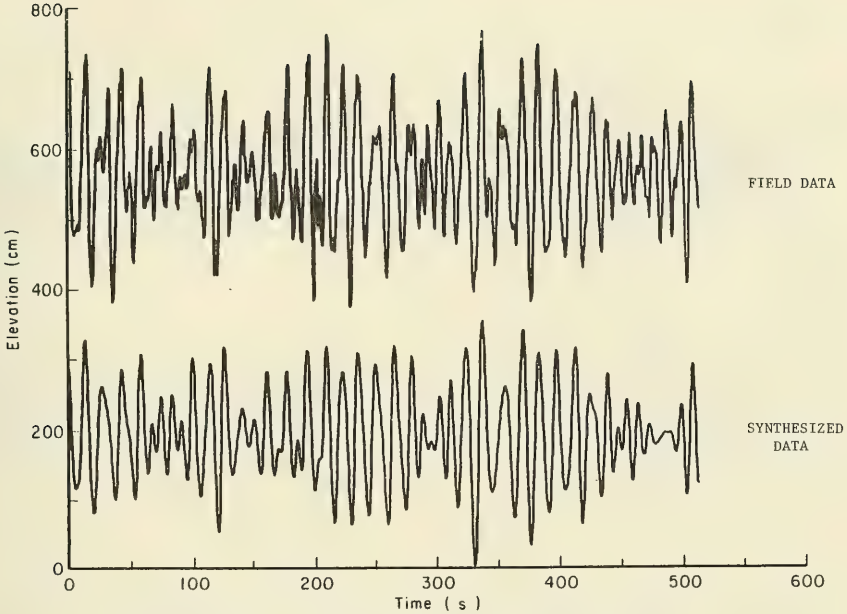

Figure B-11. Columbia Light, 1508.5 to 1517 P.d.t.

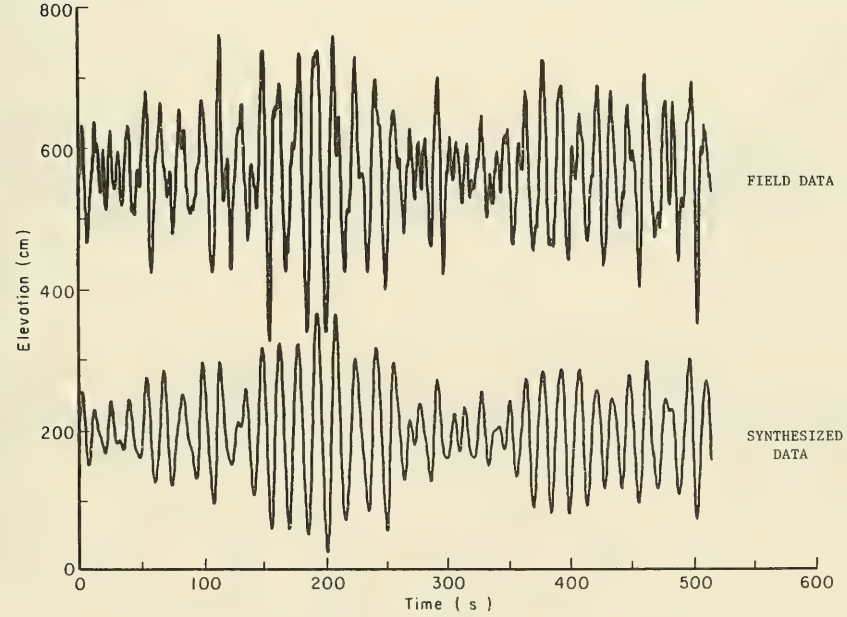

Figure B-12. Columbia Light, 1300 to 1308.5 P.d.t. (1,024-second record analyzed).

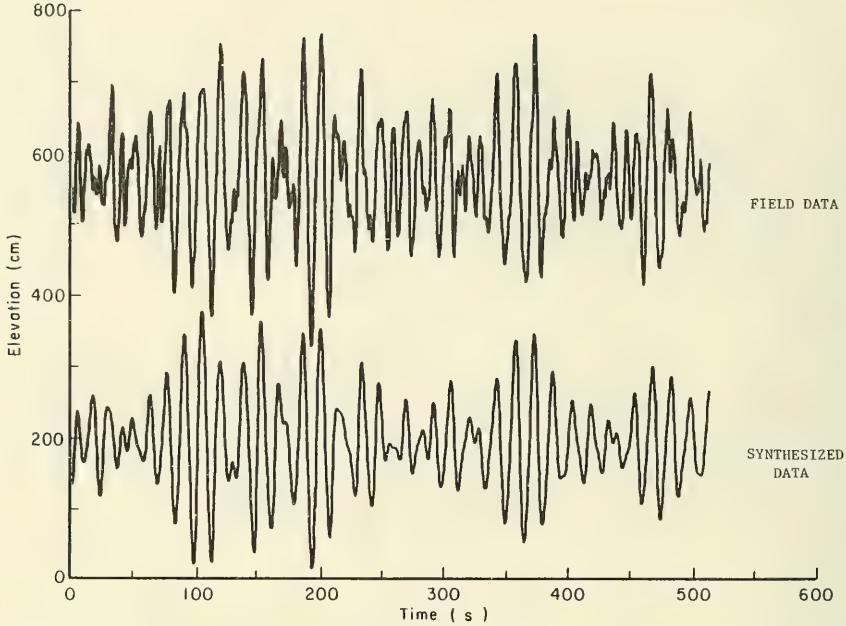

Figure B-13. Columbia Light, 1308.5 to 1317 P.d.t. (1,024-second record analyzed).

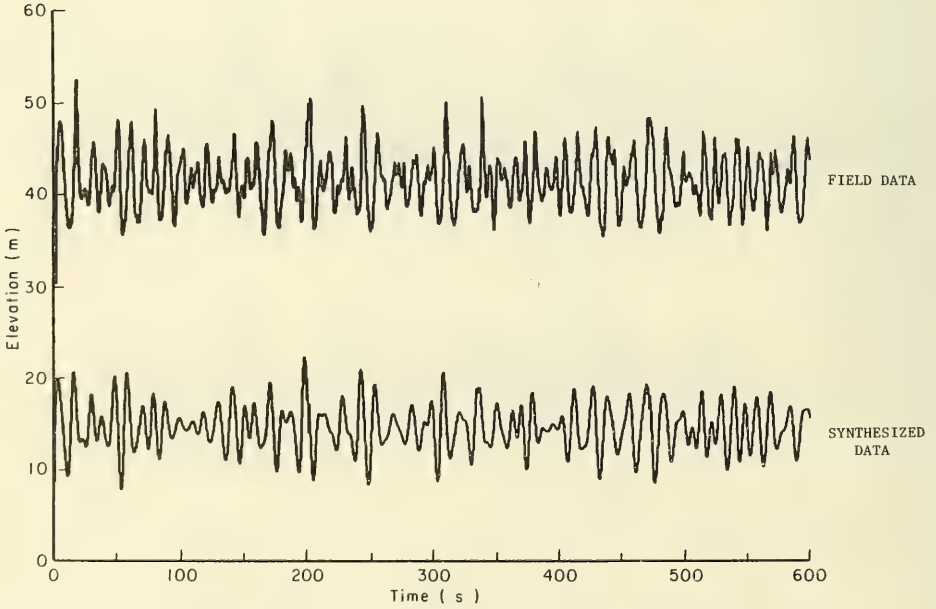

Figure B-14. South Pass, 1500 to 1510 c.d.t.

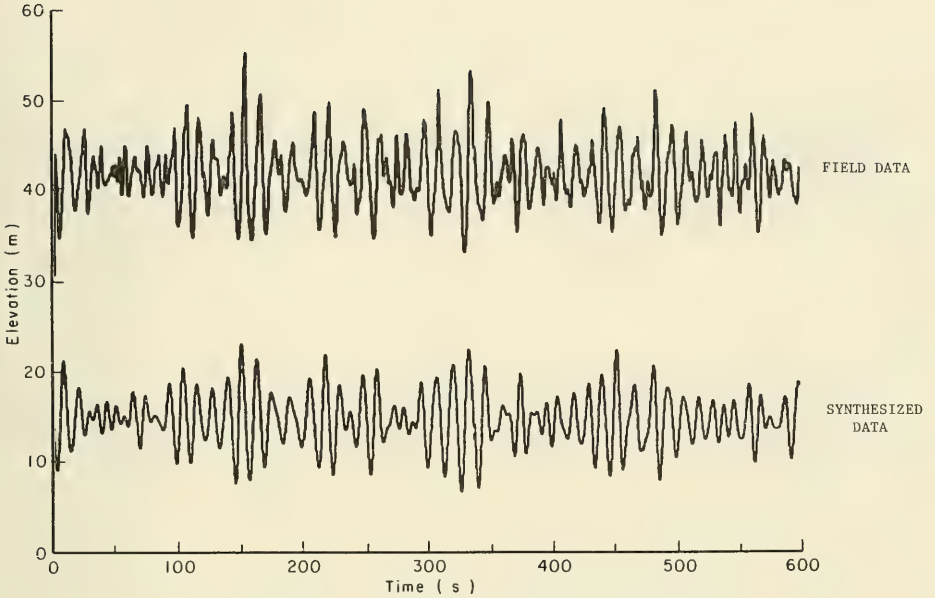

Figure B-15. South Pass, 1510 to 1520 c.d.t.

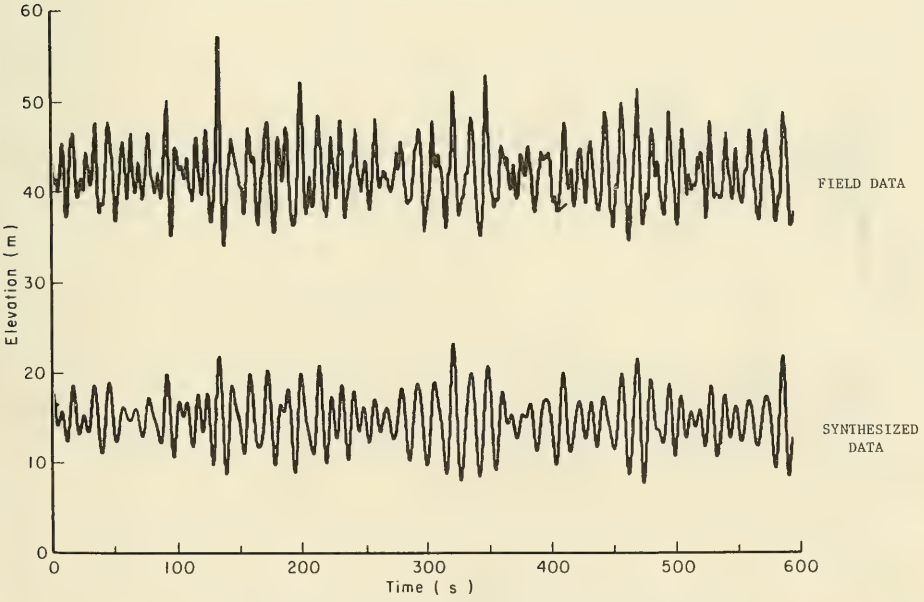

Figure B-16. South Pass, 1520 to 1530 c.d.t.

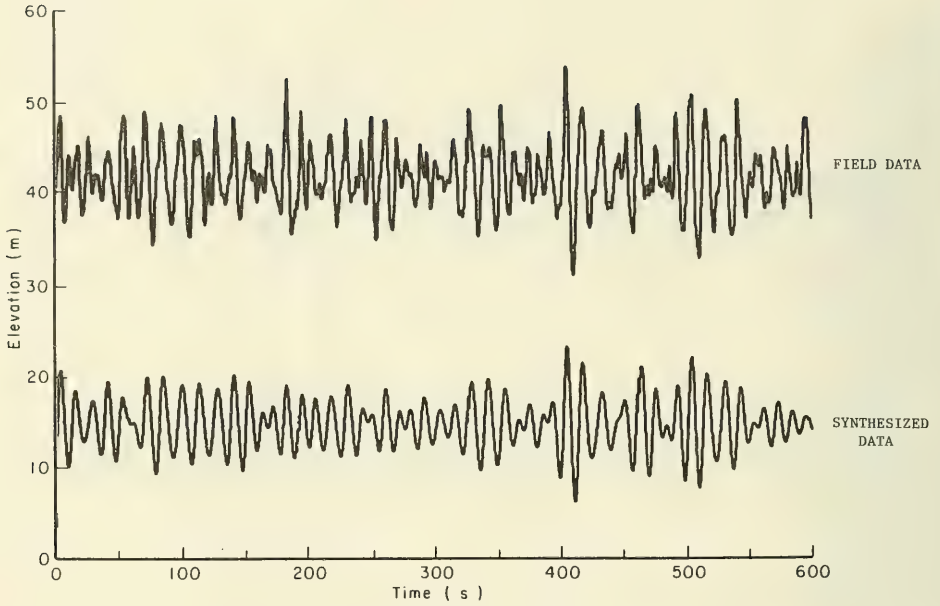

Figure B-17. South Pass, 1530 to 1540 c.d.t.

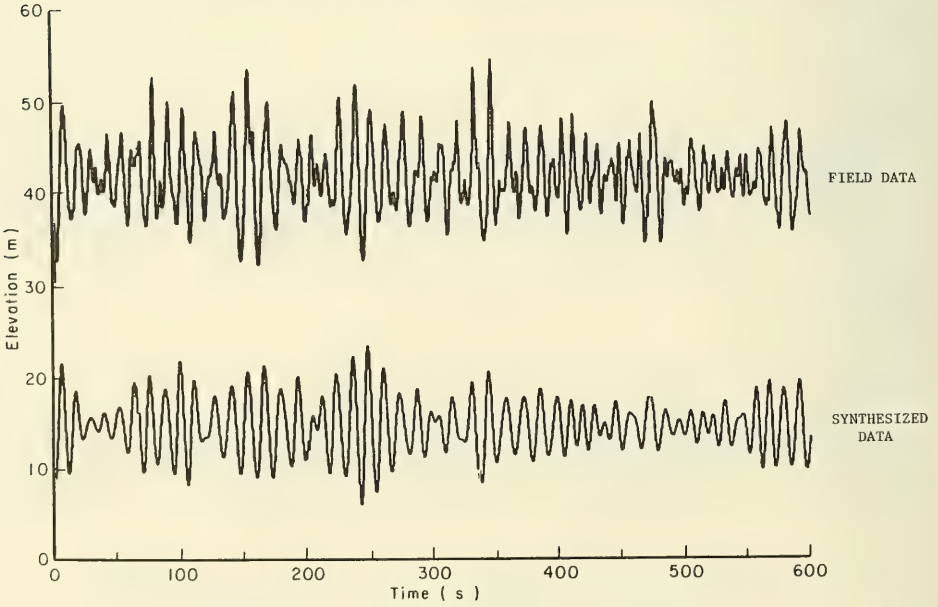

Figure B-18. South Pass, 1540 to 1550 c.d.t.

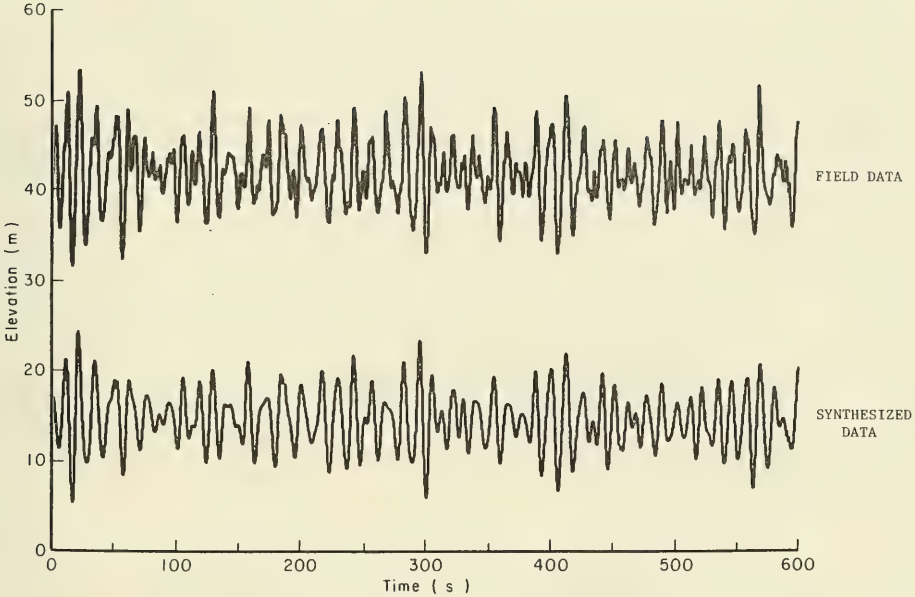

Figure B-19. South Pass, 1550 to 1600 c.d.t.

APPENDIX C

DESCRIPTION OF COMPUTER ROUTINE FOR IDENTIFYING MAJOR PEAKS AND VALLEYS IN AN IRREGULAR SIGNAL

The computer routine SMOOTH is useful for deleting small, inconsequential peaks and valleys from an irregular digital signal. Peaks and valleys that remain after application of SMOOTH represent major extrema which in many cases are more meaningful than small wiggles in the signal.

The operation of SMOOTH is most conveniently described in terms of its application to a time series of sea-surface elevations, although its other applications are analogous. The general scheme of operation consists of a check on the time difference and elevation difference between successive extrema. If either is less than the specified acceptable minimum, then one peak and one valley are deleted from the time series.

The input to SMOOTH consists of several control parameters and an array (EXTIM) containing time and elevation for each extremum in the time series. Figure C-1 shows five extrema in a hypothetical time series. If the point labeled "-1" were the first point in the time series, then the first 10 values in the EXTIM array would be

$$t_{-1},\ \eta_{-1},\ t_0,\ \eta_0,\ t_1,\ \eta_1,\ t_2,\ \eta_2,\ t_3,\ \text{and}\ \eta_3$$

where t_i and η_i are defined as the time and elevation associated with the i'th point. The control parameters which must be specified are

FURST = time associated with the first point desired in the time series.

ITEMS = total number of values in EXTIM array (= twice the number of extrema).

CHP = minimum acceptable time difference between successive points (critical half period).

HMIN = minimum acceptable elevation difference between successive points.

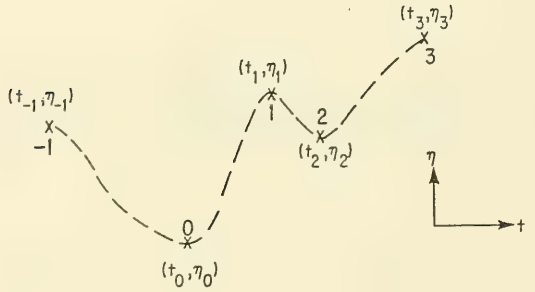

Figure C-1. Hypothetical time series (from Thompson, 1980).

After completion of SMOOTH, the times and elevations of major peaks and valleys are stored in the first ITEMS elements of EXTIM. The value of ITEMS has been reduced in accordance with the number of small peaks and valleys eliminated. Since the smoothing algorithm cannot work properly at the end of a record, the last few points are usually accepted regardless of whether or not they satisfy the acceptance criteria. Thus, the last six elements in EXTIM may not represent major peaks or valleys and should either be checked or categorically eliminated.

A complete list of subroutine SMOOTH with comments is provided in Figure C-2.

```
      SUBROUTINE SMOOTH (FURST, ITEMS)

C        SUBROUTINE SMOOTH TAKES A RECORD OF PEAKS AND VALLEYS AND
C          ELIMINATES INCONSEQUENTIAL PEAKS AND VALLEYS. THE ELIMINATION
C          CRITERIA ARE A MINIMUM DIFFERENCE BETWEEN PEAK AND VALLEY
C          ELEVATIONS (HMIN) AND A MINIMUM HORIZONTAL SPACING (BE IT
C          TIME, POSITION, ETC) BETWEEN PEAK AND VALLEY (CMP).
C        INPUT PARAMETERS ARE DEFINED AS FOLLOWS,
C     FURST = STARTING TIME
C     ITEMS = TOTAL NUMBER OF EXTREME VALUES (INCLUDES TIME AND
C                ELEVATION VALUES)
C     CMP = CRITICAL HALF PERIOD
C     HMIN = MINIMUM HEIGHT TO BE CONSIDERED
C     EXTIM(ODD) = TIME
C     EXTIM(EVEN) = EXTREME ELEVATION ASSOCIATED WITH EXTIM(EVEN-1) VALUE
C                OF TIME
      COMMON  /SHNT/  EXTIM(100)
C        SET VALUES OF CMP AND HMIN TO BE USED
      DATA CMP, HMIN / 0.00, 3.0 /
C        INITIALIZE VARIABLES AND FIND STARTING POINT FOR PROCESSING
 1503 IITEMS=ITEMS
      J=1
      ITEM7=ITEMS-7
      DO 1502 I=1,IITEMS,2
      ISKIP=I
      IF(EXTIM(I).GE.FURST) GO TO 1504
      J=J+2
      ITEMS=ITEMS-2
 1502 CONTINUE
 1504  ISTART=ISKIP
C*****************************************************************

C        BEGIN MAIN PROCESSING LOOP
      DO 1520 I=ISTART,ITEM7,2
      L=1
      IF(ISTART.GT.ITEM7)GO TO 1520
      IF(EXTIM(I)+CMP.GT.EXTIM(I+2))GO TO 1511
      IF(ABS(EXTIM(I+1)-EXTIM(I+3)).LT.HMIN)GO TO 1511
C     IF NO TRANSFER, THIS EXTREME ACCEPTED
      EXTIM(J)=EXTIM(I)
      EXTIM(J+1)=EXTIM(I+1)
      J=J+2
      GO TO 1520
C     WHEN THE NEXT INSTRUCTION IS REACHED, ONE HIGH AND ONE LOW WILL
C                BE DELETED
 1511 IF(EXTIM(I+1).GT.EXTIM(I+3))GO TO 1514
C     IF NEXT INSTRUCTION IS USED, THIS IS A LOW
      IF(EXTIM(I+5).GT.EXTIM(I+1))GO TO 1512
      IF(EXTIM(I+3).GT.EXTIM(I-1))GO TO 1513
      GO TO 1517
 1512 IF(EXTIM(I+3).GT.EXTIM(I+7))GO TO 1519
      GO TO 1516
C     WHEN NEXT INSTRUCTION IS USED, THIS IS A HIGH
 1514 IF(EXTIM(I+5).GT.EXTIM(I+1))GO TO 1515
      IF(EXTIM(I+7).GT.EXTIM(I+3))GO TO 1519
      GO TO 1516
 1515 IF (EXTIM(I+3).GT.EXTIM(I-1))GO TO 1517
      GO TO 1518
C        SET THE VALUE OF ICASE
 1516 ICASE=1
      GO TO 1521
 1517  ICASE=2
      GO TO 1521
```

Figure C-2. List of subroutine SMOOTH (from Thompson, 1980).

```
 1518  ICASE=3
       GO TO 1521
 1519  ICASE=4
 1521  J1=I-2
       J2=I+7
C         DELETE ONE HIGH AND ONE LOW ACCORDING TO THE VALUE OF ICASE
       GO TO(1522,1523,1524,1525)ICASE.
C      STORAGE PLAN A
 1522 EXTIM(J-2)=EXTIM(I-2)
       EXTIM(J-1)=EXTIM(I-1)
       EXTIM(J)=EXTIM(I)
       EXTIM(J+1)=EXTIM(I+1)
       EXTIM(J+2)=EXTIM(I+6)
       EXTIM(J+3)=EXTIM(I+7)
       GO TO 1526
C      STORAGE PLAN B
 1523  EXTIM(J-2)=EXTIM(I-2)
       EXTIM(J-1)=EXTIM(I-1)
       EXTIM(J)=EXTIM(I+4)
       EXTIM(J+1)=EXTIM(I+5)
       EXTIM(J+2)=EXTIM(I+6)
       EXTIM(J+3)=EXTIM(I+7)
       GO TO 1526
C      STORAGE PLAN C
 1524  EXTIM(J-2)=EXTIM(I+2)
       EXTIM(J-1)=EXTIM(I+3)
       EXTIM(J)=EXTIM(I+4)
       EXTIM(J+1)=EXTIM(I+5)
       EXTIM(J+2)=EXTIM(I+6)
       EXTIM(J+3)=EXTIM(I+7)
       GO TO 1526
C      STORAGE PLAN D
 1525  EXTIM(I+6)=EXTIM(I+2)
       EXTIM(I+7)=EXTIM(I+3)
       EXTIM(J-2)=EXTIM(I-2)
       EXTIM(J-1)=EXTIM(I-1)
       EXTIM(J)=EXTIM(I)
       EXTIM(J+1)=EXTIM(I+1)
       EXTIM(J+2)=EXTIM(I+2)
       EXTIM(J+3)=EXTIM(I+3)
       K1=I+4
       K2=I+10
 1526  J1=J-2
       J2=J+3
       ITEMS=ITEMS-4
       ISKIP=I+8
       J=J+4
       GO TO 1504
 1520  CONTINUE
C        END MAIN PROCESSING LOOP
C*************************************************************************
       J=J-1
       IF(I-2.EQ.ITEM7)L=I
 1530 IF(L.GT.IITEMS)GO TO 1540
       J=J+1
       EXTIM(J)=EXTIM(L)
       L=L+1
       GO TO 1530
 1540 CONTINUE
       ITEMS=J
C         IF THERE WERE ANY DELETIONS IN THIS PASS REPROCESS ALL REMAINING
C                   HIGHS AND LOWS TO MAKE FURTHER DELETIONS IF NEEDED.
       IF(IITEMS.GT.ITEMS)GO TO 1503
       RETURN
       END
```

Figure C-2. List of subroutine SMOOTH (from Thompson, 1980).--Continued

APPENDIX D

PLOTS OF PHASE VERSUS FREQUENCY FROM MRS ANALYSIS

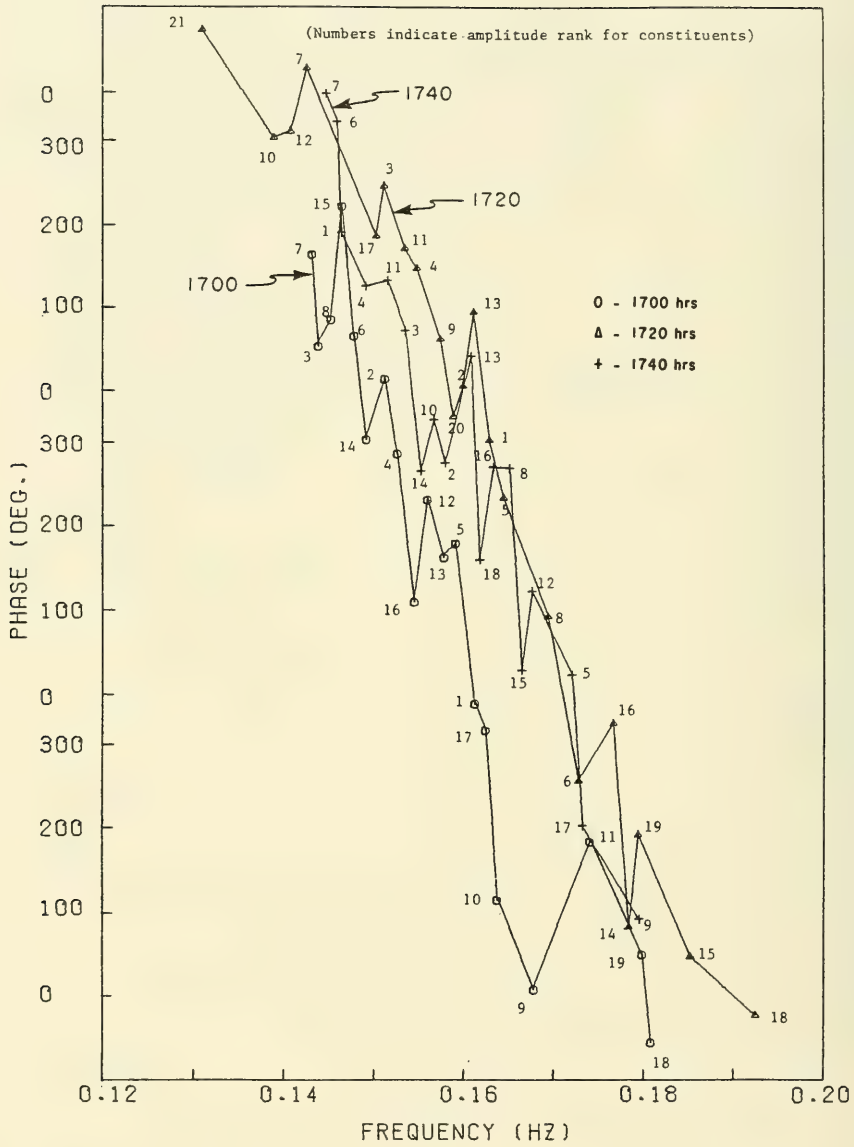

Figure D-1. South Haven, 1700 to 1800 e.s.t., 1,024-second records analyzed. Starting time of record is noted beside each curve.

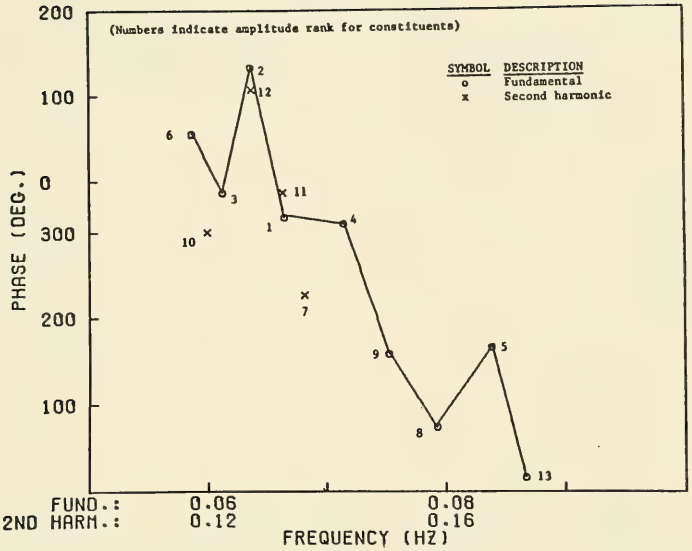

Figure D-2. Columbia Light, 1300 to 1308.5 P.d.t., 512-second record analyzed.

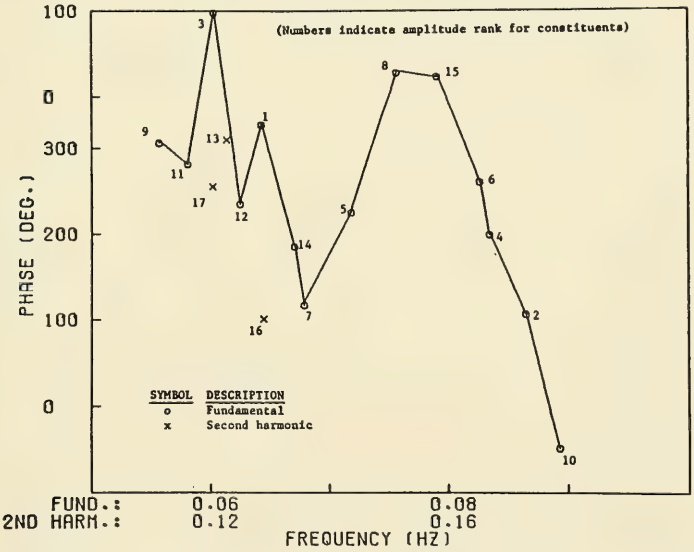

Figure D-3. Columbia Light, 1308.5 to 1317 P.d.t., 512-second record analyzed.

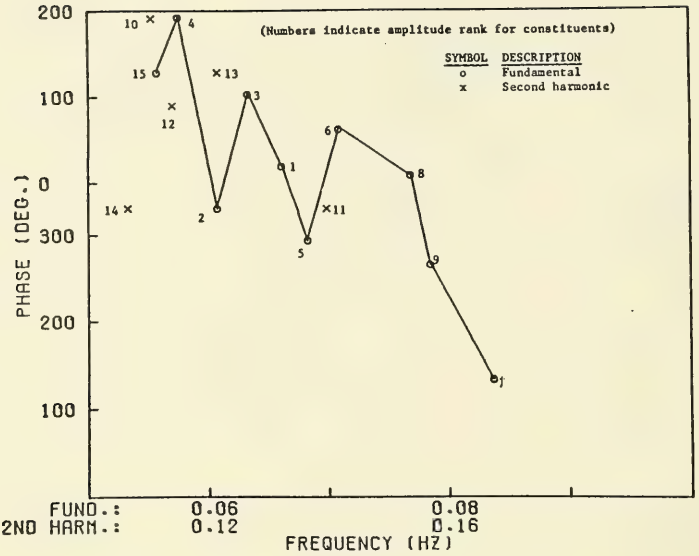

Figure D-4. Columbia Light, 1408.5 to 1417 P.d.t., 512-second record analyzed.

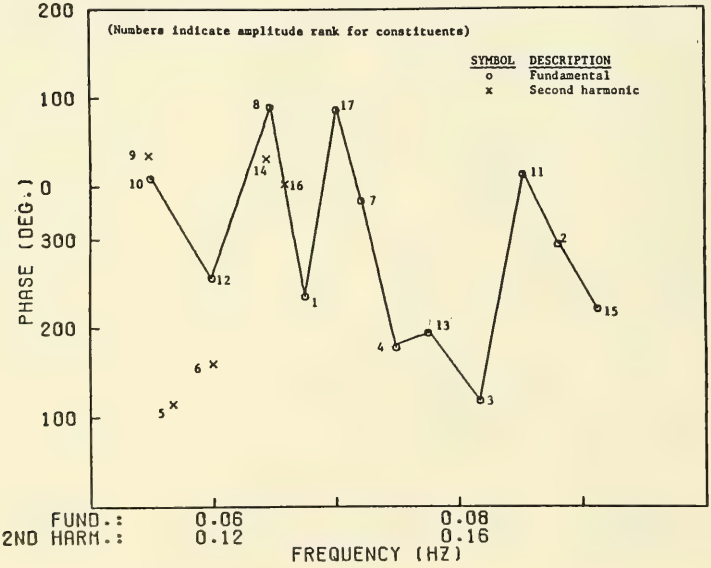

Figure D-5. Columbia Light, 1500 to 1508.5 P.d.t., 512-second record analyzed.

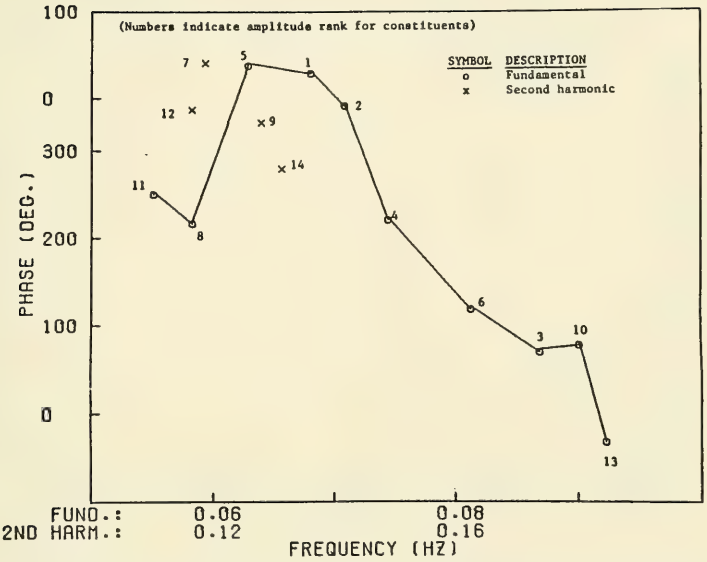

Figure D-6. Columbia Light, 1508.5 to 1517 P.d.t., 512-second record analyzed.

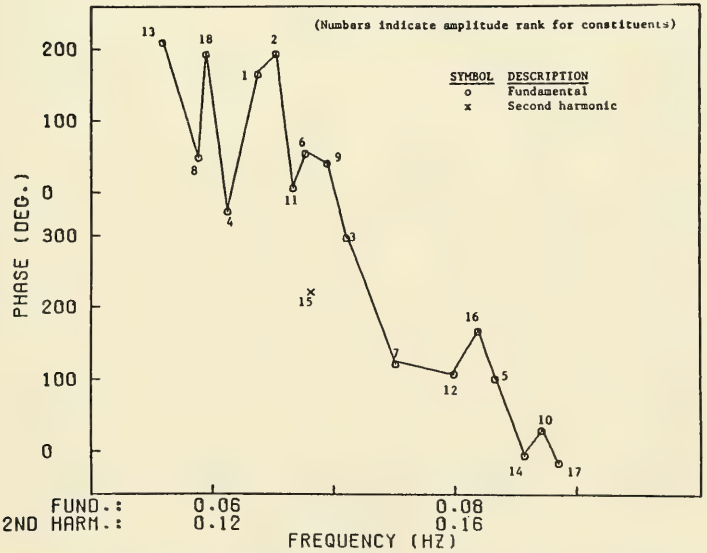

Figure D-7. Columbia Light, 1300 to 1317 P.d.t., 1,024-second record analyzed.

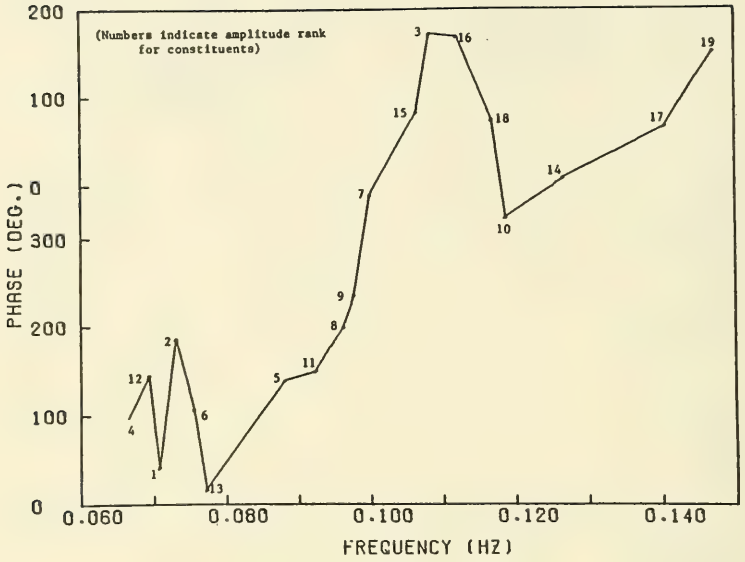

Figure D-8. South Pass, 1500 to 1510 c.d.t., 600-second record analyzed.

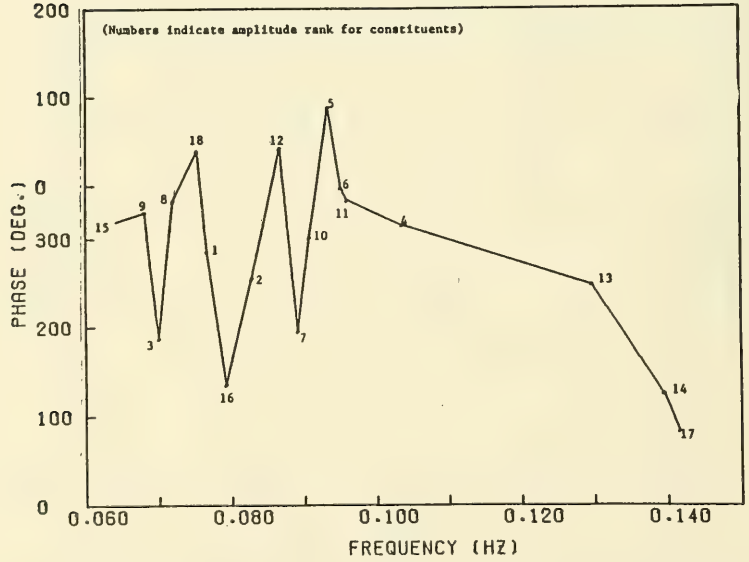

Figure D-9. South Pass, 1510 to 1520 c.d.t., 600-second record analyzed.

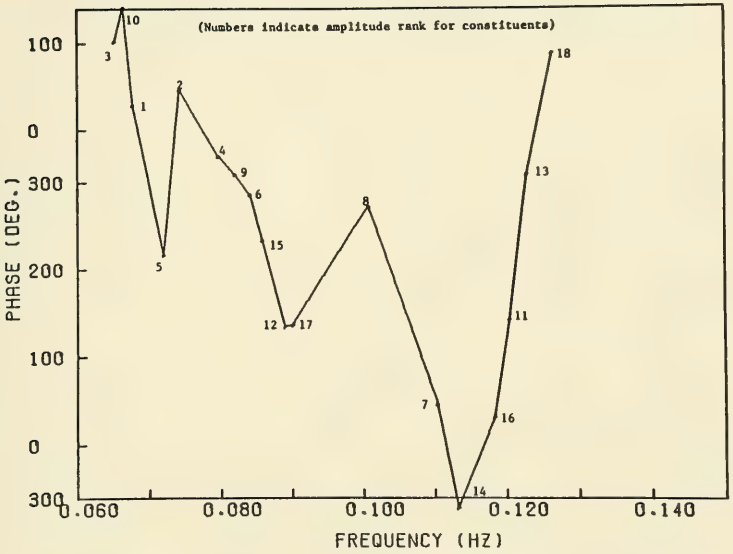

Figure D-10. South Pass, 1520 to 1530 c.d.t., 600-second record analyzed.

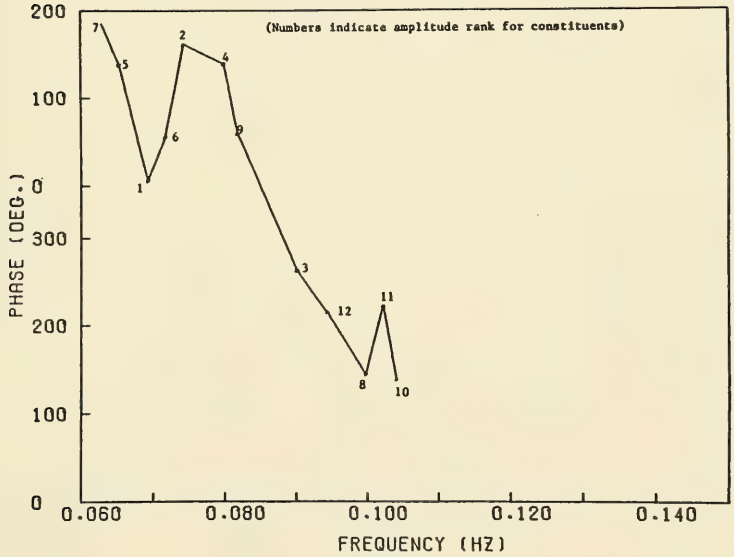

Figure D-11. South Pass, 1530 to 1540 c.d.t., 600-second record analyzed.

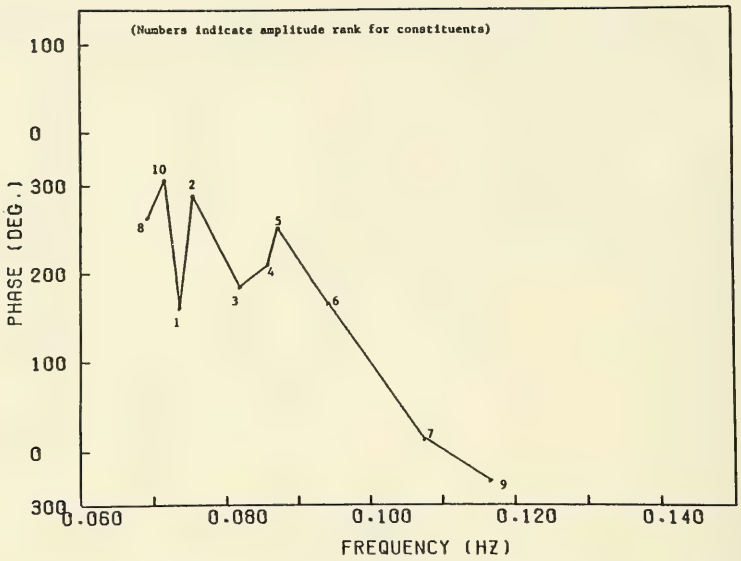

Figure D-12. South Pass, 1540 to 1550 c.d.t., 600-second record analyzed.

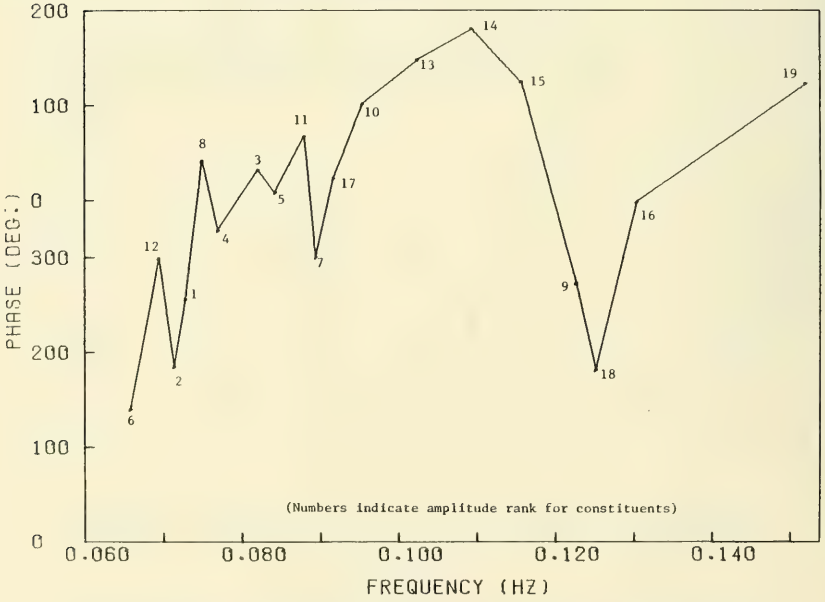

Figure D-13. South Pass, 1550 to 1600 c.d.t., 600-second record analyzed.

APPENDIX E

PLOTS OF MAJOR PEAKS AND VALLEYS IN LOCAL VARIANCE TIME SERIES

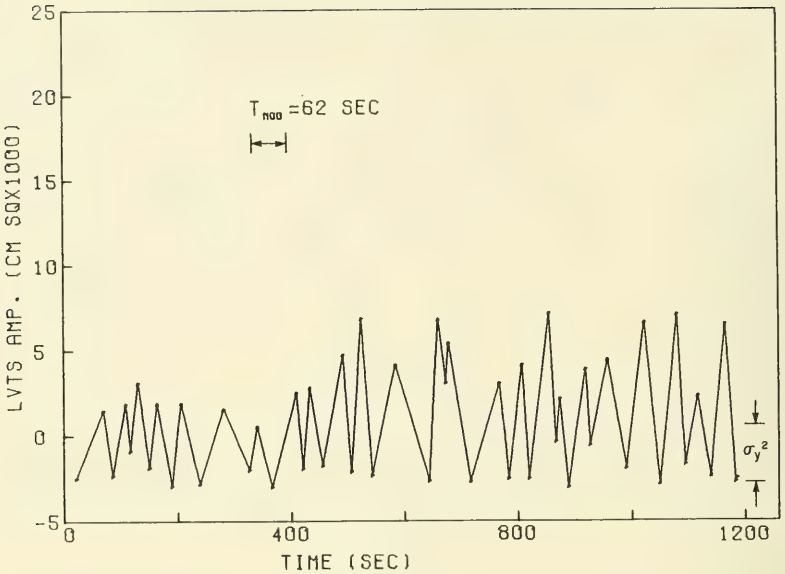

Figure E-1. South Haven, 1700 to 1720 e.s.t., I = 52, G = 0.63.

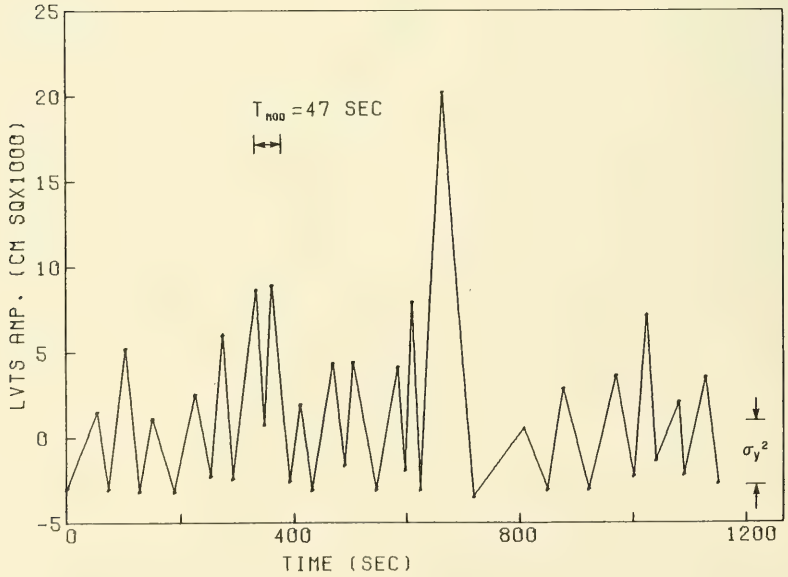

Figure E-2. South Haven, 1720 to 1740 e.s.t., I = 52, G = 0.79.

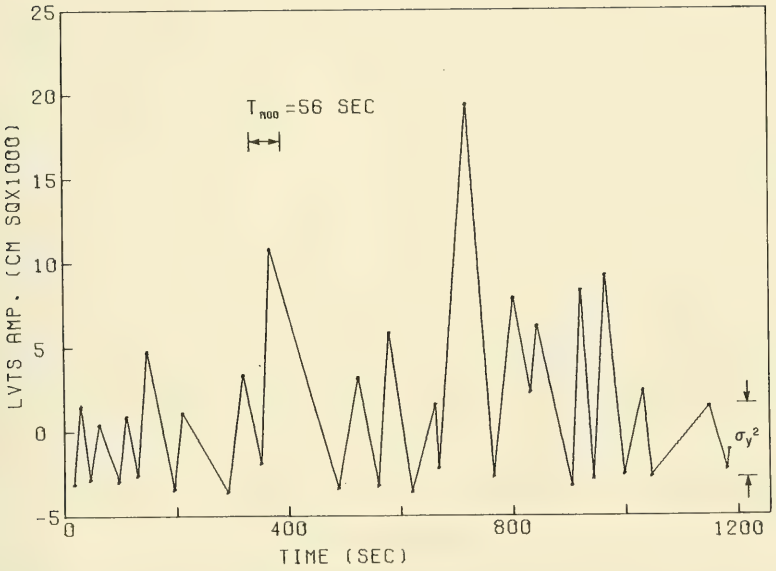

Figure E-3. South Haven, 1740 to 1800 e.s.t., I = 52, G = 0.69.

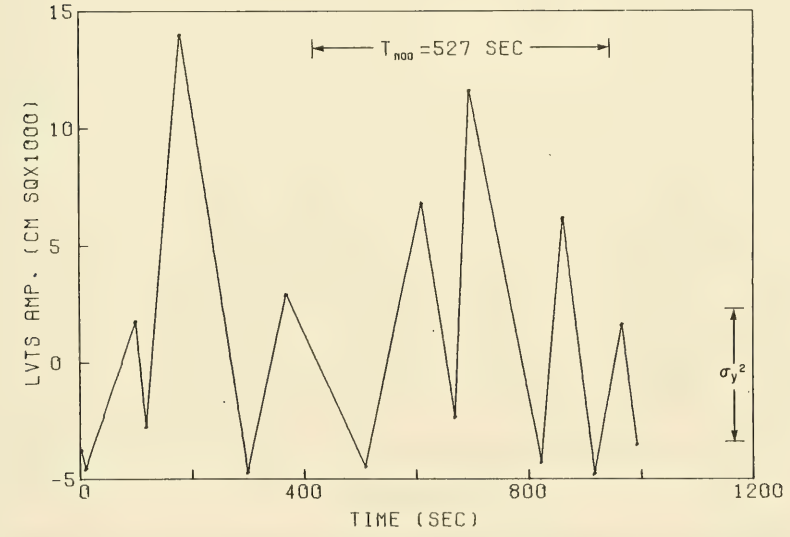

Figure E-4. Columbia Light, 1300 to 1317 P.d.t., I = 60, G = 0.67.

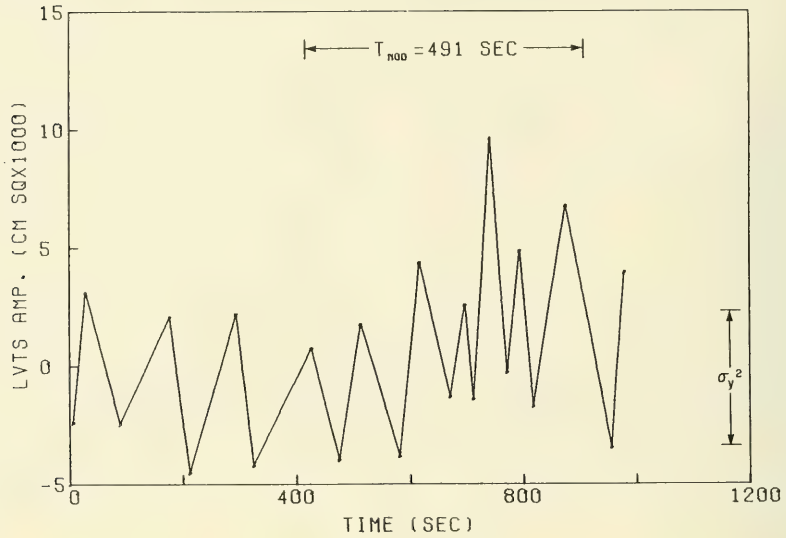

Figure E-5. Columbia Light, 1400 to 1417 P.d.t., I = 60, G = 0.50.

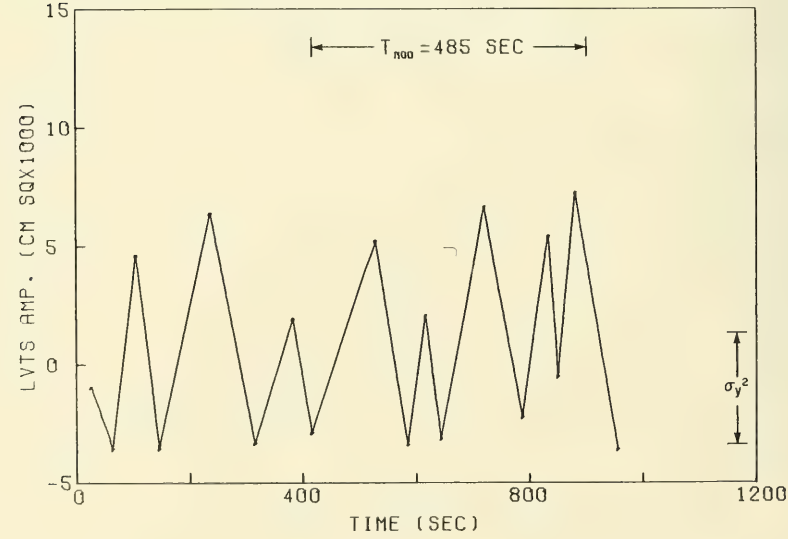

Figure E-6. Columbia Light, 1500 to 1517 P.d.t., I = 60, G = 0.60.

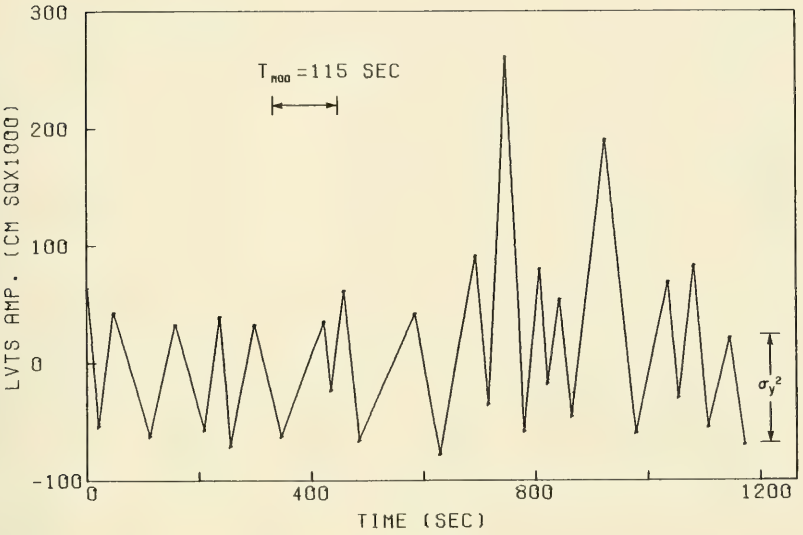

Figure E-7. South Pass, 1500 to 1520 c.d.t., I = 260, G = 0.60.

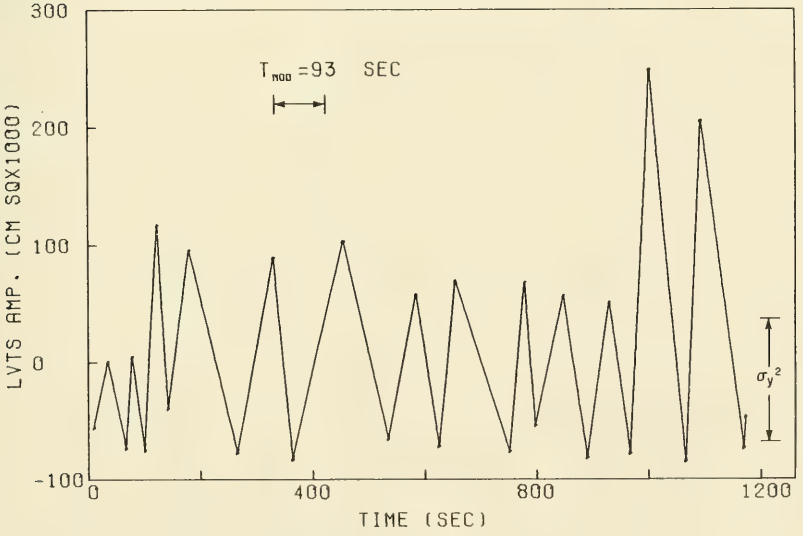

Figure E-8. South Pass, 1520 to 1540 c.d.t., I = 260, G = 0.59.

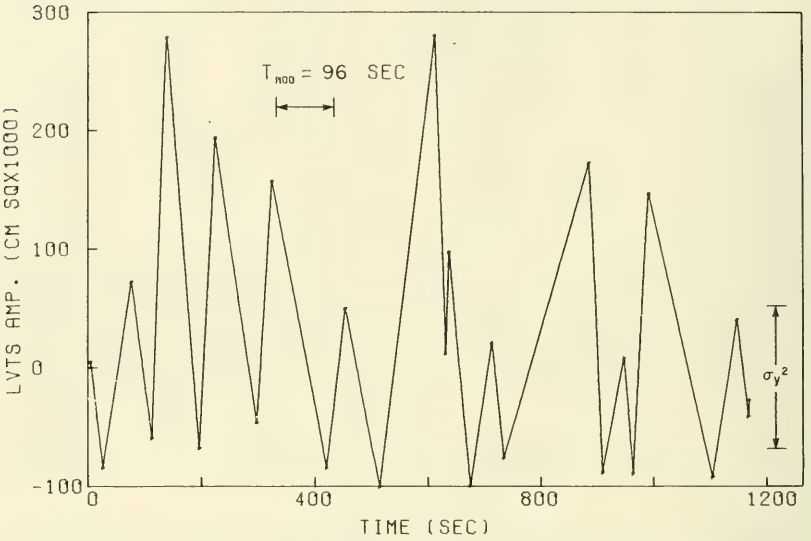

Figure E-9. South Pass, 1540 to 1600 c.d.t., I = 260, G = 0.66.

Thompson, Edward F.
Nonrandom behavior in field wave spectra and its effect on grouping of high waves / by Edward F. Thompson.--Fort Belvoir, Va. : U.S. Army Coastal Engineering Research Center ; Springfield, Va. : available from NTIS, 1982.
[110] p. : ill. : 28 cm.--(Technical report / Coastal Engineering Research Center ; no. 82-2)
Cover title.
"August 1982."
Wave measurements are examined from three relatively deepwater field sites in Lake Michigan, the Pacific Ocean, and the Gulf of Mexico. Approximately 1 hour of data representing high waves, single-peaked spectra, and nearly constant significant heights and peak spectral periods was selected for analysis. The data represent actively growing waves at two sites and swell at the third site.
1. Fourier transformations. 2. Spectral analysis. 3. Wave spectra. 4. Wave height. I. Title. II. Series: Technical report (Coastal Engineering Research Center (U.S.)); no. 82-2.
TC203 .U581tr no. 82-2 627

Thompson, Edward F.
Nonrandom behavior in field wave spectra and its effect on grouping of high waves / by Edward F. Thompson.--Fort Belvoir, Va. : U.S. Army Coastal Engineering Research Center ; Springfield, Va. : available from NTIS, 1982.
[110] p. : ill. : 28 cm.--(Technical report / Coastal Engineering Research Center ; no. 82-2)
Cover title.
"August 1982."
Wave measurements are examined from three relatively deepwater field sites in Lake Michigan, the Pacific Ocean, and the Gulf of Mexico. Approximately 1 hour of data representing high waves, single-peaked spectra, and nearly constant significant heights and peak spectral periods was selected for analysis. The data represent actively growing waves at two sites and swell at the third site.
1. Fourier transformations. 2. Spectral analysis. 3. Wave spectra. 4. Wave height. I. Title. II. Series: Technical report (Coastal Engineering Research Center (U.S.)); no. 82-2.
TC203 .U581tr no. 82-2 627

Thompson, Edward F.
Nonrandom behavior in field wave spectra and its effect on grouping of high waves / by Edward F. Thompson.--Fort Belvoir, Va. : U.S. Army Coastal Engineering Research Center ; Springfield, Va. : available from NTIS, 1982.
[110] p. : ill. : 28 cm.--(Technical report / Coastal Engineering Research Center ; no. 82-2)
Cover title.
"August 1982."
Wave measurements are examined from three relatively deepwater field sites in Lake Michigan, the Pacific Ocean, and the Gulf of Mexico. Approximately 1 hour of data representing high waves, single-peaked spectra, and nearly constant significant heights and peak spectral periods was selected for analysis. The data represent actively growing waves at two sites and swell at the third site.
1. Fourier transformations. 2. Spectral analysis. 3. Wave spectra. 4. Wave height. I. Title. II. Series: Technical report (Coastal Engineering Research Center (U.S.)); no. 82-2.
TC203 .U581tr no. 82-2 627

Thompson, Edward F.
Nonrandom behavior in field wave spectra and its effect on grouping of high waves / by Edward F. Thompson.--Fort Belvoir, Va. : U.S. Army Coastal Engineering Research Center ; Springfield, Va. : available from NTIS, 1982.
[110] p. : ill. : 28 cm.--(Technical report / Coastal Engineering Research Center ; no. 82-2)
Cover title.
"August 1982."
Wave measurements are examined from three relatively deepwater field sites in Lake Michigan, the Pacific Ocean, and the Gulf of Mexico. Approximately 1 hour of data representing high waves, single-peaked spectra, and nearly constant significant heights and peak spectral periods was selected for analysis. The data represent actively growing waves at two sites and swell at the third site.
1. Fourier transformations. 2. Spectral analysis. 3. Wave spectra. 4. Wave height. I. Title. II. Series: Technical report (Coastal Engineering Research Center (U.S.)); no. 82-2.
TC203 .U581tr no. 82-2 627